Role of NADPH oxidases and K_{DR} channels in the pathophysiology of hypoxia induced pulmonary hypertension

Inaugural Dissertation
submitted to the
Faculty of Medicine
in partial fulfilment of the requirements
for the PhD Degree
of the Faculty of Medicine
of the Justus-Liebig University Giessen

by

Manish Mittal
of
Jagadhri (Haryana), India

Giessen 2009

From the Medical Clinic II, University of Giessen Lung Centre

Chairman: Prof. Werner Seeger, M.D.

of the Faculty of Medicine of the Justus-Liebig University Giessen

First Supervisor and Committee Member: Prof. Norbert Weißmann

Second Supervisor and Committee Member: Prof. Jason Yuan, MD PhD

Committee Members: Prof. Dr. Heinz-Jürgen Thiel and Priv.-Doz. Dr. Yaser Abdallah

Date of Doctoral Defence: 26th August 2009

CONTENT

1 INTRODUCTION

1.1 Effect of hypoxia on the pulmonary vasculature

The pulmonary circulation is a low-pressure and low-resistance system that receives the entire cardiac output of the right ventricle. A unique feature of the pulmonary circulation is an ability to contract in response to hypoxia in order to divert the blood-flow from poorly to well ventilated regions of the lung, to minimise ventilation-perfusion mismatch to allow maximal oxygenation of the venous blood. This phenomenon also known as hypoxic pulmonary vasoconstriction (HPV) is a reversible physiological response of the pulmonary vasculature to acute hypoxia. The first clear description of HPV was provided by von Euler and Liljestrand in 1946 as a result of their experiments in cats, where it was found that hypoxic ventilation increased the pulmonary arterial pressure. In contrast, chronic hypoxia may lead to the development of irreversible pulmonary hypertension in humans and animals living at high altitude (Fig. 1). The pathology of this disease includes vascular remodeling which involves hypertrophy of media of the pulmonary arteries, thus narrowing the vascular lumen and leading to a permanent increase in pulmonary artery pressure (Fig. 1). The increase in pulmonary artery pressure subsequently can lead to the development of right heart hypertrophy and *cor pulmonale.*

1.2 Physiological characteristics of lung vasculature in acute hypoxia

The mechanism of HPV is particular to the lung vasculature, since the systemic vasculature undergoes relaxation in response to hypoxia. The physiologically relevant sites of HPV are thought to be the pre-capillary pulmonary arterioles [1;2]. Hypoxic pulmonary vasoconstriction occurs within seconds to few minutes of hypoxic exposure, and is a reversible process upon return to normoxic ventilation [3]. In humans and adult animals, an alveolar O_2 partial pressure (pAO_2) of 60 mm Hg or lower is sufficient to initiate HPV [3]. No visible vasoconstriction is observed at alveolar pO_2 values greater than 60 mm Hg, even when the mixed venous pO_2 falls below 10 mm Hg. This implies that the stimulus for HPV is moderate alveolar hypoxia and is independent of the pO_2 level of mixed venous blood [3]. Physiological factors such as pH and pCO_2 can affect the strength of HPV [4]. The autonomic nervous system and humoral mediators can modulate the pulmonary vascular reactivity to hypoxia, but are not the primary regulators of HPV, since HPV has been shown to persist even after denervation of the lung as well as in isolated lung perfusion models [5]. Hypoxic pulmonary vasoconstriction can be

localised to an area as small as an acinus or can include areas as large as one lung or both lungs, depending on the region of alveolar hypoxia. The increase in pulmonary arterial pressure (PAP) during HPV depends on the area of the lung that has been exposed to hypoxia. If the entire lung is exposed to hypoxia, this can result in acute hypoxia-induced pulmonary hypertension. However, a regional hypoxia leads to local vasoconstriction and effectively shifts the blood to the better ventilated areas of the lung with a very little increase in PAP [6]. The mean PAP in healthy individuals is between 20-25 mm Hg, which can increase further at high altitude. In addition, exercising at high altitude can further increase PAP values to ~ 54 mm Hg [7].

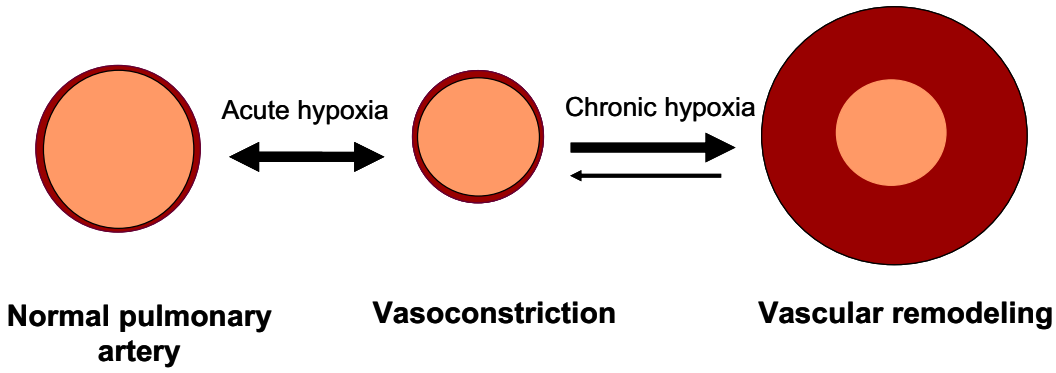

Figure 1. Effect of hypoxia on pulmonary vasculature. Acute hypoxia leads to physiological vasoconstriction which helps to minimise the mismatch between ventilation with perfusion. Chronic hypoxia leads to substantial thickening of vascular wall resulting in narrowing of the vascular lumen. Acute hypoxia induced pulmonary vasoconstriction is a reversible process whereas chronic hypoxia induced vascular remodeling is an irreversible process upon acute re-exposure to normoxia.

1.3 Mechanisms of pulmonary vascular adaptation to acute and chronic hypoxia

The cellular and molecular mechanisms governing vascular remodeling under chronic hypoxia have been suggested to be different from those mechanisms that cause HPV under acute hypoxia, however, common mediators may exist [8]. For example, an increase in cytosolic calcium levels during acute hypoxia leads to vasoconstriction but also acts as a stimulus for smooth muscle cell proliferation under chronic hypoxia which is a characteristic feature of vascular remodeling [8;9]. Similarly, an inhibition of Kv channels at the functional level under acute hypoxia is accompanied by the down-regulation of Kv channel mRNA and protein expression under chronic hypoxia (discussed in section 1.3.1.4 and 1.3.2.2). According to the generally accepted view, hypoxic pulmonary vasoconstriction is an intrinsic property of the pulmonary vaculature and specifically resides in pulmonary arterial smooth muscle cells [10]. Despite intensive research, the mechanisms of both HPV and vascular remodeling in lung have not been fully elucidated. Recent reports demonstrate the involvement of more than one pathway in controlling the reactivity of the pulmonary vasculature to hypoxia. While it is well

accepted that there is an increase in the cytoplasmic Ca^{2+} concentration $[Ca^{2+}]_{cyt}$ in smooth muscle cells under hypoxic conditions, the mechanism of this increase remains an open question. Many hypotheses have been put forward to explain the hypoxia-induced increase in Ca^{2+} in acute HPV which are summarised in Fig. 2, and are discussed in more detail in the subsequent sections.

1.3.1 Adaptation of pulmonary vasculature to acute hypoxia

1.3.1.1 Role of endothelium

Pulmonary vasoconstriction in response to acute hypoxia is biphasic, consisting of an immediate endothelium-independent constriction which peaks by ~10 min (phase 1) and an endothelium-dependent, sustained contraction phase, which peaks by ~40 min (phase 2) [7;11]. The role of the endothelium in acute HPV has been widely discussed. It was reported by several investigators that the second phase of acute HPV is abolished in the absence of the endothelium [12]. However, other reports refute the involvement of the endothelium in acute HPV [12]. The importance of the endothelium in modulating HPV response is due to its unique ability to secrete both vasoconstrictors (endothelin-1 (ET-1)) and vasodilators (nitric oxide (NO)). The action of ET-1 on pulmonary vasculature media is due to presence of endothelin receptor subtypes A and B (ET_A and ET_B) in the smooth muscle cells [13]. The significance of ET-1 as a potent vasoconstrictor can be judged from its use as a priming agent in various preparations and isolated lung perfusion models [12]. The role of ET-1 in acute HPV is controversial [12]. Some investigators have reported an increase plasma ET-1 levels under acute hypoxia, whereas other groups have not observed any changes in ET-1 levels under acute hypoxia [13]. However, the role of ET-1 in chronic hypoxia is well accepted where it may play a role in vascular remodeling process [13]. Nitric oxide is a potent vasodilator synthesised in the vascular endothelium by endothelial NO synthase (eNOS) from L-arginine and O_2. The vasodilatory properties of NO are mediated by the production of the second messenger cGMP by activating soluble guanylate cyclase (sGC) [14]. The cGMP inhibits Ca^{2+} entry in to cells by inhibiting L-type Ca^{2+} channels, and can also activate protein kinase G (PKG), which can inhibit voltage-gated Ca^{2+} channels directly [15;16]. The sGC can also be activated by hydrogen peroxide, leading to vascular relaxation and NADPH oxidase-derived hydrogen peroxide can mediate NO production by the endothelium [17;18].

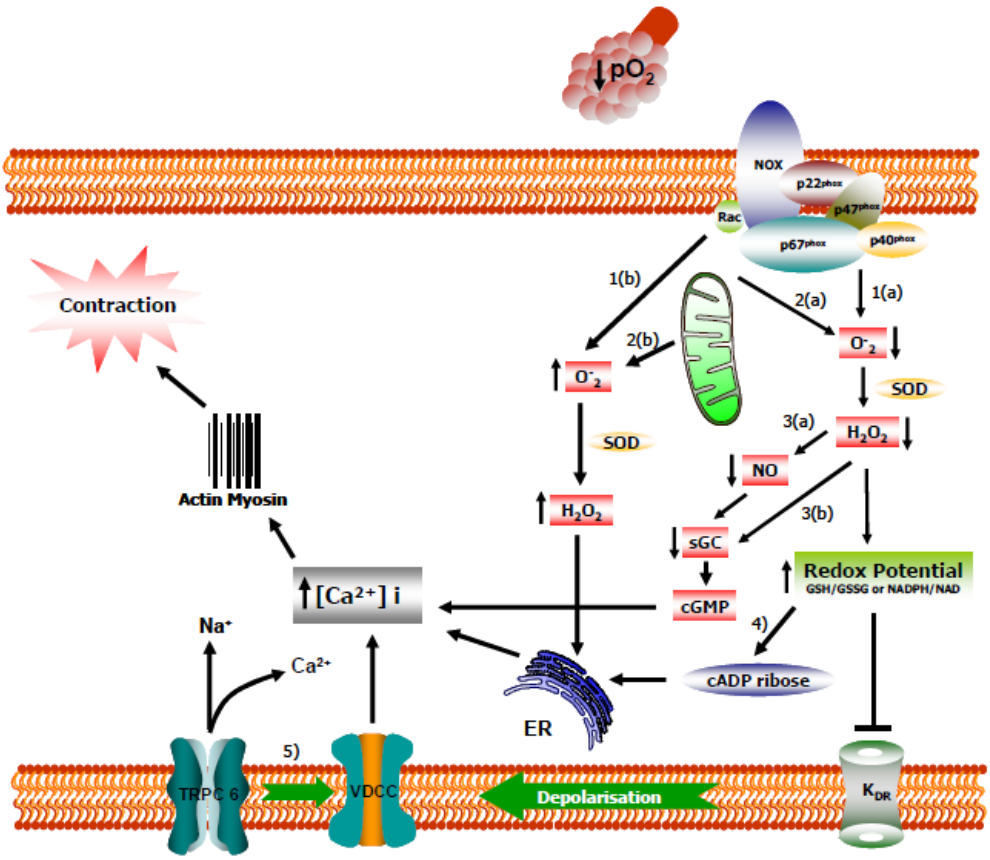

Figure 2. Schematic diagram for acute hypoxic pulmonary vasoconstriction. A decreased production of ROS by mitochondrian or NADPH oxidases have been suggested to lead to an increase in the redox status of the cell towards more reduced state leading to the closure of voltage gated K^+ channels and depolarisation of the PASMC membrane. Membrane depolarisation leads to the opening of voltage-dependent calcium channels (VDCC) leading to Ca^{2+} influx and contraction by activation of actin myosin contraction apparatus (1a, 2a). In addition, a decreased production of ROS can lead to HPV either by reduced availability of NO from endothelium or by reduced activation of sGC and hence less cGMP production (3a, 3b). Alternatively, an increased ROS production at complex I and III in mitochonria and NADPH oxidase can stimulate the release of Ca^{2+} ions from endoplasmic reticulum (ER) leading to vasoconstriction (1b, 2b). Hypoxia has also been shown to increase the ratio of NADPH/NADP leading to increased level of cADPR which activates ryanodine sensitive Ca^{2+} release channels in ER leading to vasoconstriction (4). Acute hypoxia has also been shown to increase calcium influx after activation of TRPC6 channel by involving VDCC (5).

Hypoxia has been shown to reduce the basal production of NO by reduced availability of O_2 or by reduced production of superoxide (Fig.2) [19]. But in contrast to the decrease of NO in HPV, there are arguments which favour its local increase, for example, a key stimulus for NO production is also shear stress on the vascular wall which is increased during HPV [13;20].

1.3.1.2 Role of mitochondria-derived reactive oxygen species

Molecular oxygen plays a vital role in oxidative phosphorylation in aerobic organisms where it participates in generation of high energy phosphate bonds of ATP by acting as the final electron acceptor of the cytochrome *c* oxidase complex embedded in the mitochondrial

membrane. During the process of electron transfer to molecular oxygen in the electron transport chain (ETC) in mitochondria partially-reduced and highly-reactive metabolites of O_2 are formed, such as the super-oxide (O_2^-) anion and hydrogen peroxide (H_2O_2) by one and two electron reduction of oxygen, respectively [21]. These partially-reduced metabolites of O_2 are often referred to as "reactive oxygen species" (ROS) or "activated oxygen species" (AOS) due to their considerable greater reactivities compared to molecular O_2. In addition to the production of ROS by mitochondria, there are intracellular membrane-associated (NADPH oxidase, Cytochrome P-450) and soluble enzymes (xanthine oxidase) that can generate ROS [21].

Electron transport chain consists of four mega complexes embedded in the mitochondrial membrane that catalyzes the transfer of electrons from reduced flavoprotein moieties such as NAD(P)H and $FADH_2$ to molecular oxygen (Fig. 3). Oxidation of NADH and FADH2 at complex I and complex II of the mitochondrial electron transport chain (ETC) respectively results in transfer of electrons by ubiquinone (enzyme Q) to complex III, and then to complex IV by the cytochrome *c* oxidase complex. Finally, electrons are transferred to molecular oxygen by complex IV, reducing it to H_2O. The transfer of electrons to O_2 is a tightly-controlled process to avoid the production of incompletely-reduced intermediates such as superoxide (O_2^-) and hydroxyl radicals (OH^-). However, electrons can be transferred to molecular oxygen at complex I and III to form superoxide radicals (Fig. 3). Hypoxia affects many aspects of mitochondrial function and this is current discussion with regard to generation of ROS at complex I and III, although it is controversial whether there is an increase or decrease in levels of ROS in response to acute hypoxia [22].

Pulmonary vascular tone is largely controlled by K^+ channels, which maintain the membrane of smooth muscle cells in a relaxed resting and polarised state. Any cellular changes which decrease the opening of K^+ channels result in depolarisation and subsequent contraction of smooth muscle cells. The K^+ channels are sensitive to oxidation and reduction at key thiol residues present in the intracellular side of the membrane [23]. According to the redox theory of oxygen sensing proposed by Weir and Archer, under normoxic conditions constitutive generation of ROS maintains the K^+ channels in oxidised/opened state, however, after exposure to hypoxia the electron transport through the ETC falls, thus reducing ROS production leading to reduction/closure of K^+ channels and depolarisation-dependent contraction (Fig. 2) [5;24]. Thus, inhibitors of complex I and III such as rotenone and antimycin respectively, should mimic hypoxia and vasoconstriction, and should prevent hypoxia from eliciting any further response. Indeed the application of rotenone and antimycin suppresses

HPV; however, controversy remains concerning whether rotenone and antimycin application mimics hypoxia [5;25-27]. Although some reports demonstrate an increase in pulmonary arterial pressure under normoxia upon application of rotenone, there are other reports which show no or very transient and smaller effects than on hypoxic induction [5;26;28].

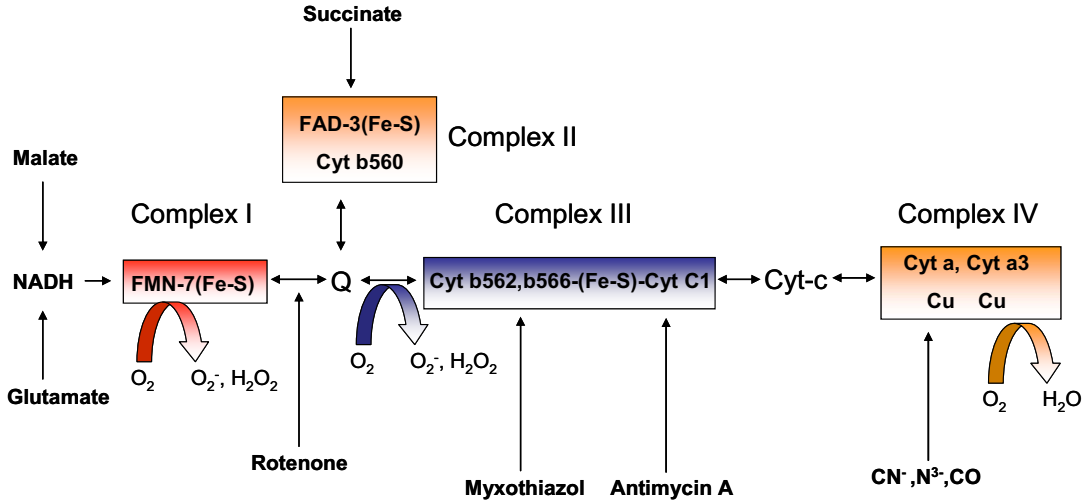

Figure 3. Schematic presentation of electron transport chain. The Mitochondrial electron transport chain consists of a series of electron carriers arranged spatially in the order of their increasing redox potential and organised in to four complexes. Arrows in the region of complexes I-IV show pathways of electron transfer between flavins (FMN-H2, FADH2), iron-sulfur centers (Fe-S), coenzyme Q (Q-QH2), cytochromes (c1, c a, a3) and molecular oxygen (O_2) resulting in the formation of H_2O. The main sites of ROS generation are complex I and III and hypoxia has been shown to affect these sites for superoxide production thus modulating HPV response.

While it seems arguably stronger to think a decrease in electron transfer via ETC in hypoxia because of decreased availability of oxygen as the final electron acceptor of ETC there is also convincing evidence which suggests that ROS is increased during hypoxia. According to Schumacker *et al.* hypoxia causes an increase in ROS from the ubisemiquinone region of complex III in mitochondria which leads to rise in intracellular Ca^{2+} level (Fig. 2) [5;27;29;30]. In line with this hypothesis the use of antioxidants and catalase as well as inhibitors which target the proximal region of complex III of ETC such as rotenone, diphenyl iodonium (DPI) and myxothiazol inhibited HPV without mimicking hypoxia. Moreover, the inhibitors which target the components of ETC distal to complex III such as cyanide (targets complex IV) did not abolish HPV [5;27;30].

1.3.1.3 Role of NADPH oxidase derived ROS

The NADPH oxidases are membrane-bound enzymes involved in superoxide production in various cell types by electron transfer from NADPH to oxygen. The classical leukocyte

NADPH oxidase plays an important role in host defense against bacterial and fungal pathogens [31;32]. This phagocytic type of NADPH oxidase consists of two membrane-bound subunits, gp91^{phox} and p22^{phox} which form the flavocytochrome b_{558} complex (Fig. 4). Superoxide production by classical gp91^{phox} is induced by assembly of the cytosolic subunits such as p40^{phox}, p47^{phox} and p67^{phox} with membrane-bound flavocytochrome b_{558} complex (Fig. 5). Such an assembly can be induced by the phosphorylation of p47^{phox} [33]. Rac GTPases are also involved in this activation process (Fig. 5). Recently, several additional isoforms of the membrane-bound subunit gp91^{phox} have been described. The first described homolog of gp91^{phox}, called mox1 (later NOX1), is primarily expressed in the colon, and is suggested to be involved in mitogenic activity [34].

Table 1 **NADPH oxidase (NOX) homologs**

	Binding partners					Tissue distribution
	p22 ^{phox}	p47 ^{phox}	p67^{phox}	p40^{phox}	Rac	
NOX1	Yes	NOXO1	NOXA1	?	?	Colon,vascular smooth muscle cells (VSM), uterus and prostate
NOX2	Yes	Yes p47 ^{phox} or	Yes p67^{phox} or	Yes	Yes	Phagocyte,endothelium,cardiomyocytes, VSM (?) and lung
NOX3	?	NOXO1	NOXA1	?	?	Innere ear, Kidney, liver, lung and spleen
NOX4 (Renox)	Yes	?	?	?	?	Kidney, VSM, endothelium, cardiomyocytes, bone,ovary,eyes placenta and skeltal muscle
NOX5	?	?	?	?	?	Lymphoid tissue, testis, prostate, breast and brain
Duox1 and Duox2	Yes	?	?	?	?	Thyroid gland cells and human bronchial epithelial cells

NOXO1, Nox-Organizing protein 1(a homologue of p47 ^{phox}) ; NOXA1, Nox-activating protein 1 (a homolgue of p67^{phox}) ; ?, unknown

Modified from: Ray R et al. Clinical science 2005; ***109****,217-226*

Additional homologs, including NOX3, NOX4 (Renox), NOX5, Duox1 and Duox2, were subsequently described [35-38] (Table 1). According to this new nomenclature, gp91^{phox} is synonymous with NOX2. It was suggested that each of these homologs can replace gp91^{phox} in the NADPH oxidase complex, and it has been demonstrated that these non-phagocytic NADPH oxidases releases lower amounts of superoxide [39-41]. However, very recently two new isoforms of the cytosolic subunits p47^{phox} and p67^{phox} have been identified. These new subunits, NOXO1 and NOXA1, have been demonstrated to interact with NOX1 to generate significant amounts of superoxide without being activated by protein kinase C-dependent phosphorylation [42;43] (Table 1). Isoforms of gp91^{phox} have been identified in different organs and cell types, including the colon, kidney, uterus, testis, liver, vascular smooth muscle cells, fibroblasts, endothelial cells, pancreatic islets and lymphocytes [31;33;39;44-46] (Table 1).

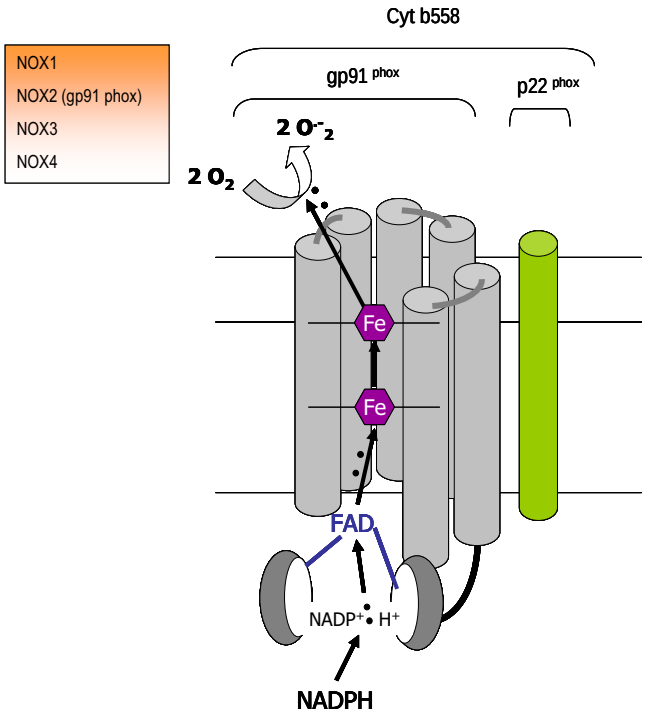

Figure 4. Topological structure of NOX enzymes. NADPH oxidase I (NOX1), NOX3 and NOX4 share a similar catalytic core of well studied gp91 ^{phox} or NOX2 consisting of 6 transmembrane α helices at N-terminus. The histidine residues in helices 3 and 5 coordinate with the iron atoms at the centre of 2 heme molecules. The iron residue in the heme molecule is responsible for undergoing oxidation and reduction reaction in electron transfer process. The two heme moieties are located within two leaflets of the membrane bilayer thus providing an electron channel across the membrane. The C-terminal portion of the protein forms a globular cytoplasmic domain harboring the prosthetic group FAD and the binding site for NADPH.
Modified from: Lassegue B et al. (40)

NADPH oxidases have been shown to behave as oxygen sensors at least in neuroepithelial bodies where a role of mitochondria seems to be unimportant for oxygen sensing [5]. According to Wolin et al. there is decreased superoxide production from NADH oxidase in hypoxia causing reduced stimulation of soluble guanylate cyclase (sGC) which results in vasoconstriction due to decreased production of cGMP (Fig. 2) [47]. Thus, loss of a normoxic vasodilation in hypoxia resulted in HPV. The opponents of this hypothesis have shown that in hypoxia there is a paradoxical increase in ROS production rather than a decrease (Fig. 2). Marshall *et al.* characterised an NADPH oxidase with a low redox potential which is activated by hypoxia resulting in increased ROS production in isolated smooth muscle cells of resistance pulmonary arteries [48]. Previous investigations from our laboratory suggested the involvement of a p47^{phox}-containing NADPH oxidase in the regulation of vascular tone in acute hypoxia since p47^{phox} knockout mice exhibit a reduced acute HPV as compared to wild type and gp91^{phox} knockout mice [49]. Recently it has been shown by Rathore et al. that acute

hypoxia activated NADPH oxidase and increased Ca^{2+} in PASMC and inhibitor of NADPH oxidase such as apocynin inhibited the acute hypoxia induced increase in Ca^{2+} [50].

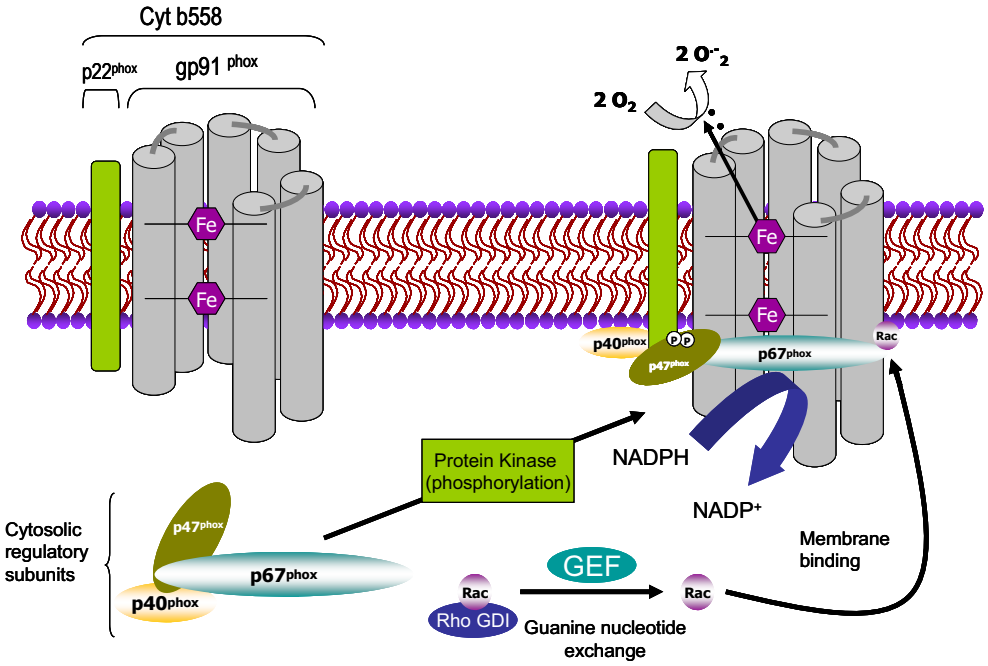

Figure 5. Activation mechanism of NADPH oxidases. Two independent events are required for the activation of $gp91^{phox}$ resulting in the assembly of the cytosolic regulatory proteins ($p40^{phox}$,$p47^{phox}$ and $p67^{phox}$) with the flavocytochrome b_{558} (made up of the membrane associated catalytic subunit $gp91^{phox}$ and $p22^{phox}$). One of the two events is the activation of protein kinases such as protein kinase C and AKT which phosphorylate the autoinhibitory region (AIR) of $p47^{phox}$ thus relieving its inhibition from the autoinhibitory loop and allowing $p47^{phox}$ to bind with $p22^{phox}$. The second event results in replacement of GDP residue with GTP by a guanine nucleotide exchange factor (GEF) resulting in conformational change of Rac protein by relieving inhibition from RhoGDP-dissociation inhibitor (RhoGDI) and promoting its binding with $p67^{phox}$ and finally resulting in the formation of active complex.

1.3.1.4 Role of calcium channels and redox sensitive Kv channels

According to the classical view of oxygen sensing, the calcium influx under acute hypoxia is mediated mainly by voltage-dependent calcium channels (such as L-type Ca^{2+} channels) which open in response to membrane depolarisation by hypoxia. However, recently it has been recognised that under acute hypoxia, apart from L-type Ca^{2+} channels, additional ion channels may also play a regulatory role in calcium influx. Non-selective cation channels have been identified as important players in the regulation of vascular tone by their role in mediating the entry of cations including Ca^{2+} and Na^{+} [51]. Amongst other non-selective cation channels, the family of classical transient receptor potential (TRPC) channels has been shown to be expressed in pulmonary arterial smooth muscle cells (PASMC) [52;53]. Moreover, TRPC6 has recently been shown to be essential in acute hypoxic pulmonary vasoconstriction in mice. Genetic deficiency of TRPC6 resulted in a complete loss of hypoxic pulmonary

vasoconstrictor response; however, the chronic hypoxic pulmonary vasoconstrictor response was unaltered in these mice [54]. In addition to calcium influx from the extracellular space, the release of calcium ions from intracellular stores such as the endoplasmic reticulum (ER) has been shown to play an important role in acute HPV [55]. Endoplasmic reticulum possesses calcium release channels termed as ryanodine receptors (RyRs) based on their ability to bind to the plant alkaloid ryanodine with high affinity. Hypoxia has been shown to increase the level of ADP ribosyl cyclase (cADPR), a metabolic product of β NAD^+ [56] (Fig.2). The cADPR is a well-known endogenous activator of ryanodine receptor Ca^{2+} release channels present in endoplasmic reticulum (ER) and can sensitise the release of Ca^{2+} from the ER store. Based on the role of cADPR in Ca^{2+} mobilisation from the intracellular ER stores, Wilson *et al.* suggested that cADPR acts as an oxygen sensor in the pulmonary artery [57]. Alternatively, Okabe *et al.* have suggested that the cADP-ribose system can also be regulated by interference with ROS, since low levels of superoxide stimulated calcium release via cADPR [58]. However, ROS mediated release of Ca^{2+} ions via cADP ribose system requires further investigation.

Potassium (K^+) is the most abundant intracellular cation in most excitable cells, including vascular smooth muscle cells and cardiac myocytes. The intracellular concentration of K^+ in such cells is around 150 mM compared to the extracellular concentration, which is 5 mM [59]. Due to the high concentration gradient, K^+ ions are passively carried out of the cell according to the electrochemical gradient. Due to the movement of K^+ ions across the insulated lipid bilayer, an electrical potential difference is created between the interior and exterior of the cell which is termed as membrane potential or *Vm*. Potential differences between two points that are separated by an insulator are larger than the differences between these points separated by a conductor. Thus, the lipid membrane, which is a good insulator, has a high electrical potential difference across the membrane which can vary between −40 and −60 mV for vascular smooth muscle cells. Due to this potential difference, the plasma membranes of most living cells exist in an electrically polarised state. The membrane potential of polarised cells is termed as resting membrane potential or *Em* [59]. The *Em* value for pulmonary vascular smooth muscle cells varies between -55 to -60 mV. The negative *Em* value of vascular smooth muscle cells literally implies that the interior of the resting cell is about 60 mV more negative than exterior [59].

It is generally agreed that the *Em* is largely determined by the ionic concentration gradients generated by K^+ channels rather than the ion pumps [59]. Thus *E*m is directly related to the level

of whole cell K^+ current or *I*K(V), which is determined by *I*K(V)= $N \times i \times Po$, where *N* is the number of Kv channels present in the membrane, *i* is the single-channel Kv current, and *P*o is the steady-state open probability of the Kv channel [60].

A decrease in K^+ currents through plasmalemmal K^+ channels, either by a decrease in *N* due to downregulation of the channel expression, or a decrease in *Po* due to the blockade of the channel conductance, causes membrane depolarisation (making *Em* more positive), whereas an increase in K^+ currents either by an increase in the *Po* or *N* causes membrane hyperpolarisation (making *Em* more negative) [60]. Any cellular changes which bring depolarisation in the PASMC makes the cell contract on the other hand the hyperpolarisation brings relaxation to PASMC. Due to the role of K^+ channels in regulating the vascular tone, McMutry *et al.* suggested that HPV might be induced by inhibition of K^+ channels [60].

Functionally, K^+ channels can be classified in to five groups: 1) voltage-gated K^+ (Kv) channels, 2) Ca^{2+}-activated K^+ channels, 3) ATP-sensitive K^+ channels, 4) inward rectifier K^+ channels, and 5) voltage-insensitive background K^+ channels. On the basis of the membrane topological structure K^+ channels can be classified as: 1) channels with one pore and six-transmembrane domains (For example, Kv channels and its subfamilies such as delayed rectifier K^+ channels (K_{DR}), A-type K^+ channels (K_A), outward rectifying, inward rectifying , slowly activating and Ca^{2+}-activated K^+ channels), 2) channels with one pore and two-transmembrane domains (For example, ATP-sensitive K^+ (K^+_{ATP}) and inward rectifier K^+ channels (Kir)), and 3) channels with two-pore and four-transmembrane domains (e.g., weakly inward rectifying K^+ channels (TWIK)) [60-62].

The family of K^+ channels with one pore and six-transmembrane domains (Kv channels and Ca^{2+}-activated K^+ channels) form the largest group of Potassium channel family and have also been suggested to show sensitivity to hypoxia leading to HPV [60;61]. However, the majority of reports indicate greater contribution by the Kv family in O_2 sensing in PASMC [60;61]. Functional Kv channels are either homomeric or heterotetramers consisting of pore forming α subunits or P-subunits and cytoplasmic or regulatory β subunits (Fig.6). The α subunit determines the selectivity of K^+ ions and is a conserved domain in all K^+ channels from bacteria to humans [62].

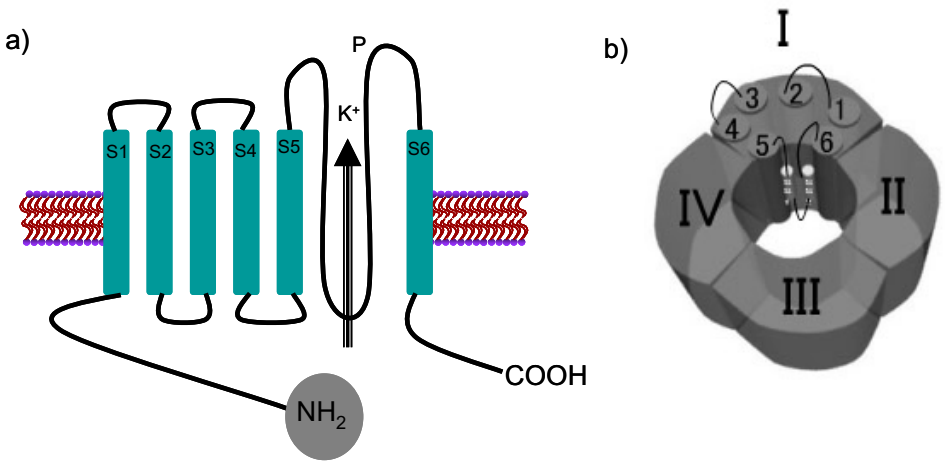

Figure 6. Schematic drawing of the α subunit of K+ channel. a) The α subunit forms the ionic pore in a tetrameric configuration. Each α subunit has six transmembrane domains. Both N and C terminal portions of α subunit are intracellular. A positively-charged amino terminal ball domain occludes the ionic pore of K^+ channels under hypoxic conditions resulting in their inactivation. Reactive oxygen species produced by NADPH oxidase can inactivate the channel by oxidising specific cysteine residues in the N-terminus which forms the disulfide bridges with the other cysteine residues in the channel thus occluding the pore by immobilising the balls. b) Cross section of the α subunit in tetrameric configuration.

There are only three regulatory β subunits identified to date (β 1-3). Heteromultimeric association of β subunits with α subunits increases the complexity of Kv channels. The α and β subunits associate in a 1:1 stoichiometry thus four subunits of α associate with four subunits of β creating $\alpha_4\beta_4$ heterotetramers. Homotetrameric gene products of Kv1.2, Kv2.1 and Kv3.1 and heterotetramers of Kv1.2/Kv1.5, Kv2.1/Kv9.3 and Kv4.2/Kv β 1.2 have been shown to be sensitive to hypoxia (Table 2) [60;62]. There are two types of K^+ channels which are abundant in pulmonary arterial smooth muscle cells: 1) The K_{DR} channels which open by membrane depolarisation and are preferentially inhibited by hypoxia and 4-AP and 2) the Ca^{2+}dependent K^+channel (KCa^{2+}) which opens with membrane depolarisation and intracellular Ca^{2+} and is specifically inhibited by charybdotoxin, iberiotoxin and tetraethylammonium (TEA) [63]. A list of various hypoxia sensitive Kv channels expressed in the pulmonary vasculature is given in Table 2. Proximal and distal segments of the pulmonary vasculature possess different electrophysiologically distinct SMC populations. Archer et al. have shown that the proximal portion of the pulmonary vasculature harbors a higher percentage of KCa^{2+} channels compared to the cells of the distal segment, which are enriched in K_{DR} channels [63]. Out of the 542 cells identified in the proximal segment, 15% were KCa^{2+}cells and 15% were K_{DR} expressing cells; however, in the distal segment 65% of a total of 342 cells were found to be K_{DR} expressing cells and only 3% were KCa^{2+} expressing cells [63]. Due to these electrophysiologically distinct smooth muscle cell populations, different portions of pulmonary vasculature exhibit different reactivity to hypoxia [63]. The inhibitor, 4-

Aminopyridine, which is a blocker of K_{DR} channels, causes membrane depolarisation and , increases $[Ca^{2+}]_{cyt}$ induces cell contraction in the distal portion of the pulmonary vasculature [64;65]. Acute hypoxia significantly reduced whole cell *I*K(V) currents and caused membrane depolarisation in PASMC but not in smooth muscle cells of systemic arteries [66]. Furthermore, HPV was impaired in Kv1.5 knockout mice and enhancing the expression of Kv1.5 channel via adenoviral gene transfer could restore HPV and the O_2 sensitive K^+ current in PASMC [67;68].

Table 2: List of various K_v α and β subunits expressed in pulmonary vasculature and channels which are potentially involved in oxygen sensing

Subfamily	***Channel subunit***	***mRNA expression***	***Protein expression***	***Sensitivity to hypoxia***
Delayed rectifier	Kv 1.1	Yes	Yes	
Delayed rectifier	Kv 1.2	Yes	Yes	Yes
Delayed rectifier	Kv 1.3	Yes	Yes	
Delayed rectifier	Kv 1.4	Yes	Yes	
Delayed rectifier	Kv 1.5	Yes	Yes	Yes
Delayed rectifier	Kv 1.6	Yes	Yes	
Delayed rectifier	Kv 1.7	Yes		
Delayed rectifier	Kv 2.1	Yes	Yes	Yes
Delayed rectifier	Kv 2.2	Yes	Yes	
Delayed rectifier	Kv 3.1	Yes	Yes	Yes
A-type	Kv 3.3	Yes		
A-type	Kv 3.4	Yes		
A-type	Kv 4.1	Yes		
A-type	Kv 4.2	Yes		
A-type	Kv 4.3	Yes		Yes
Modifier/silencer *	Kv 5.1	Yes		
Modifier/silencer	Kv 6.1	Yes		
Modifier/silencer	Kv 9.1	Yes		
Modifier/silencer	Kv 9.2	Yes		
Modifier/silencer	Kv 9.3	Yes		Yes
	Kv β 1.1	Yes		Yes
	Kv β 1.2	Yes		Yes
	Kv β 1.3	Yes		
	Kv β 2.1	Yes		
	Heteromeric α/α or α/β channel			
	Kv 1.2/ Kv 1.5			Yes
	Kv 2.1/ Kv 9.3			Yes
	Kv 4.2/ Kv β 1.2			Yes

Modified from: Jason X.-J. Yuan.(60)

** Modifiers/ silencers are unable to form functional channels but associate with the other α subunits to form conductive pores.*

1.3.2 Adaptation of pulmonary vasculature to chronic hypoxia: pathomechanisms

1.3.2.1 Structural changes in the pulmonary vasculature under chronic hypoxia

The pulmonary vasculature undergoes morphological changes in response to chronic hypoxia, although the severity of these changes depends on the species, genotype, sex and developmental stage. Some animal species such as pikas, yaks, snow pigs and llamas are resistant to hypoxia-induced pulmonary vascular remodeling, whereas neonatal calves are highly susceptible animals to chronic hypoxia [69;70]. The endothelium of the pulmonary vasculature undergoes minimal changes in response to chronic hypoxia in rats, however, an extreme elevation in the PAP is observed in neonatal calves in response to chronic hypoxia, where a more pronounced intimal thickening similar to humans was observed [8;70]. In addition to vascular remodeling, some reports have indicated a reduction in the cross-sectional area of the pulmonary vascular bed due to loss of small blood vessels during chronic hypoxia. This mechanism is also known as rarefaction or pruning [71;8].

The proximal portion of the pulmonary vasculature undergoes thickening of both media and adventitia in response to chronic hypoxia in large mammalian species such as cows, lambs, pigs and humans, however, in rodents adventitial thickening is more prominent compared to medial thickening [8]. The media of conduit pulmonary and systemic vessels in large mammalian species, including humans, is more complex compared to rodents and has a distinct smooth muscle–like (SM-like) subpopulation residing within the media [8;72;73]. This SM-like population exists in a relatively "undifferentiated state" in comparison to other smooth muscle cells within the vessel wall, and only these less-differentiated SM-like cells proliferate in response to hypoxic exposure [8].

The distal portion of the pulmonary vasculature is the site of HPV and it undergoes significant changes in response to chronic hypoxia in both rodents and large mammalian species. This portion of pulmonary vasculature also has a SM-like subpopulation of the cells which exhibit greater proliferative response to chronic hypoxia compared to similar cells from the proximal portion [8]. The most dramatic change that is observed in the distal portion of pulmonary vasculature is the muscularisation of partial and non-muscularised vessels. The distal muscularisation is believed to occur due to the presence of some specialised cells known as “pericytes” or “intermediate cells” which exhibit SM- like characteristics. These cells undergo proliferation and differentiation in response to chronic hypoxia and contribute to muscularisation of otherwise non muscularised vessels [8].

The mechanisms operating under chronic hypoxia induced vascular remodeling are not fully understood. Current reports have suggested that under chronic hypoxia there is a change in the endothelial and smooth muscle cell phenotype. A functional decreased production of NO from the endothelium has been reported under chronic hypoxia [19]. Furthermore, endothelial nitric oxide synthase 3 (NOS3) knockout mice have been shown to exhibit increased right ventricular pressure and vascular remodeling under chronic hypoxia [74;75].

Changes in smooth muscle cell phenotype includes hypertrophy, migration and excessive proliferation of PASMC [8]. These changes in the smooth muscle cell phenotype are thought to be caused by the increased production of growth factors by endothelial cells under chronic hypoxia such as platelet derived growth factor-beta (PDGF-beta), vascular endothelial growth factor (VEGF), basic fibroblast growth factor (bFGF), serotonin, endothelin-1 (ET-1) and a loss of prostacyclin. The PDGF-beta is a potent mitogen for PASMC and it has been recently shown that inhibition of the PDGF receptor using STI571 (imatinib) completely reverses hypoxia-induced pulmonary vascular remodeling in mice [76]. Similar to PDGF, ET-1 is a potent mitogen for PASMC and also behaves as a vasoconstrictor in isolated pulmonary arterial ring preparation and in isolated lung perfusion models. The use of BQ123 (an ET_A receptor blocker) and bosentan (mixed ET_A and ET_B receptor blocker) caused the partial reversal of increased pulmonary arterial pressure induced by hypoxia in new-born lambs and rats respectively [13]. The roles of bFGF, VEGF and serotonin have also been discussed widely in chronic hypoxia induced pulmonary hypertension models [8;77-82].

1.3.2.2 Role of calcium and Kv channels

The differences in the regulation of K^+ ion and Ca^{2+} ion homeostasis under acute and chronic hypoxia have been reported by several investigators [55;60;83;84]. Acute hypoxia-mediated inhibition of Kv channels in PASMC is quite evident from several reports, however under chronic hypoxia, this inhibition reflects a substantial down-regulation of Kv channels at both the mRNA and protein levels [60]. Smirnov *et al.* provided the first evidence of reduced function of Kv channels under chronic hypoxia [84;85]. Later, Wang *et al*. provided the first evidence of down-regulation of Kv1.1, Kv1.5, Kv2.1, Kv4.1 and Kv9.3 channels in cultured PASMC under chronic hypoxia, which has been confirmed by other groups [86;87]. The down-regulation of Kv channels in chronic hypoxia was also found to be specific to PASMC as smooth muscle cells from systemic arteries did not show any changes in Kv channel expression [86;87]. Multiple hypotheses have been suggested explaining the regulation of Kv channels under chronic hypoxia, including regulation by ROS produced by NADPH oxidases

and transcriptional regulation by transcription factors such as HIF-1 alpha, c-jun and NF-ATc [88]. It has recently been shown that overexpression of c-jun gene significantly decreased whole cell Kv currents and mRNA levels of Kv1.5 channels [89]. Decreased expression of Kv channels can modulate the proliferation of PASMC in two ways: 1) sustained inhibition of K^+ efflux via Kv channels in chronic hypoxia leads to influx of Ca^{2+} ions from both extracellular and intracellular stores. Recent reports have suggested that Ca^{2+} ions not only activate the contractile machinery of the cell but are also responsible for the transcription of genes which control progression of the cell through cell cycle and hence, control cell proliferation [55] and 2) inhibition of K^+ efflux leads to a high cytoplasmic concentration of K^+ ions which attenuate the activity of caspases and inhibits cytochrome *c* release thus making the cell more resistant to apoptosis (Fig. 7) [59;90].

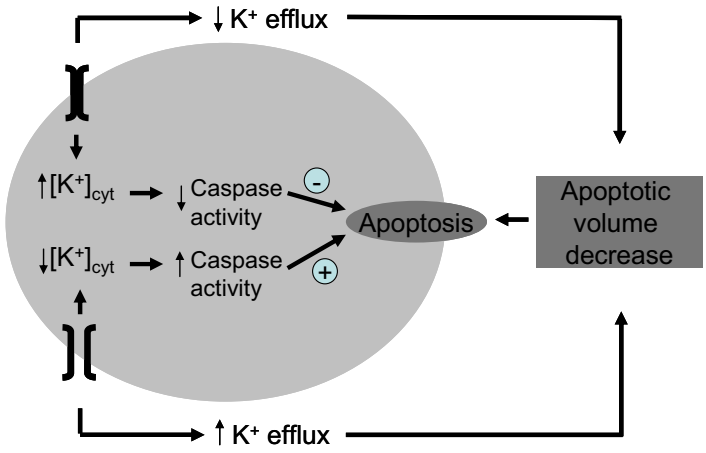

Figure 7. Intracellular $[K^+]_{cyt}$ concentration influences the apoptosis of the cell. High levels of intracellular $[K^+]_{cyt}$ leads to suppression of cytoplasmic caspase activity thus making the cell more resistant to apoptosis. Opening of K^+ channels on the other hand will accelerate the apoptosis by increasing K^+ efflux.
Modified from: Remillard C V et al. (59).

In addition to the changes in the regulation of K^+ ion homeostasis, substantial changes are observed in the regulation of calcium influx during chronic hypoxia. While under acute hypoxia calcium influx is due to opening of L-type voltage-gated Ca^{2+} channels by membrane depolarisation, under chronic hypoxia, the role of L-type Ca^{2+} channels is controversial [91]. According to Shimoda *et al.*, the membrane of PASMC already exists in depolarised stated under chronic hypoxic conditions due to highly reduced K^+ efflux. In accordance, further membrane depolarisation had no impact on the opening of L-type calcium channels [92]. However, there might be other pathways regulating L-type Ca^{2+} channels under chronic hypoxia which have not been implicated in vascular remodeling. Alternative mechanisms of calcium influx have recently been identified that are responsible for calcium influx under

chronic hypoxia, which include: 1) store-operated Ca^{2+} channels (SOC) activated by depletion of Ca^{2+} from intracellular stores and 2) receptor operated Ca^{2+} channels (ROC) which are activated by interaction of an agonist with membrane receptors [93].

1.3.2.3 Role of NADPH oxidase and mitochondria derived ROS

The role of ROS in altering smooth muscle cell phenotype by increasing hypertrophy and proliferation has been widely reported [94]. Increased ROS production leads to oxidative stress, which is an imbalance between oxidant production and the antioxidant capacity of the cell to prevent oxidative injury [94]. Recently Wu *et al.* have demonstrated that chronic hypoxia increases ROS production in cultured PASMC, however, decreases ROS production in the coronary arterial smooth muscle cells [95]. The possible sources of increased ROS production under chronic hypoxia may include NADPH oxidases and mitochondria. Chronic hypoxia induced up-regulation of ROS via NADPH oxidases is highly likely since NADPH oxidases have been shown to be activated by enodthelin-1 which is up-regulated under chronic hypoxia [96;97]. Moreover, NADPH oxidases are the major ROS-producing enzymes in the vascular system [94;98]. However, few reports exist which have addressed a role for NADPH oxidase-derived oxidative-stress in pulmonary hypertension. Liu *et al.* have recently demonstrated that chronic hypoxia-induced pulmonary hypertension was abolished in $gp91^{phox}$ knockout mice [99]. No investigations have been performed exploring the role NOX1 and NOX4 in chronic hypoxia induced vascular remodeling. Increased ROS production can modulate vascular remodeling process by enhancing the deposition of extracellular matrix proteins [94]. In addition, increased ROS production can activate matrix metalloproteinases (MMPs) such as MMP2 and MMP9, which can accelerate degradation of basement membrane and elastin in cultured human SMC [94]. Investigations related to the role of NADPH oxidases generated oxidative stress under chronic hypoxia in the pulmonary vaculature are hampered by the unavailability of specific and safe inhibitors for long term application under chronic hypoxia. Most of the studies have relied on the use of DPI and apocynin, which are non-specific inhibitors of NADPH oxidases. Diphenyl iodonium in general is an inhibitor of flavocytochromes and may inhibit nitric oxide synthase (NOS), and mitochondrial ETC [98]. However, the role of NADPH oxidases in cardiovascular diseases such as atherosclerosis, hypertension, myocardial infarction, ischemia-reperfusion injury has been widely discussed [41;98;100]. Moreover, the antioxidant therapy using N-acetyl cystine (NAC) has been shown to be effective in preventing the development of hypoxia induced pulmonary hypertension in chronically hypoxic rats [101]. There are scanty reports in the literature which have evidenced

the role of mitochondria derived ROS production in vascular remodeling under chronic hypoxia. Zungu et al. have recently shown that mitochondrial regulatory genes are up-regulated under chronic hypoxia in hypertrophied right heart ventricle leading to increased respiratory capacity and enhanced efficiency to sustain contractile function [102]. In addition, Bonnet *et al.* has shown that fawn hooded rats have abnormal mitochondria which contribute to the pathogenesis of pulmonary arterial hypertension by activation of hypoxia inducible transcription factors (HIF).

2 AIM OF THE STUDY

Against the background given in introduction, we investigated the regulation of NADPH oxidase homologs under chronic hypoxia by employing a mouse model of chronic hypoxia-induced pulmonary hypertension and studied the down-stream signaling pathway of NADPH oxidases to assess a possible role in hypoxia-induced vascular remodeling with special focus on PASMC. Thus this study aimed:

1) To assess whether NADPH oxidase homologs are regulated under chronic hypoxia in the murine lung.

2) To decipher the localisation of NADPH oxidase homologs and further screening of the up-regulated candidates at the mRNA and protein levels.

3) To assess the possible role of NADPH oxidases in the progression of hypoxia-induced pulmonary hypertension.

4) To study the functional aspects such as proliferation and ROS production in PASMC with regard to NADPH oxidases.

5) To elucidate the down-stream signaling pathway of candidate NADPH oxidases at a functional level (by electrophysiology) in isolated PASMC.

3 MATERIALS

3.1 Western blotting

Complete	Roche	Mannheim, Germany
Sodium vanadate	Sigma	Hamburg, Germany
PMSF	Sigma	Hamburg, Germany
Rotiphorese Gel 30 Acrylamide	Roth	Karlsruhe, Germany
TEMED	Sigma	Hamburg, Germany
Ammonium persulphate	Sigma	Hamburg, Germany
Tris-HCl	Roth	Karlsruhe, Germany
Methanol	Fluka Chemie	Buchs, Swiss
Milk powder	Roth	Karlsruhe, Germany
Tween-20	Sigma	Hamburg, Germany
Mini-PROTEAN vertical electrophoresis system	Bio-Rad	München,Germany
Blotting papers	Bio-Rad	München,Germany
Semi dry blotting machine	Keutz Labortechnik	Reiskirchen,Germany
PVDF membrane	Pall Corporation	Dreieich, Germany
Medical X-Ray film	Agfa	Mortsel, Belgium
X-Ray cassette (18 x 24)	Kisker biotech	Steinfurt, Germany
Medical X-Ray film processor (curix 60)	Agfa	Mortsel, Belgium
Restore plus western blot stripping buffer	Pierce	Bonn,Germany
Full range Rainbow ™ molecular weight marker	Bio-Rad	München,Germany
ECL plus western blot detecting system	Amersham	Freiburg, Germany

3.2 siRNA and proliferation assay

Xtreme transfection reagent	Roche	Mannheim, Germany
NOX4 siRNA (Human)	Eurogentec	Seraing, Belgium
NOX4 siRNA (Rat)	Biospring	Frankfurt, Germany
Scrambled siRNA-FITC	Invitrogen	Karlsruhe, Germany
H^3 thymidine	Amersham	Munich, Germany

3.3 Cell culture

Chamber slides (permanox) 8	Nunc	Wiesbaden,Germany

well		
48-well cell culture plates	Greiner bio-one	Frickenhausen,Germany
100 mm cell culture plates	Greiner bio-one	Frickenhausen,Germany
DMEM	Gibco	Karlsruhe, Germany
OPTI-MEM medium	Gibco	Karlsruhe, Germany
M199 SMC medium	Gibco	Karlsruhe, Germany
DPBS	PAN	Aidenbach,Germany
FCS		
Pipettes (10ml, 5ml)	BD Falcon	Heidelberg,Germany
Antibiotic solution (Penicillin+Streptomycin)	PAN	Aidenbach,Germany
Trypsin	PAN	Aidenbach,Germany

3.4 RNA extraction

Rneasy RNA extraction kit	Qiagen	Hilden, Germany

3.5 RT PCR

Random hexamers	Promega	Mannheim, Germany
RNAse inhibitor	Peqlab	Erlangen, Germany
Moloney murine leukemia virus reverse transcriptase	Invitrogen	Karlsruhe, Germany
5X RT buffer	Invitrogen	Karlsruhe, Germany
0.1 M dithiothreitol	Invitrogen	Karlsruhe, Germany
dNTP	Peqlab	Erlangen, Germany
Thermal Cycler	Biometra	Goettingen, Germany

3.6 Real time PCR

Platinum SYBR green qPCR superMix-UDG	Invitrogen	Karlsruhe, Germany
ROX	Invitrogen	Karlsruhe, Germany
MgCl2	Invitrogen	Karlsruhe, Germany
ABI prism 7700 detection system	Applied Biosystem	Weiterstadt, Germany

3.7 Riboprobes for in situ hybridization

Digoxigenin-11-uridine triphosphate	Roche	Mannheim, Germany
5X transcription buffer	Promega	Mannheim, Germany
RNAse inhibitor	Peqlab	Erlangen, Germany

T3 or T7 phage polymerase	Promega	Mannheim, Germany
Qiagen PCR purification kit	Qiagen	Hilden, Germany

3.8 Non isotopic *in situ* hybridization

Cryostat CM1850 UV	Leica Microsystems	Nussloch, Germany
TissueTek	Sakura	Heppenheim,Germany
Diethylpyrocarbonate	Sigma	Hamburg, Germany
Proteinase K	Qiagen	Hilden, Germany
Glycine	Roth	Karlsruhe, Germany
Paraformaldehyde	Roth	Karlsruhe, Germany
Triethanolamine		
Ethanol 70%, 80% and 90%	Fischer	Saarbrücken, Germany
Salmon sperm DNA	Sigma	Hamburg, Germany
Yeast tRNA	Sigma	Hamburg, Germany
EDTA	Roth	Karlsruhe, Germany
Tris.HCl	Roth	Karlsruhe, Germany
Di-Natriumhydrogenphosphat Dihydrat	Merck	Darmstadt, Germany
Kaliumdihydrogenphosphat	Merck	Darmstadt, Germany
NaCl	Roth	Karlsruhe, Germany
Dextran sulphate		
Blocking reagent	Roche	Mannheim, Germany
BSA	Sigma	Hamburg, Germany
Triton X-100		
Alexa fluor 488 tyramide	Molecular Probes, Invitrogen	Karlsruhe, Germany
Hoechst-33258	Invitrogen	Karlsruhe, Germany
Digital Cameral Fluorescence Microscope DSML	Leica Microsystems	Nussloch, Germany

3.9 Histology

Automated microtom RM 2165	Leica Microsystems	Nussloch, Germany
Flattening table HI 1220	Leica Microsystems	Nussloch, Germany
Flattening bath for paraffin sections HI 1210	Leica Microsystems	Nussloch, Germany
Tissue embedding machine EG 1140H	Leica Microsystems	Nussloch, Germany
Cooling plate EG 1150C	Leica Microsystems	Nussloch, Germany
Tissue processing automated machine TP 1050	Leica Microsystems	Nussloch, Germany
Stereo light microscope	Leica Microsystems	Nussloch, Germany

DMLA		
Digital camera microscope DC 300F	Leica Microsystems	Nussloch, Germany
Ethanol (70%, 95%, 99,6%)	Fischer	Saarbrücken, Germany
Isopropanol (99,8%)	Fluka Chemie	Buchs, Swiss
Methanol	Fluka Chemie	Buchs, Swiss
Formaldehyd alcohol free ≥37%	Roth	Karlsruhe, Germany
Roti-Histol (Xylolersatz)	Roth	Karlsruhe, Germany
Xylol	Roth	Karlsruhe, Germany
Hydrogen peroxide 30%	Merck	Darmstadt, Germany
Cover slips 24x36mm	Menzel	Germany
Paraffin embedding medium Paraplast Plus	Sigma Aldrich	Steinheim, Germany
Mounting medium perte	Medite GmbH	Burgdorf, Germany
Trypsin	Zytomed	Berlin, Germany
Avidin-Biotin-blocking kit	Vector/ Linaris	Wertheim-Bettingen, Germany
Normal goat serum	Alexis Biochemicals	Grünberg, Germany
Normal Rabbit Serum	Alexis Biochemicals	Grünberg, Germany
Vectastain Elite ABC kit (anti rabbit)	Vector/ Linaris	Wertheim-Bettingen, Germany
Vector VIP substrat kit	Vector/ Linaris	Wertheim-Bettingen, Germany
Methylgreen counterstain	Vector/ Linaris	Wertheim-Bettingen, Germany

3.10 SMCs isolation from precapillary pulmonary arteries (rat and mouse)

Surgical instruments	Martin Medizintechnik	Tuttlingen, Germany
Surgical threads, non-absorbable, Size 5-0	Ethibond Excel	Norderstedt, Germany
Napkins	Tork	Mannheim, Germany
Medical adhesive bands 3M	Durapore®	St. Paul, MN, USA
Low melting agarose	Sigma	Hamburg, Germany
Fe3O4 Iron particles	Sigma	Hamburg, Germany
M199 SMCs growth medium	Gibco	Karlsruhe, Germany
Collagenase type IV	Sigma	Hamburg, Germany
Narcorin	Merial GmbH	Hallbergmoos, Germany
Physiological saline solution	DeltaSelect GmbH	Dreieich, Germany
Heparin	Rathiopharm GmbH	Ulm, Germany
Plastic Syringe (10ml & 20ml)	Braun	Melsungen,Germany
Needle (20G, 1 1/2",0,9x40mm)	BD Microlance	Becton Dickinson, Germany
Neelde (18G,1	Unolok	Horsham,U.K

1/2",1,20x38mm)		
DPBS	PAN	Aidenbach,Germany
Catheter (for trachea & pulmonary artery)	Made manually from BD Microlance 3 15 or 20G shortened to 1,5cm	Becton Dickinson, Germany
Antibiotic solution	PAN	Aidenbach,Germany

3.11 EMSA and nuclear isolation

LightShift chemiluminescent EMSA kit	Pierce	Bonn,Germany
Biotinylated oligonucleotides	Metabion	Martinsried, Germany
Hybond-N^+ nylon membrane	Amersham	UK
HEPES	Sigma	Hamburg, Germany
KCl	Sigma	Hamburg, Germany
EDTA,	Sigma	Hamburg, Germany
EGTA,	Sigma	Hamburg, Germany
Nonidet P-40,	Sigma	Hamburg, Germany
Glycerol	Sigma	Hamburg, Germany

3.12 Electrophysiology

Flaming/Brown micropipette puller	Sutter Instrument	Novato, CA, USA
Filamented borosilicate capillary glass,1.2 mm OD, 0.69 mm ID	World Precision Instruments	Sarasoda, FL, USA
Axopatch 200A amplifier	Axon Instruments	Foster City, CA, USA
pClamp6 software	Axon Instruments	Foster City, CA, USA

3.13 Antibodies

Anti rabbit-HRP labeled	Promega	Mannheim, Germany
Anti mouse HRP labeled	Promega	Mannheim, Germany
Cy3 labelled α SM-Actin	Sigma	Hamburg, Germany
Kv1.5 and Kv2.1	Sigma	Hamburg, Germany
HIF-1α and HIF-2α	Novus Biologicals	Hiddenhausen Germany
HIF-3 α	Abcam	Cambridge, UK
Cy3-conjugated anti-goat antibody	Dako	Denmark

3.14 General Consumables

Single use syringes Inject Luer®, 1ml, 2ml, 5ml, 10ml	Braun	Melsungen, Germany
Single use gloves Transaflex®	Ansell, Surbiton	Surrey, UK
Napkins	Tork	Mannheim, Germany
Pipette filter tips, blue and yellow	Eppendorf	Hamburg, Germany

4 METHODS

4.1 Animals

Adult male Sprague-Dawley rats (200-250 grams body weight) and mice (C57BL/6N) of either sex weighing 20-22 g were obtained from Charles River Laboratories (Sulzfeld, Germany). Animals were housed under controlled temperature (≈22 °C) and lighting (12/12-hour light/dark cycle), with free access to food and water. All experiments were performed according to the institutional guidelines that comply with national and international regulations. The experiments were approved by the local ethic commission.

4.2 Hypoxia induced pulmonary hypertension in mice

Pulmonary hypertension was induced in mice by exposure to hypoxia (10 % O_2) in a normobaric chamber for 3, 7 and 21 days. The level of hypoxia was held constant by an autoregulatory control unit (O_2 controller model 4010; Labotect, Göttingen, Germany) supplying either nitrogen or oxygen. Excessive humidity in the re-circulating system was prevented by condensation in a cooling system. Carbon dioxide was continuously removed by soda lime. Cages were opened once per day for cleaning, as well as food and water supply. Control mice were exposed to normoxia (21 % O_2) under identical conditions for 21 days.

4.3 Isolation of mouse organs

After 3, 7 and 21 days of hypoxia, the animals were euthanized by intraperitoneal injection of a lethal ketamine and xylazine dose, and the lungs were flushed through a catheter in the pulmonary artery with Krebs Henseleit buffer (125.0 mM NaCl, 4.3 mM KCl, 1.1 mM KH_2PO_4, 2.4 mM $CaCl_2$, 1.3 mM $MgCl_2$ and 13.32 mM glucose) at a pressure of 20 cm H_2O at room temperature. The buffer was pre-equilibrated with a gas mixture of 3%O_2, 5.3%CO_2, balanced N_2. $NaHCO_3$ was adjusted to result in a pH of 7.4. During perfusion of the lungs, the buffer was allowed to drain freely from a catheter in the left ventricle. Once the effluent was clear of blood, lungs were dissected from the thoracic cavity and immediately frozen in liquid nitrogen for mRNA analysis.

For immunohistochemistry, *in situ* hybridization and laser assisted microdissection, 800 µl pre-warmed TissueTek® (Sakura Finetek, Zoeterwoude, Netherlands) was instilled into the airways via a tracheal cannula. After ligation of the trachea, the lungs were excised and immediately snap frozen in melting isopentane. Preparation of the hypoxic animals was

performed continuously in a hypoxic environment (10% O_2). Lungs from normoxic animals (control) were prepared accordingly under normoxic conditions.
The right ventricular wall (RV) was separated from the left ventricle plus septum (LV+S) to calculate the ratio of RV/(LV+S) of the dehydrated heart tissue. For analysis of colon, heart, and pulmonary arteries, these tissues and organs were removed immediately after the lungs have been flushed.

4.4 Laser-assisted microdissection

Laser-microdissection was performed as described previously[103-106]. In brief, 10 µm thick cryosections of TissueTek® embedded mouse lungs were mounted on glass slides. After hemalaun staining for 30 s, sections were subsequently immersed in 70% (v/v) and 96% (v/v) ethanol and stored in 100% (v/v) ethanol until use. Not more than 10 sections were prepared at the same time to restrict storage time. Intrapulmonary vessels (~100 µm diameter) were microdissected under visual control using the Laser Microbeam System (P.A.L.M., Bernried, Germany) and isolated by a sterile 30 G needle. Needles with adherent material were transferred into a reaction tube containing the lysis buffer RLT (Qiagen, Hilden, Germany) with β-mercaptoethanol.

4.5 Isolation of RNA and cDNA synthesis

The RNA was extracted from cells using spin-columns (RNeasy, Qiagen, Germany). For reverse transcription (RT) of extracted RNA, 1 µg of total RNA in a total volume of 10µl was mixed with 1µl of dNTP and 1µl of random hexamers (Promega, Mannheim, Germany) and denatured at 75 °C for 3 min. After cooling on ice, the following components were added to the samples: 4 µl of 5× RT buffer, 2 µl of 0.1 M dithiothreitol, 1µl of RNAse inhibitor (Peqlab, Erlangen, Germany) and 1 µl Moloney murine leukemia virus reverse transcriptase (MMLV) (Invitrogen, Karlsruhe, Germany) and then incubated at 25°C for 10 min and 37°C for 1h.

4.6 Real-time PCR

Relative quantification of NOX4 was done using ABI prism 7700 detection system (Applied Biosystem, Weiterstadt, Germany). All of the primers used in the real time PCR experiments were intron-spanning. The reaction mixture (25 µl) consists of 2 µl of cDNA (equivalent to 20-30 ng of RNA), 12.5 µl of Platinum SYBR Green qPCR SuperMix-UDG (Invitrogen,

Karlsruhe, Germany), 0.5 µl of ROX, 0.2 µM each of forward and reverse primers, 2 mM $MgCl_2$ and 8 µl of autoclaved water. The Ct values of NOX4 were normalized to the endogenous control B2M (β_2-microglobulin) in both mouse and human samples [107]. The PCR cycling conditions were as follows: 50 °C for 2 min, 95 °C for 6 min, 95 °C for 5 s, 59 °C for 5 s, 72 °C for 10 s. Specificity of the products was verified by dissociation curves and by analysis on an ethidium bromide-stained agarose gel. The fold change $2^{\Delta\Delta Ct}$ was calculated as described previously [105]. The sequences of primers used in real time PCR experiment are given in Table 3.

4.7 Synthesis of riboprobes for in situ hybridization

Single-stranded digoxigenin (DIG)-labeled riboprobes for non-isotopic *in situ* hybridization were generated by the *in vitro* transcription method. The template for the generation of single-stranded RNA probes was amplified by nested PCR. Briefly, 1 µg of the purified PCR-amplified template harboring T3 and T7 RNA polymerase promoter sequences was mixed with 2 µl digoxigenin-11-uridine triphosphate (Roche, Mannheim, Germany), 4 µl of 5× transcription buffer (Promega, Mannheim,Germany), 1 µl of RNasin (Peqlab, Erlangen, Germany) and 2 µl of T3 or T7 Phage polymerase (Promega, Mannheim, Germany) in a total reaction volume of 20 µl. The reaction mixture was incubated at 37 °C for 2 h. The RNA probes were purified with a Qiagen PCR purification kit (Qiagen, Hilden, Germany).

4.8 Non isotopic in situ hybridization on mouse lung sections

The non-isotopic *in situ* hybridization (NISH) was performed on 8 µm thick TissueTek®-embedded mouse lung cryostat sections. The sections were heated at 55 °C for 15 min followed by transferring the sections in to 2× SSC buffer for 30 min at 70 °C, diethylpyrocarbonate-treated water for 1 min, Proteinase K (5 µg/ml) for 10 min at room temperature, 0.2% (m/v) glycine in PBS solution (for the inactivation of Proteinase K) for 30 s, PBS for 30 s, freshly prepared cold 4% (m/v) paraformaldehyde for 20 min, PBS for 5 min, 0.1 M acetylated triethanolamine (0.5 ml of acetic anhydride/200 ml of triethanolamine) on a shaking platform for 10 min, PBS for 3 min, followed by dehydration of slides by passing through 70% (v/v), 80% (v/v) and 90% (v/v) ethanol (each for 2 min). The slides were then pre-hybridized with 2× Prehyb solution (1 M NaCl, 0.02 M Tris (pH 7.5), 2× Denhardt's reagent, 2 mM EDTA, 10 mg/ml salmon sperm DNA, 0.2 mg/ml yeast tRNA) at 55 ° C for 2-3 h in a humidified chamber, followed by hybridization with a denatured antisense NOX4 probe in 2× hybridization solution (1 M NaCl, 0.02 M Tris (pH7.5), 2×

Denhardt's reagent, 2 mM EDTA, 2 g dextran sulphate, 0.2 mg/ml yeast tRNA) at 55 °C for overnight. The following day, slides were washed from low to very highly stringent conditions as follows: on shaking platform 2× SSC for 1 h at room temperature, 0.1× SSC at 60 °C and finally to pre-heated 0.1x SSC (at 60 °C), followed by incubation at room temperature. The sections were treated with blocking buffer (2% Blocking reagent (Roche, Mannheim, Germany), 0.1% (m/v) BSA, 0.1 M Tris (pH 7.5), 5 M NaCl) for 30 min at room temperature, followed by incubation with a peroxidase-labeled anti-DIG antibody (Roche, Mannheim, Germany) in 1:20 dilution for 2 h at room temperature. After antibody incubation, sections were washed in TBT buffer (50 mM, 1 M Tris-HCl (pH 7.5), 150 mM NaCl and 0.1% Triton X-100; 3 × 15 min). The fluorescent substrate Alexa fluor 488 tyramide (Molecular Probes, Invitrogen, Karlsruhe, Germany) at a dilution of 1:60 in amplification buffer was applied to the sections for 2 h. Subsequently, sections were washed (3 × 20 min) in PBT buffer (PBS, 0.1% (v/v) Tween 20) and incubated with a mouse monoclonal Cy3-labeled α-smooth muscle actin antibody (Sigma, Hamburg, Germany) at 1:500 in PBS, for 1 h. The sections were washed (3 × 3 min) in PBS and subsequently incubated with Hoechst-33258 (1:10.000 in PBS; Invitrogen, Karlsruhe, Germany) for 10 min, washed and mounted in carbonate-buffered glycerol (pH-8.6).

4.9 Immunofluorescence on mouse lung sections

Cryosections (10 μm) were fixed in ice-cold acetone for 10 min and unspecific binding of primary antibodies was blocked by incubation with 50% (v/v) heat-inactivated normal swine serum in phosphate buffered saline (9.1 mM dibasic sodium phosphate, 1.7 mM monobasic sodium phosphate and 150 mM NaCl, pH 7.4 (PBS)) with double the salt concentration (PBS+S) for 1 h. Incubation was performed overnight with an affinity-purified rabbit polyclonal anti-NOX4 antibody diluted 1:200, together with a mouse monoclonal FITC-conjugated α-smooth muscle actin antibody (clone 1A4, 1:500; Sigma, Deisenhofen, Germany) in PBS+S [108]. After washing in PBS, the sections were incubated with a Cy3-conjugated donkey anti-rabbit antibody (Chemicon, Hofheim, Germany) diluted 1:2000 in PBS+S for 1 h, and after a final wash step, the sections were mounted with carbonate-buffered glycerol, pH 8.6. To test specificity, the NOX4 antibody was pre-incubated for 1 h with the corresponding peptide antigen (20 μg/ml). All labeling reported here was specific as judged from its absence in sections incubated with pre-adsorbed antibody. Immunoreactivity was evaluated using an Axioplan 2 imaging epifluorescence microscope (Zeiss, Göttingen, Germany) equipped with a Axiocam digital camera, Axiovision software (Zeiss, Göttingen,

Germany), and with appropriate filter sets for Cy3 and FITC or with a TCS-SP2 AOBS confocal laser scanning microscope (Leica, Heidelberg, Germany).

4.10 Quantitative analysis of mouse lung sections

Examination of sections was performed blinded. For every animal, 50 α-smooth muscle actin-immunoreactive vessels were evaluated for anti-NOX4-immunoreactive cells in the vessel wall, and the vessel diameter was measured using the Axiovision software. To restrict analysis to smaller blood vessels, vessels with a diameter larger than 60 µm were not examined.

4.11 Immunohistochemistry on human lung sections

Lung tissue samples from healthy individuals and from patients with IPAH were formalin-fixed, paraffin-embedded and cut into 3 µm sections. After deparaffinization, rehydration and blocking of endogenous peroxidase, proteolytic antigen retrieval was performed (Digest All 2, Zytomed, Berlin, Germany). After incubation with normal goat serum for 1 h, the tissue sections were incubated overnight at 4 °C with primary custom-made rabbit anti-human NOX4 polyclonal antibody. Signal amplification was achieved with a biotinylated goat anti-rabbit IgG secondary antibody employing the avidin-biotin-horseradish peroxidase method (Vectastain Elite ABC Kit, Vector/ Linaris, Wertheim-Bettingen, Germany). The purple chromogen Vector VIP was used to visualize immune complexes, and nuclear counterstaining was performed with methyl green (both from Vector/ Linaris, Wertheim-Bettingen, Germany).

4.12 Western blotting

Protein extracts for western blotting from human lung were prepared in RIPA buffer (containing 1 mM sodium vanadate, Protease-Inhibitor Mix complete (Roche, Mannheim, Germany) and 0.1 mM PMSF). The permission to use human tissue was obtained from local ethic commission. The proteins were denatured in the presence of β-mercaptoethanol and 1X LDS sample buffer (Nu PAGE, Invitrogen, Karlsruhe, Germany) at 100°C for 10 min. For NOX4 immunoblot equivalent amounts of protein were resolved on 10% SDS polyacrylamide gels at 100V, 400 mAmp, and 150W for 90 min. Proteins were transferred to polyvinylidene fluoride (PVDF) membranes (Pall Corporation, Dreieich, Germany) by semi-dry electro-blotting at 100V, 115 mAmp, and 150W for 75 min. Nonspecific antibody binding was blocked by incubation in 6% (m/v) non-fat dry milk powder in T-TBS (20 mM Tris-Cl, pH

7.5, 150 mM NaCl, 0.1% (v/v) Tween 20) at room temperature for 1 h. Incubation with a 1:5000 diluted custom made rabbit polyclonal anti-NOX4 primary antibody was performed at 4 °C overnight [109].After washing the membranes in T-TBS buffer, specific immunoreactive signals were detected by enhanced chemiluminescence (ECL, Amersham, Freiburg, Germany) using a secondary antibody coupled to horseradish-peroxidase.

4.13 Human, rat and mouse cell culture

Smooth muscle cells from human, rat and murine pulmonary arteries were isolated and cultured as described previously[110;111]. For the investigation of the effect of hypoxia on NOX4 mRNA levels, cells were either exposed to 1% O_2 (hypoxia) or to 21% O_2 (normoxia).

4.14 Immunocytochemistry of murine pulmonary arterial smooth muscle cells

Isolated PASMC were cultured on chamber slides, treated as indicated, fixed in acetone and methanol (1:1), and blocked with 3% (m/v) BSA in PBS for 1 h, followed by overnight incubation with an anti-NOX4 antibody (1:25) diluted in 3% (m/v) BSA in PBS. Indirect immunofluorescence was obtained by incubation with a Cy3-conjugated anti-goat antibody (Dako, Denmark) diluted 1:100 in PBS, for 90 min. Nuclear counterstaining was performed with Hoechst-33258 (1:10.000 dilution in PBS) (Invitrogen, Karlsruhe, Germany) for 10 min.

4.15 RNA interference and proliferation assay for human PASMC

Human pulmonary arterial smooth muscle cells (10,000 cells per well) from passage five were cultured in 48-well tissue culture plates, and used for the RNA interference and proliferation assays. Transfection of NOX4 siRNA was performed in low-serum and antibiotic-free medium (1% (v/v) FCS in DMEM). The medium was changed at least 4 h before transfection. Approximately 100 nM of NOX4 siRNA (Eurogentec, Seraing, Belgium) was transfected using 1 µl X-tremeGENE siRNA Transfection Reagent (Roche, Mannheim, Germany) per cm^2 of the well. Both siRNA and transfection reagent were diluted in OPTI-MEM medium (Gibco, Karlsruhe, Germany). For controls, a FITC-labelled, scrambled siRNA (Invitrogen, Karlsruhe, Germany) was employed. After five hours of transfection, the medium was changed to low-serum medium containing antibiotics (1% (v/v) FCS, 1% (m/v) penicillin and streptomycin in DMEM and incubated overnight for cellular synchronisation. The following day, the cells were stimulated with smooth muscle cell medium (Promocell, Heidelberg, Germany) supplemented with medium containing 5% (v/v) FCS and 1% (m/v) penicillin and streptomycin for 20 h, followed by ^{3}H-thymidine (Amersham, Munich, Germany) addition for

4 h. Subsequently, cells were washed 3× with ice-cold PBS and lysed with NaOH on a shaker for 4 h. The radioactivity in the lysate was measured by liquid scintillation counting (Rotiszint® eco plus, Roth, Germany) with a Packard liquid scintillation counter.

4.16 ROS measurement and quantification

ROS in human PASMC were measured using superoxide sensitive dye DHE (Dihydroethidium, Invitrogen). The cells were grown on chamber slides at the density of 10.000 /cm^2, transfected with scrambled and NOX4 siRNA and incubated in normoxic and hypoxic chambers for 24 h. After 24 h the cells were incubated with 5 µM of DHE for 15 min in normoxic and hypoxic chamber. Subsequently the cells were washed in PBS, fixed in acetone and methanol mixture (1:1) for 10 min and stained with nuclear stain Hoechst-33258. The cells were visualized under a fluorescent microscope (excitation: 514 nm; emission: 560 nm). A total of eight images was captured from each group in a blinded fashion and were quantified using Image J software (U.S. National Institutes of Health, Bethesda, MD).

ROS measurement in isolated rat PASMC (passage two or three) was done using oxidation sensitive dye Dichloroflourescein diacetate (DCF-DA). The cells were grown on 6 well plates. The treatment of rat PASMC with NOX4 siRNA was done as described in previous section. At the conclusion of treatment, the cells were incubated with 10µM DCF-DA dissolved in HEPES-Ringer buffer (HRB (in mM): 136.4 NaCl, 5.6 KCl, 1 $MgCl_2$, 2.2 $CaCl_2$, 10 HEPES, 5 glucose, 0.1% BSA, pH 7.4) in the dark for 5 min at room temperature. The cells were subsequently washed twice and fluorescence was measured with Infinite 200 microplate reader (TECAN, Crailsheim, Germany) at excitation/emission wavelength of 502/530 respectively. The flourescence values were collected from 12 different areas of well. The cells were stimulated with 20 nM of ET-1 and recordings were made immediately (0 min), 5 min and after 10 min of ET-1 stimulation.

4.17 Immunofluorescence on rat lung sections

Immunofluorescence was performed on 8 µm thick cryosections from the rat lung. The cryosections were dried at room temperature for 1 h, then fixed in acetone/methanol mixutre (1:1) for 10 min, dried at room temp for 1 h and subsequently blocked by 3% BSA in PBS for 1 h at room temperature.After completion of the blocking step, the sections were incubated with the directly labelled primary antibodies overnight at 4°C. Subsequently the sections were

washed 2-3 times in PBS and refixed in 4% PFA in PBS for 15 min at room temperature, washed with PBS and mounted using DAKO (DAKO, Denmark) fluorescent medium. All fluorescent slides were stored at 4°C.

The direct labelling of primary NOX4 (custom made), Kv2.1 (Sigma, Hamburg, Germany) and Kv1.5 (Sigma, Hamburg, Germany) antibodies was done using rabbit IgG tricolor labelling kit (Invitrogen, Karlsruhe, Germany) according to manufacturers instructions. The labeled reaction mix was diluted up to 100µl with 3% BSA in PBS.

4.18 Hypoxic exposure, siRNA and apocynin treatment of rat PASMC

Rat PASMC were exposed to hypoxia (1% O_2, 5% CO_2) in 1% (v/v) FCS and 1% (m/v) penicillin and streptomycin M199 medium for indicated period of time. Rat PASMC were transfected with two different sequences of siNOX4. Approximately 100 nM of Cy3 labeled NOX4 siRNA (Biospring-Frankfurt, Germany) was transfected using X-tremeGENE siRNA transfection reagent (1:200 dilution) (Roche, Mannheim, Germany). Following NOX4 siRNA sequences were used: siNOX4 seq-1: GGUGUCUGCAUGGUGGUGGUAUU, siNOX4 seq-2: CGAGAGACUUUACCGAUGCAUCAUGAUGC. Both siRNA and transfection reagent were diluted in OPTI-MEM medium (Gibco, Karlsruhe, Germany). For controls, a similar Cy3 labeled, scrambled siRNA (Biospring-Frankfurt, Germany) was employed. After five hours of transfection, the medium was changed to low-serum medium containing antibiotics (1% (v/v) FCS, 1% (m/v) penicillin and streptomycin) in M199 and were left under normoxic conditions for 3-days to bring down the level of NOX4 protein. After this 3-day incubation period, the hypoxic group of the cells was transferred to hypoxic conditions (1% O_2, 5% CO_2) for the indicated period of time whereas normoxic group of the cells stayed under normoxia (21% O_2, 5% CO_2).

For apocynin experiment, the rat PASMC were treated with the indicated concentration of apocynin dissolved in 1% (v/v) FCS and 1% (m/v) penicillin and streptomycin M199 medium and then were transferred under normoxic and hypoxic incubator (1% O_2) for three days. The control group of cells was treated with DMSO (di-methyl sulfoxide) solvent control in the similar manner.

4.19 Electrophysiology

Electrodes for whole cell recording were pulled on a Flaming/Brown micropipette puller (Model P-87, Sutter Instrument, Novato, CA, USA) from filamented borosilicate capillary glass (1.2 mm OD, 0.69 mm ID, World Precision Instruments, Sarasoda, FL, USA). The

electrodes were fire-polished, and resistances were 2–5 MΩ for voltage-clamp experiments using above-mentioned solutions. Membrane potentials (V_m) were recorded in the current-clamp mode at the moment of establishment of a whole cell configuration. Input resistance (R_m) was calculated at –70 mV as 1/slope of the current trace evoked by a ramp voltage from –160 to 100 mV in the voltage-clamp mode. Membrane potential and membrane currents were recorded with an Axopatch 200A amplifier (Axon Instruments, Foster City, CA). Signals were obtained at sampling rates of 5 kHz, filtered at 2 kHz and stored on the hard disk of a personal computer. Stimulus generation and data acquisition were controlled with the ClampEx program in the pClamp6 software package (Axon Instruments). Before seals were made on cells, liquid junction potentials were nulled for each individual cell with the Axopatch 1C amplifier. The series resistances were primarily under 10 MΩ. Current traces in voltage clamp were leak-subtracted.

The bath or extracellular solution used for the voltage-clamp experiments contained (in mM) 130 NaCl, 3 KCl, 1 $CaCl_2$, 1 MgCl2, 10 HEPES, and 10 glucose and pH was adjusted to 7.4 with NaOH. The pipette solution contained (in mM) 138 KCl, 0.2 $CaCl_2$, 1 $MgCl_2$, 10 HEPES (Na^+ salt), and 10 EGTA and pH was adjusted to 7.4 with Tris. Osmolarity of all solutions was adjusted to 290 mOsm. All recordings were performed at room temperature (22–24°C). The rat PASMC in passage one or two were transfected with NOX4 siRNA and were exposed to normoxic or hypoxic conditions as described in previous sections. At the conclusion of the treatment, the cells were trypsnized, re-suspended in extracellular solution and were kept in the incubator at 37°C for 1-2 h to adhere at the bottom. The cells that were exposed to hypoxia were kept in the hypoxic incubator during this period. The cells at this stage look flat and round with a prominent nucleus and still do not gain their normal morphology. For dissecting out the current specific to Kv1.5 and Kv2.1 channels, the antibodies against both channels were dissolved in the pipette solution at the dilution of 1:100. The control experiments were done without any antibody in the pipette solution. The current specific to K_{DR} channels was analysed using custom made software (designed by Dr. Xiang Q Gu at the University of California San Diego (UCSD)) which averaged 21 data points shortly before the termination of voltage commands.

4.20 Calcium measurement

Calcium measurement was done on isolated rat PASMC. PASMC on coverslips were loaded with fura-2 acetoxymethyl ester (5 μM) in Hepes-Ringer buffer (HRB; 136.4mM NaCl/5.6 mM KCl/1 mM $MgCl_2$/2.2 mM $CaCl_2$/10 mM Hepes/5 mM glucose/0.1% BSA, pH 7.4) at

37°C for at least 60 min. Coverslips were then placed on the inverted microscope in an open heating chamber maintained at 36 ^{o}C. PASMC were stimulated with 20nM entohtelin-1 directly in the medium. Cells were analysed using a Polychrome II monochromator and an IMAGO CCD camera (Till Photonics, Martinsried, Germany) coupled to an inverted microscope (IX70; Olympus, Hamburg, Germany) at 340 and 380 nm for measuring [Ca^{2+}]i.

4.21 Statistics

Values are given as mean ± SEM (Standard Error of the Mean) if not indicated differently. Statistical significance of the data in the western blotting, electrophysiology, ROS measurement and proliferation assay was calculated by two tailed student's t-test. Comparison of the groups in the real time PCR experiments was done by one way ANOVA using LSD test. For NOX4 quantification in mouse lung sections, two conditions were evaluated: 1) is the number of NOX4 immunoreactive vessels different between the groups and 2) is the mean diameter of NOX4 immunoreactive vessels different between the groups. Statistical analysis was performed by a non-parametric variance analysis (Kruskal-Wallis-test). If p in this test was < 0.05, a comparison of the groups amongst each other was done using a Mann-Whitney-test, where $p < 0.05$ was regarded as significant. Comparison of groups was stopped after $p > 0.05$ to prevent α-inflation. A p-value of less then 0.05 was considered significant in all experiments.

Table 3: Nucleotide sequences of primers used for quantitative real time PCR

Organism	*Primer*	*Orientation*	*Sequence*	*Accession Number*
Mice	NOX1	Sense	5′-TGGCTAAATCCCATCCAGTC-3′	NM_172203
		Antisense	5′-CCCAAGCTCTCCTCTGTTTG-3′	
	NOX2	Sense	5′-TCGCTGGAAACCCTCCTATG-3′	NM_007807
		Antisense	5′-GGATACCTTGGGGCACTTGA-3′	
	NOX4	Sense	5′-ACTTTTCATTGGGCGTCCTC-3′	NM_015760
		Antisense	5′-AGAACTGGGTCCACAGCAGA-3′	
	$p22^{phox}$	Sense	5′-CAGATCGAGTGGGCCATGT-3′	NM_007806
		Antisense	5′-AGCACACCTGCAGCGATAGA-3′	
	$p47^{phox}$	Sense	5′-GTCCCTGCATCCTATCTGGA-3′	NM_010876
		Antisense	5′-TATCTCCTCCCCAGCCTTCT-3′	
	$p67^{phox}$	Sense	5′-CAGACCCAAAACCCCAGAAA-3′	NM_010877
		Antisense	5′-AGGGTGAATCCGAAGCTCAA-3′	
	$p40^{phox}$	Sense	5′-TTTGAGCAGCTTCCAGACGA-3′	NM_008677
		Antisense	5′-GGTGAAAGGGCTGTTCTTGC-3′	
	NOXO1	Sense	5′-TTCCTGATGCTCCATTGCTG-3′	NM_027988
		Antisense	5′-GGTTGGGATAAGGGCTCCTC-3′	
	NOXA1	Sense	5′-AGCTGCAGAGGTTCCAGGAG	NM_172204
		Antisense	5′-GATGTCTTGAGCCCCCTCTG	
	B2M	Sense	5′-AGCCCAAGACCGTCTACTGG-3′	NM_009735
		Antisense	5′-TTCTTTCTGCGTGCATAAATTG-3′	
Human	NOX4	Sense	5′-GGTTAAACACCTCTGCCTGTTC-3′	NM_016931
		Antisense	5′-CTTGGAACCTTCTGTGATCCTC-3′	
	B2M	Sense	5′-CTGTGCTCGCGCTACTCTCT-3′	NM_004048
		Antisense	5′-CTTCAATGTCGGATGGATGAA-3′	

5 RESULTS

5.1 NADPH oxidases in hypoxia induced pulmonary hypertension

5.1.1 Hypoxic regulation of NADPH oxidase subunits in mouse lungs

The hypoxic regulation of various NADPH oxidase subunits was investigated by real time PCR in the lung homogenate of the mice exposed to 3 days and 3 weeks of hypoxia. Real time PCR measurement showed that NOX4 was the only non phagocytic NADPH oxidase significantly up-regulated in homogenised tissue over the time-course of exposure to chronic hypoxia (Fig. 8 a, b). In contrast NOX2, NOXA1, and p67phox were not significantly regulated and NOX1 as well as the other cytosolic NADPH oxidase subunits exhibited an overall down-regulation after 21 days of chronic hypoxia (Fig. 8 a, b).

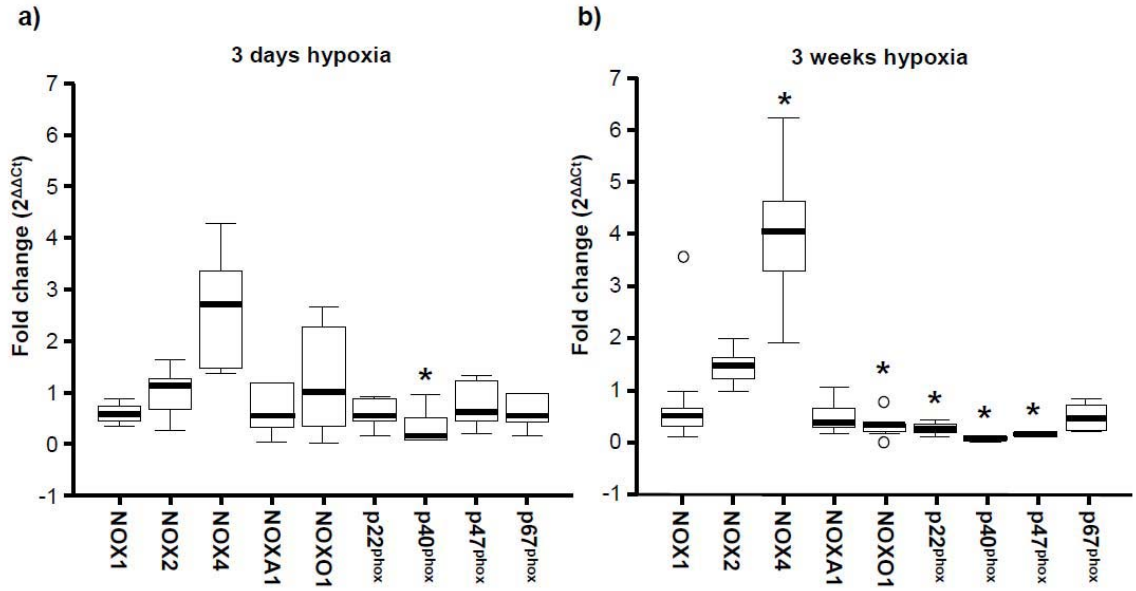

Figure 8. Real time PCR quantification of NADPH oxidase subunits in homogenised lungs after 3 days and 3 weeks of hypoxia.
Real time PCR quantification of NADPH oxidase subunits in the lung homogenate after 3 days a) and 3 weeks of hypoxia b). * indicate significant difference compared to normoxic controls; boxes: percentiles 25 and 75, black bar: median, whiskers: percentiles 0 and 100, O = value is more than 1.5 lengths of a box away from the edge of a box. n= 3 mice for 3-days hypoxia; n=5 mice for 3-weeks hypoxia.

5.1.2 Regulation of NOX2 and NOX4 in microdissected mouse pulmonary arteries during the course of hypoxia

Considering that NOX4 was prominently up-regulated and NOX2 was previously suggested to play an important role in hypoxia-induced pulmonary hypertension [99], further invesigations were made regarding the expression of NOX4 and NOX2 in microdissected small pulmonary

arterial vessels (~100 µm diameter), the major site of pulmonary vascular remodeling in chronic hypoxia by real-time PCR (Fig. 9 a, b, c).

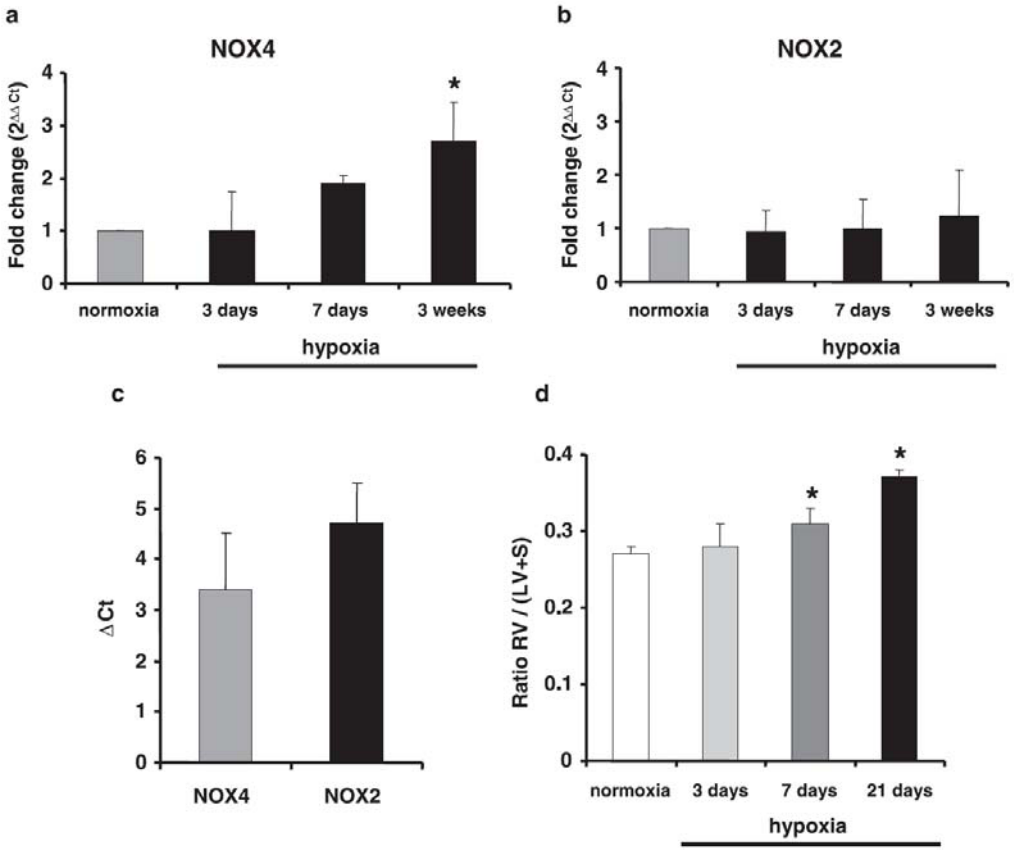

Figure 9. NOX4 and NOX2 mRNA quantification of microdissected pulmonary arteries by real time PCR during development of hypoxia-induced pulmonary hypertension
a, b) Microdissected small pulmonary arteries (~100 µm diameter) from cryosections of mouse lungs were employed for the quantification of NOX4 and NOX2 mRNA. Mice were maintained under normoxic or hypoxic conditions for up to 21 days. The NOX2 and NOX4 mRNA levels were quantified by real-time PCR normalized to β_2-microglobulin mRNA levels. c) Delta Ct values of NOX4 and NOX2 from microdissected pulmonary arteries of normoxic mice. Values are duplicate measurements of n=16 vessels from n=3 lungs each. d) Right ventricular hypertrophy after exposure of mice to chronic hypoxia. The right ventricle (RV) to left ventricle (LV) + septum (S) ratio was quantified from mouse hearts after exposure to chronic hypoxia (10% O_2 for 3, 7 and 21 days, respectively, n=5). * indicate significant differences as compared to normoxic controls, $p<0.05$.

Comparing these vessels from animals exposed to normoxic (21% O_2) and chronic hypoxic (10% O_2) conditions for up to 3, 7 and 21 days, it was observed that NOX4 mRNA expression was up-regulated in the pulmonary arteries over the course of exposure to hypoxia, with the highest elevation after 3 weeks (Fig. 9 a). In contrast to NOX4, no regulation of NOX2 was observed (Fig. 9 b).

Under normoxic conditions NOX2 mRNA levels were not different from those of NOX4 (Fig. 9 c). The hypoxic up-regulation of NOX4 paralleled the development of pulmonary

hypertension in mice induced by chronic hypoxia. The ratio of the right to the left ventricular mass was 0.27 ± 0.01 in mice maintained under normoxic conditions, and increased to 0.28 ± 0.03, 0.31 ± 0.02, and 0.37 ± 0.01 (n=5 each) after 3, 7 and 21 days of hypoxia, respectively (Fig. 9 d).

5.1.3 Localisation of NOX4 by in situ hybridization on mouse lung sections

Further investigations by *in situ* hybridization were performed to localize NOX4 mRNA on mouse lung sections.

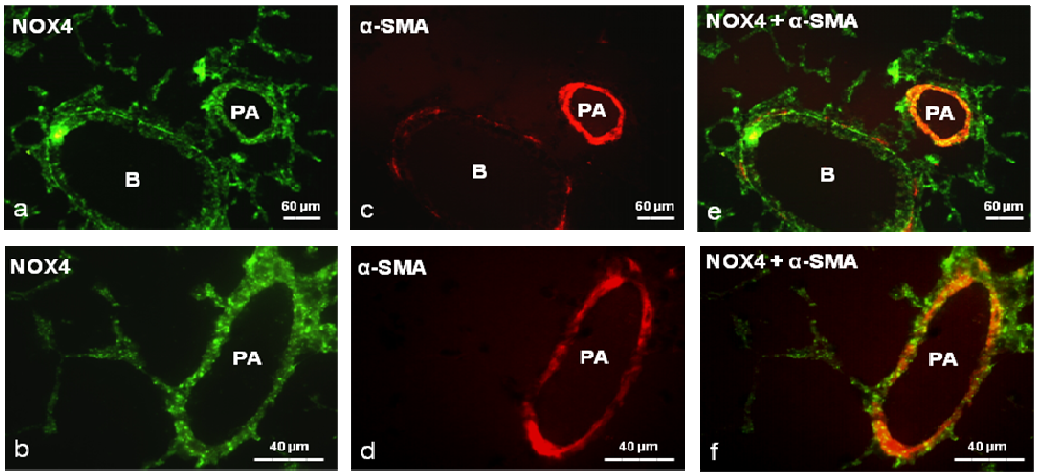

Figure 10. Localization of NOX4 in mouse lung sections by *in situ* hybridization (ISH)

a, b) Hybridization of the NOX4 antisense probe to mouse lung cryosections (green fluorescence). c, d) The same sections stained with a Cy3-labelled antibody directed against α-smooth muscle actin (SMA, red fluorescence). e, f) Overlay of the images a and b depicting predominant co-localisation of NOX4 transcripts with SMA in the smooth muscle cell layer of the pulmonary artery (yellow fluorescence). B: bronchus, PA: pulmonary artery.

The transcripts of NOX4 were localized in different cell types with prominent presence in the vessel media, as confirmed by its co-localisation with α-smooth muscle actin (Fig. 10). In addition, the NOX4 merged staining showed that the transcripts were present in non-vascular compartments comprising of bronchial smooth muscle cells and alveolar type II cells. In this regard, NOX4 transcripts were detected in isolated alveolar type II cells from mouse (data not shown).

5.1.4 Hypoxic regulation of NOX4 at protein level in mice lung

In addition to the observations that NOX4 mRNA was predominantly present in the vessel media, the presence of NOX4 protein in the vessels was further confirmed by immunostaining on mouse lung sections (Fig. 11)[1].

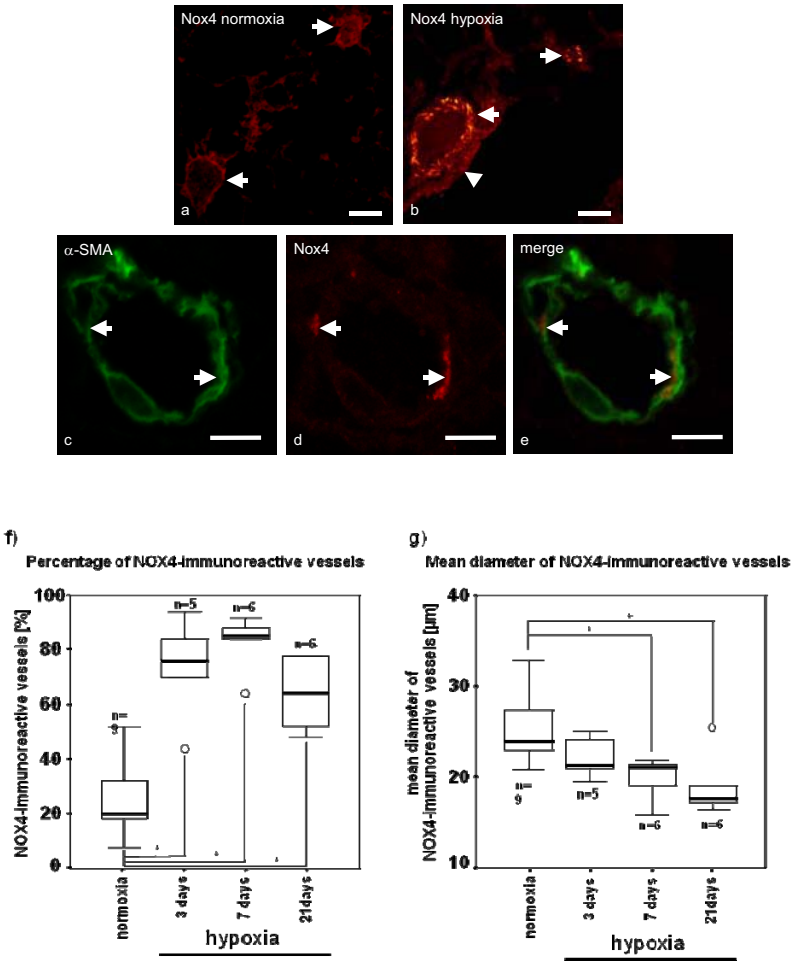

[1] Figure 11. NOX4 immunostaining comparing mice maintained either under normoxic (21% O_2) or hypoxic (10% O_2) conditions

a) In the normoxic mice, the majority of vessels displayed very less NOX4 immunoreactivity (arrows) . b) Under hypoxia, the majority of vessels were immunoreactive for NOX4 (arrows). Note the slight autofluorescent bronchial epithelium (arrowhead). c, d) Labeling of NOX4 and α-smooth muscle actin (SMA), confocal image. A subgroup of SMA-immunoreactive cells in the vessel wall was also NOX4 immunoreactive (arrows), as evident for the merged images c and d (e). f) Percentage of NOX4 immunoreactive vessels in normoxic mice and mice exposed to chronic hypoxia (10% O_2) for up to 21 days. The mean value for every animal is shown in the box plot. g) Mean diameter of NOX4 immunoreactive vessels during development of hypoxia-induced pulmonary hypertension. The mean value for every animal is shown in the box plot; n = number of animals examined per experimental condition, *$p<0.05$; boxes: percentiles 25 and 75, black bar: median, whiskers: percentiles 0 and 100, O = value is more than 1.5 lengths of a box away from the edge of a box.

[1] Imaging and quantification was performed and data were provided by Dr. Peter König.

NOX4-immunoreactivity was observed in a subset of cells of the medial wall of the pulmonary artery, as well as in some smaller pulmonary arteries (Fig. 11 a-e). After exposure to chronic hypoxia, the number of NOX4 positive vessels was significantly increased after three days of exposure to hypoxia (Fig. 11 f). The number of small NOX4 immunopositive vessels was also significantly increased after 7 and 21 days of hypoxia (Fig. 11 g), indicating that the newly-formed and muscularized smaller vessels were also NOX4-immunoreactive.

5.1.5 Sub-cellular localisation of NOX4 in isolated mouse pulmonary arterial smooth muscle cells and its regulation in hypoxia

At the sub-cellular level, NOX4 protein exhibited a predominantly perinuclear localisation in mouse PASMC (Fig. 12 a, b). The intensity of staining increased after 48 h of hypoxic incubation as compared to normoxic control (Fig. 12 c, d). The perinuclear localisation of NOX4 reflects the presence of NOX4 protein in the endoplasmic reticulum.

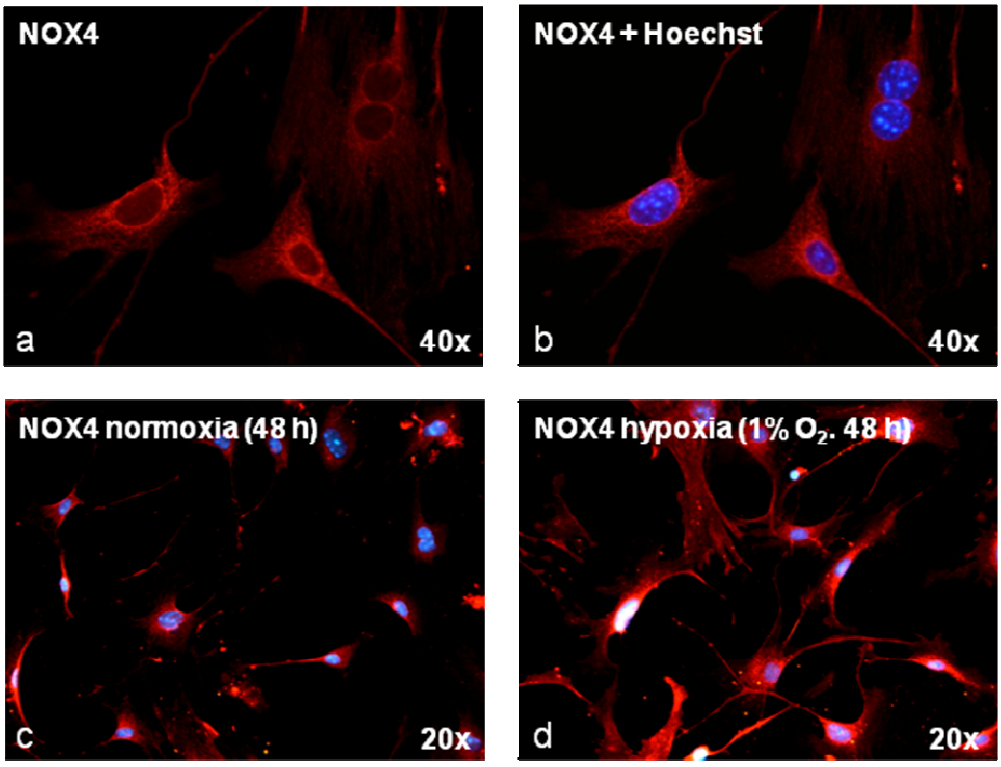

Figure 12. Cellular NOX4 localisation in mouse pulmonary arterial smooth muscle cells by immunofluorescence.
The NOX4 immunostaining of isolated murine pulmonary arterial smooth muscle cells revealed a perinuclear localisation, and a slight increase of NOX4 immunoreactivity when PASMC were incubated for 48 h under hypoxic conditions, compared to cells incubated under normoxic conditions. a) Murine PASMC stained with an anti-NOX4 antibody and b) with an additional nuclear marker (Hoechst). c) NOX4 immunoreactivity of murine PASMC after 48 h under normoxic (21% O_2), compared to d) hypoxic (1% O_2), conditions.

5.1.6 Immunostaining of NOX4 and NOX2 on human lung sections

Histological staining of human lung sections from healthy donors and from patients with idiopathic pulmonary arterial hypertension (IPAH) confirmed NOX4 expression in the vessel media of the pulmonary arteries (Fig. 13 a-d). In contrast to NOX4, NOX2 was primarily expressed in the endothelial layer of the human pulmonary arteries (Fig. 13 e, f).

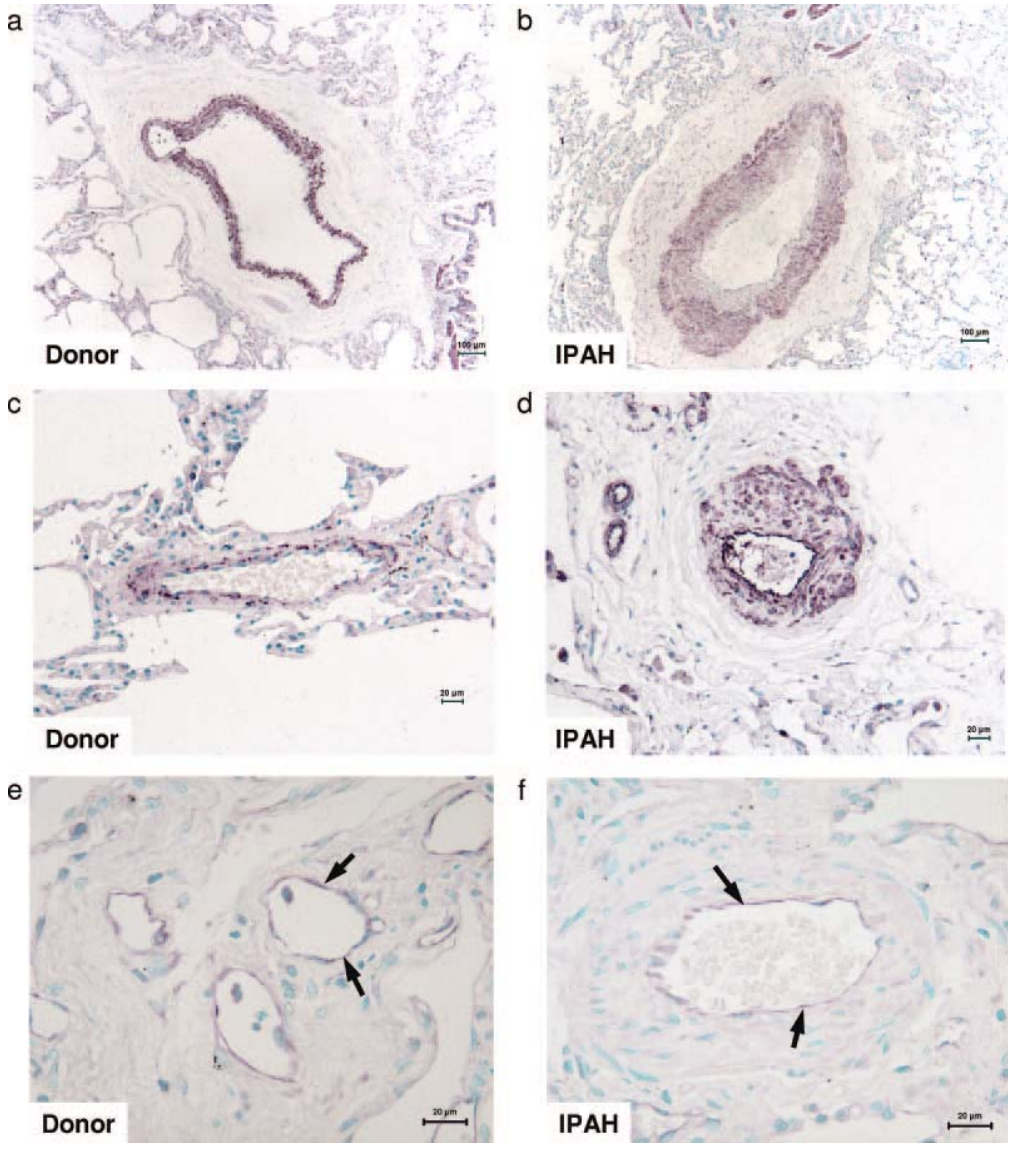

Figure 13. Localisation of NOX4 and NOX2 in human donor and IPAH lungs.
The NOX4 immunostaining of human donor (a, c) and IPAH (b, d) lung sections revealed a localisation of NOX4 predominantly in the medial layer of pulmonary arteries. In contrast NOX2 immunostaining was localized mainly in the endothelium of human donor (e) and IPAH (f) lung sections (arrows).

5.1.7 Regulation of NOX4 in idiopathic pulmonary arterial hypertension (IPAH)

Western blot analysis of lung homogenate from IPAH patients compared to healthy donor lungs revealed a significant ($p<0.001$) 2.5-fold higher NOX4 protein level in IPAH patients (Fig. 14).

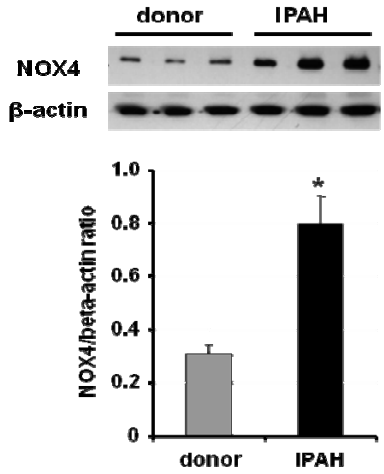

Figure 14. Detection of NOX4 by western blot in human donor and IPAH lungs
a) Western blots of human IPAH lungs (n=4) compared to healthy donor lungs (n=6) revealed a 2.5-fold up-regulation of NOX4 expression in human IPAH lungs (specific band at 64 kDa). The NOX4 was normalized to β-actin. * indicates significant difference as compared to donor lungs.

5.1.8 Effect of hypoxia on NOX4 mRNA levels in human PASMC

In addition, NOX4 transcripts quantified by real-time PCR were increased in human donor PASMC from passage 3 exposed to hypoxia for 24 h, compared to normoxic controls (Fig. 15).

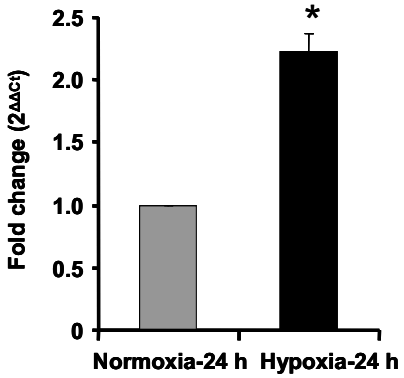

Figure 15. Hypoxia induced up-regulation of NOX4 in isolated human pulmonary artery smooth muscle cells. Isolated human pulmonary arterial smooth muscle cells (PASMC) were maintained under hypoxic (1% O_2) or normoxic (21% O_2) conditions for 24 h. The NOX4 mRNA levels were quantified by real-time PCR and standardized to β_2-microglobulin mRNA levels. A significant increase in NOX4 mRNA was observed after 24 h of hypoxic *versus* normoxic treatment (*). Data are derived from duplicate measurement of n=3 independent cell preparations.

5.1.9 Role of NOX4 in the proliferation of human PASMC

To investigate a possible functional role of NOX4 for cell proliferation, it was demonstrated that siRNA directed against human NOX4 significantly reduced the NOX4 mRNA level (Fig. 16 a) and suppressed the proliferation of human passage 3 PASMC (Fig. 16 b) correlating with a decrease of reactive oxygen species (ROS) generation (Fig. 16 c).

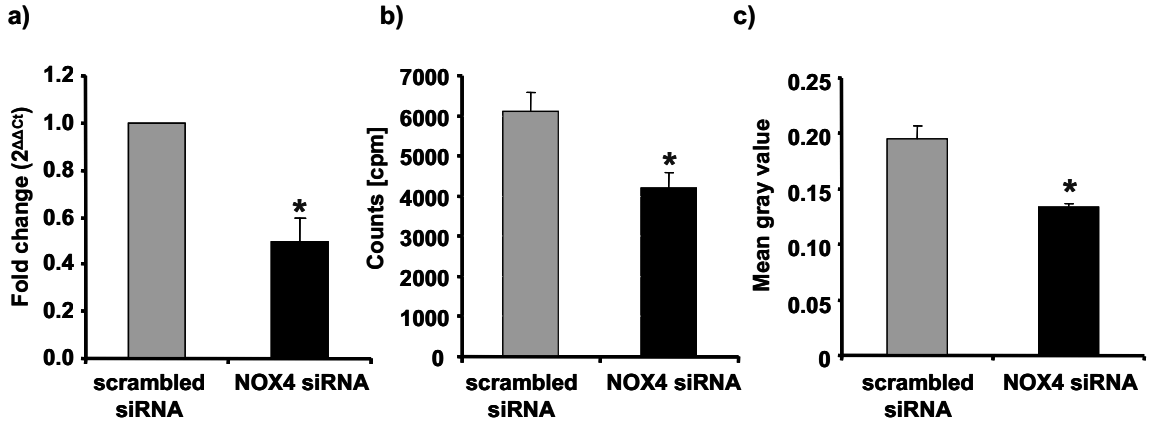

Figure 16. Suppression of human pulmonary arterial smooth muscle cell proliferation and reactive oxygen species generation by siRNA directed against NOX4
a) Quantification of NOX4 in siNOX4 transfected human PASMC showing significant down-regulation of NOX4 as compared to scrambled control. b) The normoxic proliferation of PASMC was investigated using ^{3}H-thymidine. c) Reactive oxygen species quantification by dihydroethidium fluorescence in scrambled and NOX4 siRNA transfected human PASMC. *indicate significant differences between NOX4 siRNA and scrambled siRNA experiments. Data are derived from duplicate cell isolations of n=5 independent lungs. cpm, counts per minute.

5.2 Effect of NOX4 on K_{DR} channel function in rat PASMC under chronic hypoxia

5.2.1 Co-localisation of NOX4 with K_{DR} channels in the rat lung sections

Reduced function and expression of K_{DR} channels in chronic hypoxia is considered as an important key event in the pathogenesis of hypoxia induced pulmonary hypertension. Previous reports have indicated that the Kv channel gating can be affected by the oxidative modification at the N-terminal cytoplasmic inactivation domain [112-114]. Despite the presence of both NOX2 and NOX4 in the pulmonary vasculature, the fact that only NOX4 is up-regulated under chronic hypoxia, leads to the question about a functional link between NOX4 derived oxidative stress and K_{DR} channels. The realationship between NOX4 and K_{DR} channels was investigated in isolated rat PASMC because of the technical difficulty in handling mouse PASMC and in getting enough material for expression analysis.

To explore a functional link between NOX4 and K_{DR} channels, it was first examined if NOX4 and K_{DR} channel are co-localised under *in vivo*.

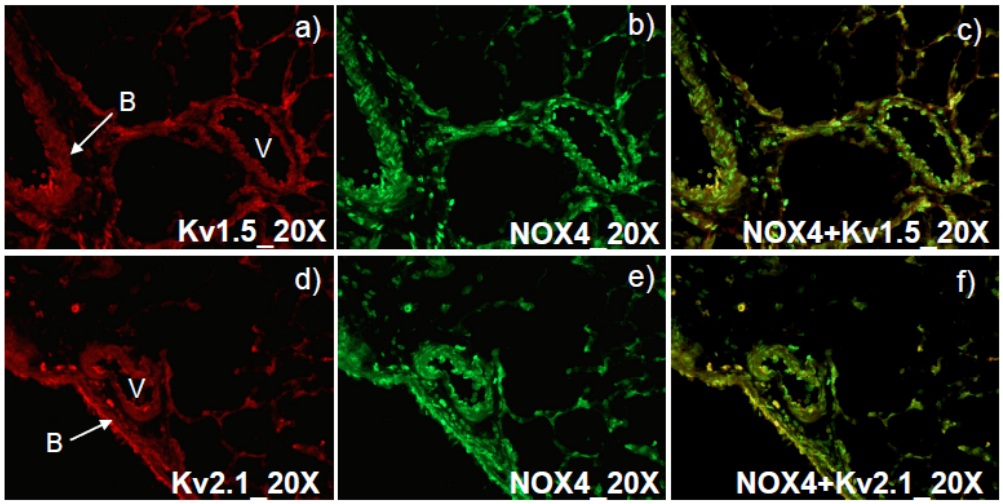

Figure 17. Co-localisation of NOX4 with Kv1.5 and Kv2.1 channels on rat lung sections. (a and b) Immunostaining on rat lung sections using Kv1.5 antibody (red) and NOX4 antibody (green). (d and e) Immunostaining on rat lung sections using Kv2.1 (red) and NOX4 antibody (green). (c and f) an overlay of images a and d depicting the co-localisation of Kv1.5 and Kv2.1 channels with NOX4. B: Bronchus; V: Vessel.

Immmunofluorescence on rat lung sections revealed a strong co-localisation of NOX4 with Kv1.5 and Kv2.1 channels in the vessels, bronchus and alveolar space (Fig. 17).

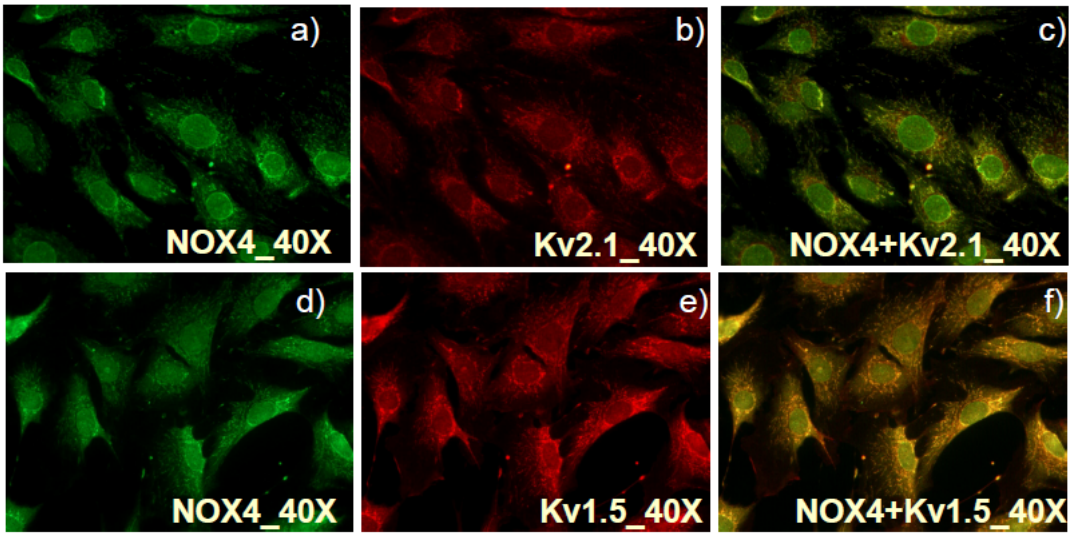

Figure 18. Co-localisation of NOX4 with Kv1.5 and Kv2.1 channels in isolated rat PASMC. (a and b) Immunostaining on rat PASMC using a directly labelled NOX4 antibody (green) and Kv2.1 antibody (red). (c and d) Immunostaining on rat PASMC using a directly labelled NOX4 antibody (green) and Kv1.5 antibody (red). (c and f) An overlay of images in a and d depicting colocalisation of NOX4 wit Kv2.1 and Kv1.5 channels.

The co-localisation of NOX4 with Kv1.5 and Kv2.1 channels was further confirmed in isolated rat PASMC (Fig. 18). NOX4 showed a strong co-localisation with Kv1.5 and Kv2.1 channels on plasma membrane and in perinuclear space.

5.2.2 Effect of chronic hypoxia on the delayed rectifier K^+ current

The whole cell patch clamp technique was used to measure the delayed rectifier K^+ current (K_{DR}) in rat PASMC exposed for 48 h in hypoxia (1% O_2). Membrane currents were recorded in response to the voltage steps from -70 mV to 90 mV in a 20 mV increment from a holding potential of –50 mV. When the current densities (whole cell currents divided by its capacitance) were plotted against V_m, it was observed that hypoxic treatment significantly reduced the current density of delayed rectifier K^+ channels of rat PASMC at all positive V_m (Fig. 19).

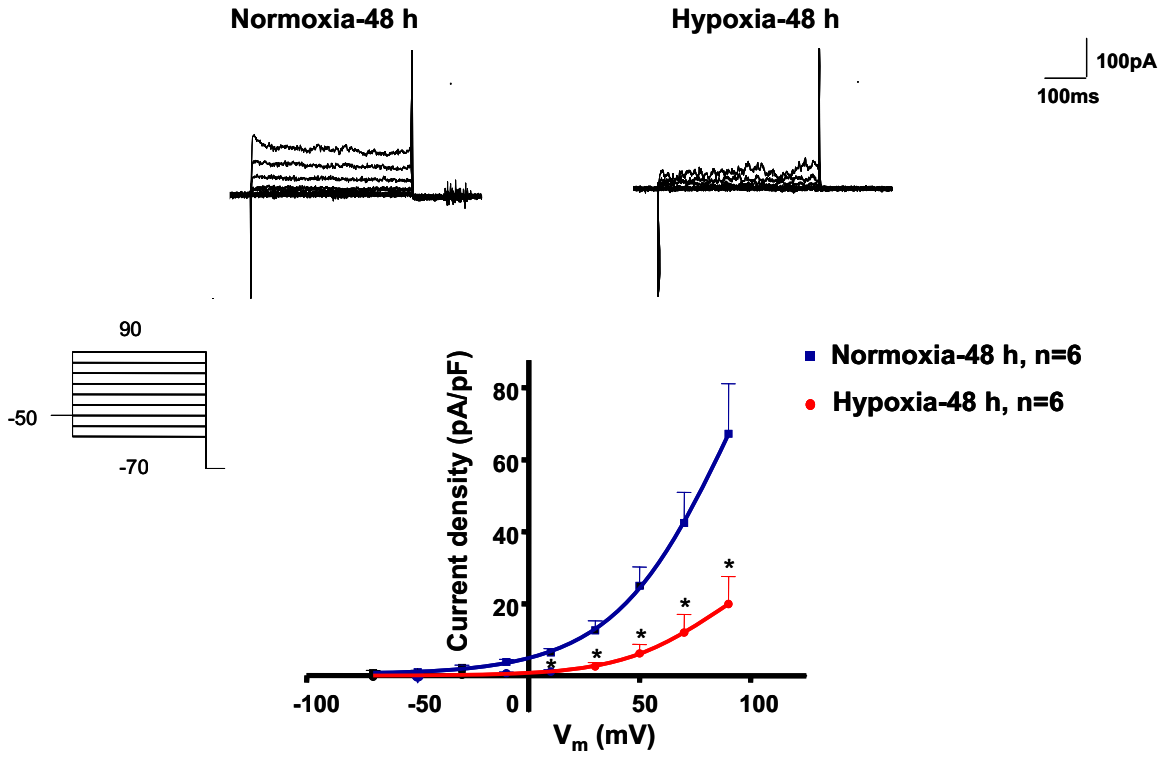

Figure 19. Chronic hypoxia treatment decreased the whole cell delayed rectifier K^+ current of rat PASMC.
Rat PASMC were exposed for 48 h in hypoxia (1% O_2) and whole cell delayed rectifier K^+ currents were measured from the voltage steps of -70 mV to 90 mV in a 20 mV increment from a holding potential of -50 mV. At -50 mV greater than 90% of K_A current was not available so that mainly the current from delayed rectifier K^+ channels was recorded. An *I-V* plot showed a significant reduction in the K_{DR} current density in rat PASMC exposed for 48 h in hypoxia in all positive *Vm*. n= number of the cells. * $p<0.05$ compared to normoxic cells.

5.2.3 Effect of apocynin on the delayed rectifier K^+ current in rat PASMC

Whole cell patch clamp recordings revealed that apocynin treatment significantly increased the K_{DR} current density of rat PASMC by approximately 2.7 fold at 90 mV compared to DMSO (solvent control) treated control cells under hypoxic conditions (Fig. 20 b, Table 5). The K_{DR} current density at 90 mV on the DMSO treated hypoxic cells was 15.2±1.8 pA/pF, which was increased to 41.4±8.7 pA/pF ($p<0.05$) with apocynin treatment.

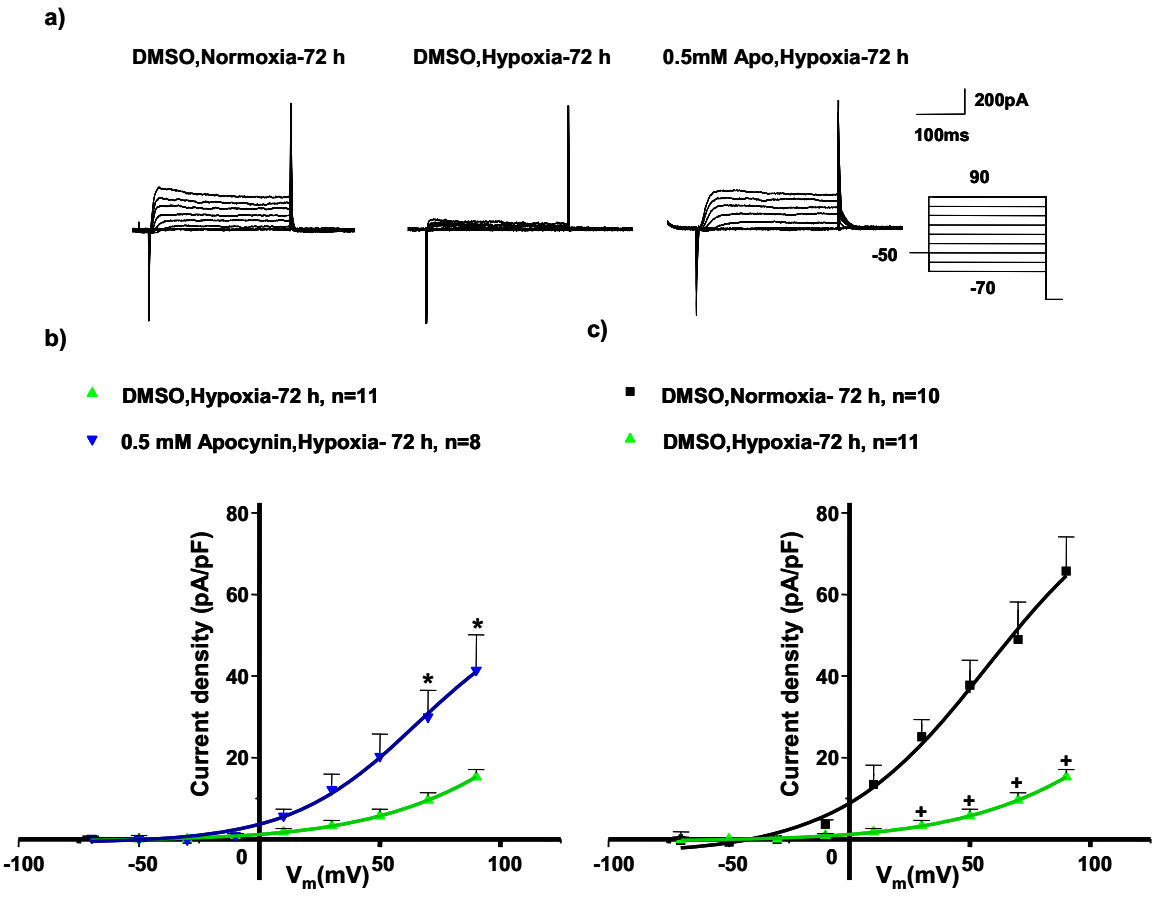

Figure 20. Treatment of rat PASMC with 0.5mM apocynin significantly increased the whole cell K_{DR} current as compared to control cells.
a) Representative recordings of whole cell K_{DR} currents showing an increase in K_{DR} currents in response to 0.5 mM apocynin treatment under hypoxic conditions. Whole cell K_{DR} currents were collected from -70 mV to 90 mV voltage steps from a holding potential of -50 mV in a 20 mV increment step. b) *I-V* curve expressed as the whole cell K_{DR} current density against V_m. A significant increase in K_{DR} current density was observed under hypoxic conditions from treatment with 0.5 mM apocynin as compared to DMSO treatment. c) Hypoxia significantly decreased the K_{DR} current density in DMSO treated hypoxic cells compared to DMSO treated normoxic cells. n=number of the cells from two rats. * $p<0.05$ compared to DMSO treated hypoxic cells. $^+p<0.05$ compared to DMSO treated normoxic cells.

The density of K_{DR} current was significantly reduced in DMSO treated hypoxic rat PASMC as compared to DMSO treated normoxic cells (Fig. 20 c) (Table 5).

Table 5: Comparison of K_{DR} current densities of rat PASMC under normoxic and hypoxic conditions with apocynin treatment and solvent control (DMSO)

V_m (mV)	*Normoxia-72 h DMSO (n=10) pA/pF*	*Hypoxia-72 h, DMSO (n=11) pA/pF*	*Hypoxia-72 h 0.5mM Apocynin (n=8) pA/pF*
-70	-0,3±0,4	-0.1±0.1	0.7±0.3
-50	-0,7±0.2	0.0±0.08	0.0±0.2
-30	0.0±0.5	0.0±0.1	-0.2±0.4
-10	3.6±1.2	0.9±0.4	0.8±0.5
10	13.4±2.7	1.7±0.9	5.7±1.7
30	25.1±4.2	3.3±1.3^{+}	12.2±3.7
50	37.8±6.1	5.7±1.7^{+}	20.3±5.5
70	49.0±7.3	9.6±1.7^{+}	30.0±6.6*
90	65.8±8.4	15.2±1.8^{+}	41.4±8.7*

Values are given as Mean ± SEM (standard error of mean)
* $p<0.05$ compared to DMSO treated hypoxic cells
$^{+}p<0.05$ compared to DMSO treated normoxic cells

5.2.4 Increased current density of Kv2.1 and Kv1.5 channels after apocynin treatment

The currents specific to Kv2.1 and Kv1.5 channels were dissected out from the whole cell K_{DR} currents using the antibodies specific to Kv2.1 and Kv1.5 channels [115;116]. The membrane currents from normoxic rat PASMC were recorded at voltage steps from -70 mV to 90 mV with Kv1.5 and Kv2.1 antibodies in the intracellular pipette solution (Fig. 21 a).

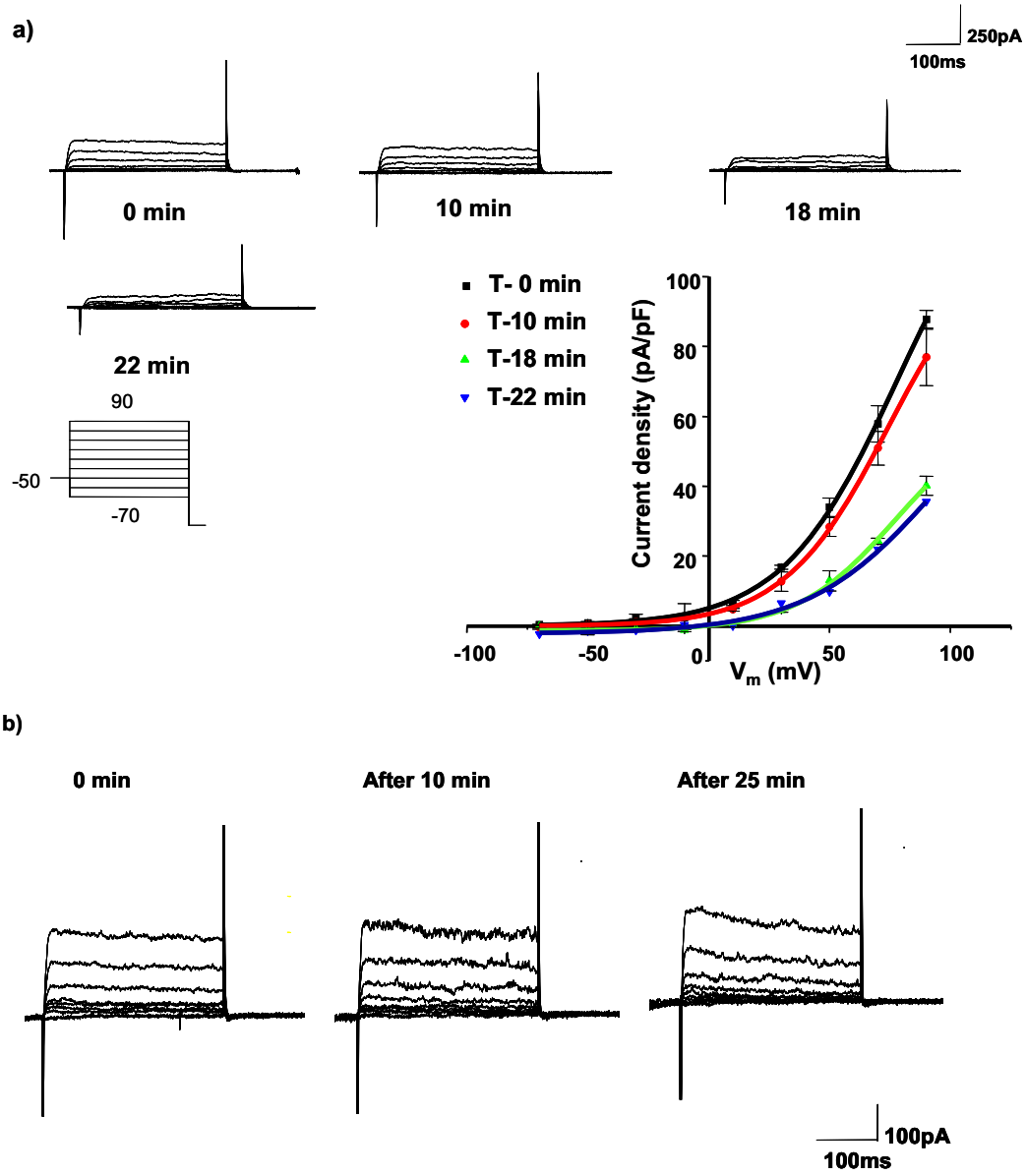

Figure 21. Time course of inhibition of K_{DR} current with Kv1.5 and Kv2.1 antibodies in the intracellular pipette solution and *I-V* curve expressed as current densities against V_m.
a) Both antibodies at dilution of 1:100 were dissolved in the intracellular pipette solution. T-0 represents the recording made immediately after the membrane rupture. Further time points represent the time taken by the antibodies to diffuse in to the cell from the pipette pore to block the Kv1.5 and Kv2.1 specific current. *I-V* curve revealed a 55% inhibition of K_{DR} current density after 22 min of dialysis with Kv2.1 and Kv1.5 antibodies. b) No run down was observed of the whole cell K_{DR} current even after 25 min of the establishment of the whole cell configuration in the absence of antibodies in the intracellular solution.

The initial recording of the whole cell K_{DR} current was made immediately after the establishment of a whole cell configuration and is represented by T-0. Further recording at different time intervals revealed a gradual decrease in the K_{DR} current density with increasing time. A 55% inhibition of K_{DR} current was observed after 22 min of the break in which could indirectly represent the percentage of Kv1.5 and Kv2.1 specific current in the whole cell K_{DR} current (Fig. 21 a). No effect of run down on the K_{DR} current was observed in the normoxic

rat PASMC even after 25 min in to the whole cell configuration in the absence of antibodies (Fig. 21 b).

Interestingly, the inhibition of K_{DR} current by Kv1.5 and Kv2.1 antibodies was observed only in the hypoxic group of PASMC treated with apocynin, no inhibition of K_{DR} current was observed in the control DMSO treated hypoxic rat PASMC (Fig. 22 a). Moreover, the current density was significantly higher even after antibody blockage in apocynin treated hypoxic PASMC compared to DMSO treated hypoxic control (Fig. 22 a).

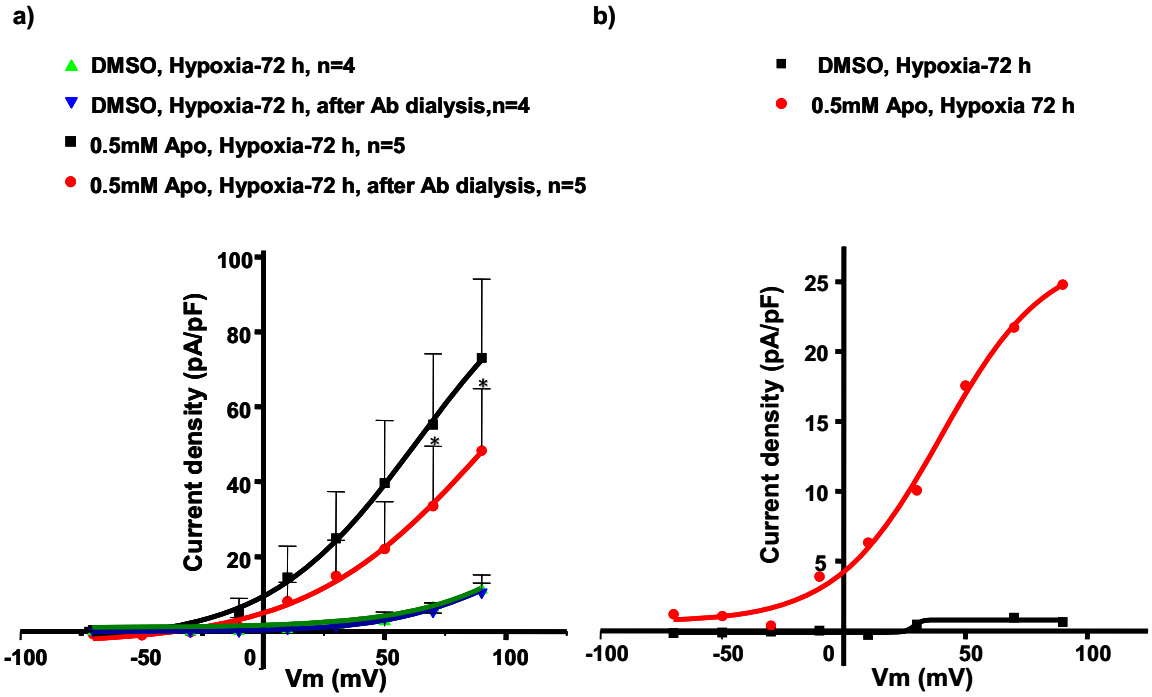

Figure 22. Effect of inhibition on the whole cell K_{DR} currents by Kv1.5 and Kv2.1 antibodies in DMSO treated and apocynin treated hypoxic rat PASMC at different V_m.
a) *I-V* curve revealed an inhibition of the K_{DR} current by Kv2.1 and Kv1.5 specific antibodies in the apocynin treated rat PASMC whereas no inhibition was observed in the DMSO treated hypoxic rat PASMC. b) Apocynin treatment under hypoxia increased the current density of Kv2.1 and Kv1.5 channels on rat PASMC at all positive V_m. n= number of the cells from two rats. * indicates $p<0.05$ compared to DMSO treated hypoxic cells after antibody dialysis. * $p<0.05$ compared to DMSO hypoxic cells. Ab; antibody.

The difference in currents before and after antibody blockage revealed a specific increase in the current density of Kv1.5 and Kv2.1 channels on rat PASMC treated with apocynin under hypoxia at all positive V_m (Fig. 22 b).

5.2.5 Treatment with NOX4 siRNA in rat PASMC increased the K_{DR} current density

To investigate the role of NOX4 in the regulation of hypoxia sensitive K_{DR} channels, rat PASMC were transfected with the NOX4 specific siRNA and were kept under normoxic conditions for three days to lower down the level of NOX4 protein. After this period, cells

were transferred to hypoxic conditions for 48 h and normoxic cells stayed under normoxia up to the same time period.

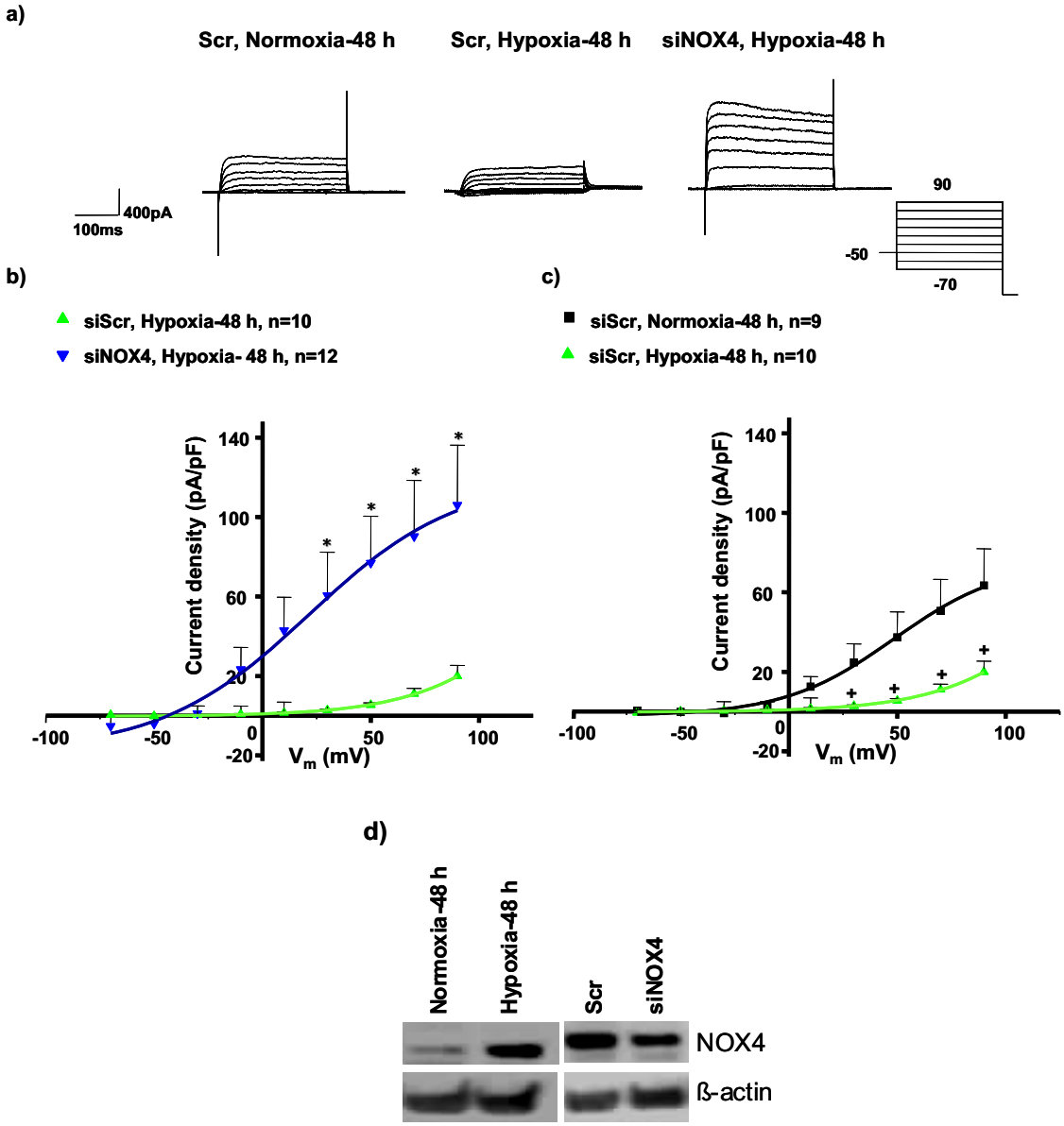

Figure 23. Treatment of rat PASMC with siNOX4 increased the K_{DR} current density under hypoxic conditions. a) Representative recordings of K_{DR} current revealed a significant increase on siNOX4 treatment under hypoxia. b) *I-V* curves revealed a significant 5 fold increase in the K_{DR} current density at all positive V_m on rat PASMC transfected with NOX4 siRNA as compared to scrambled siRNA treated cells under hypoxic conditions. c) Hypoxia significantly decreased the K_{DR} current density of scr siRNA treated hypoxic PASMC as compared to scrambled siRNA treated normoxic cells. d) Immunoblot revealed that chronic hypoxia increased NOX4 protein level in PASMC and siNOX4 treatment decreased the NOX4 protein. n=number of the cells from two rats. * $p<0.05$ compared to scrambled siRNA treated hypoxic cells. $^{+}p<0.05$ compared to scrambled siRNA treated normoxic cells.

I-V curve revealed that the K_{DR} current increased significantly by 5 fold in the rat PASMC transfected with NOX4 siRNA at V_m of 90 mV as compared with scrambled (Scr) siRNA

treated cells under hypoxic conditions (Fig. 23 b, Table 6). The mean K_{DR} current density of scrambled siRNA treated hypoxic rat PASMC was 19.9±5.4 pA/pF (n=10) at V_m of 90 mV which increased up to 105.9±30.2 pA/pF (n=12, $p<0.05$) on siNOX4 treatment (Table 6). Hypoxia significantly decreased the K_{DR} current density at all positive V_m on the scrambled siRNA treated hypoxic cells as compared to scrambled siRNA treated normoxic cells (Fig. 23 c, Table 6). Similar to up-regulation of NOX4 in the mouse and human PASMC, an up-regulation of NOX4 protein was also observed in the isolated rat PASMC exposed to 48 h of hypoxia and treatment with NOX4 siRNA decreased the NOX4 protein levels (Fig. 23 d).

Table 6: Comparison of K_{DR} current density of rat PASMC after treatment with scrambled and NOX4 siRNA under normoxic and hypoxic conditions

V_m (mV)	*Scr Normoxia- 48 h (n=9) (pA/pF)*	*Scr Hypoxia-48 h (n=10) (pA/pF)*	*siNOX4 Hypoxia-48 h (n=12) (pA/pF)*
-70	0.4±0.3	-0.6±0.2	0.0±0.5
-50	-0.2±0.2	0.0±0.1	-0.3±0.5
-30	-0.8±0.7	0.4±0.1	3.7±3.0
-10	3.0±1.9	0.8±0.3	26.1±11.2
10	12.5±5.1	1.5±0.4	45.6±17.4*
30	24.7±9.3	2.7±0.6^{+}	63.1±22.6*
50	37.3±12.8	5.4±1.1^{+}	77.5±26.1*
70	50.6±15.9	11.0±2.7^{+}	91.9±29.4*
90	63.4±18.5	19.9±5.4^{+}	105.9±30.2*

Values are given as Mean ± SEM (standard error of mean)
$^{+}$ $p<0.05$ compared to Scr normoxic cells
*$p<0.05$ compared to Scr hypoxic cells

5.2.6 NOX4 siRNA affected the activation kinetics of K_{DR} current under chronic hypoxia

The treatment of rat PASMC with NOX4 siRNA under chronic hypoxia resulted in a significant hyperpolarising shift of the voltage dependent activation and a reduction in the slope factor *K* (Fig. 24 a). The steady state activation kinetics was fitted to the Boltzman equation $G/Gmax=1/(1+e^{-(V-V_{1/2})}/K)^n$. Whereas $V_{1/2}$ is the half maximal activation potential of

K_{DR} current and *K* is the slope factor. The Boltzman distribution of scr siRNA treated hypoxic cells had a $V_{1/2}$ = 11.43 mV (n=5) which was shifted to hyperpolarising direction of $V_{1/2}$ = -9.89 mV (n=9) by siNOX4 treatment under chronic hypoxia. This hyperpolarising shift was accompanied by a decrease in the value of slope factor *K* from 15.80 in scr siRNA treated cells to 12.77 in NOX4 siRNA treated cells under hypoxia.

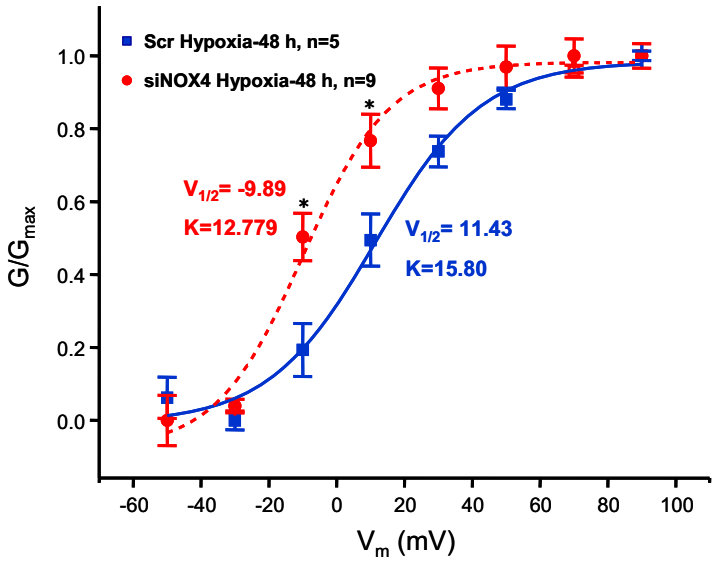

Figure 24. Conductance voltage relationship of K_{DR} current in rat PASMC transfected with NOX4 siRNA under chronic hypoxia. The conductance was calculated from the peak current amplitude divided by the K^+ ion driving force calculated from the Nernst equation and normalised with the maximal conductance in a given series of voltages. NOX4 siRNA significantly affected the half maximal activation potential ($V_{1/2}$) of K_{DR} current and shifted it towards more hyperpolarising potentials accompanied by a decrease in the slope factor (*K*).

5.3 Effect of NOX4 on calcium influx and ROS production in rat PASMC under chronic hypoxia

5.3.1 Treatment of rat PASMC with apocynin reduced the endothelin-1 (ET-1) stimulated calcium influx under chronic hypoxia

Further investigations were performed to explore the possibility of NADPH oxidase derived ROS production in regulation of calcium influx in rat PASMC using apocynin. The treatment of rat PASMC with 0.5 and 2 mM apocynin under hypoxia resulted in the disappearance of the transient calcium peak induced by endothelin-1 (ET-1) and delayed the sustained increase in calcium by approximately 200 s compared to DMSO treated hypoxic cells (Fig. 25). The overall ET-1 induced calcium influx was much reduced in the apocynin treated hypoxic PASMC compared to DMSO (solvent) control.

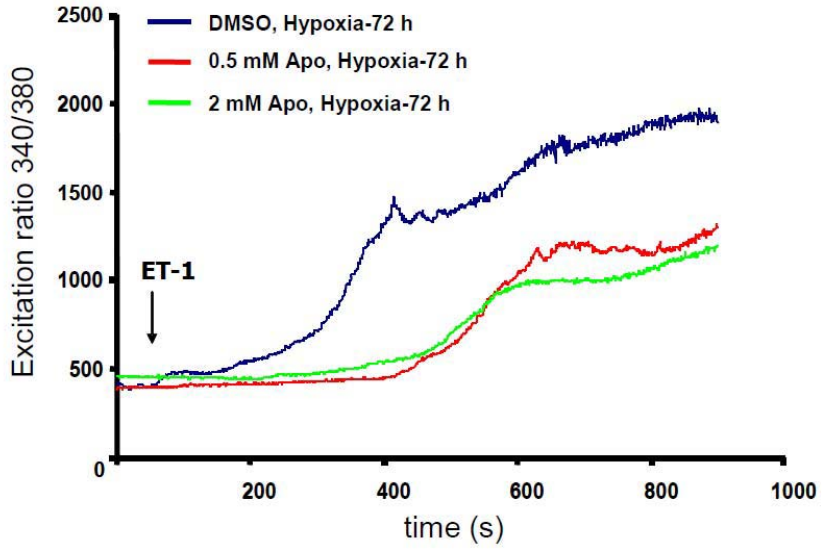

Figure 25. Measurement of intracellular calcium concentration in rat PASMC treated with apocynin under chronic hypoxia. Pharmacological inhibition of NADPH oxidases with apocynin resulted in reduced calcium influx under hypoxic conditions. Calcium measurement was done using the calcium sensitive dye Fura-2. The PASMC were loaded with Fura-2 for 1 h at 37 ^{o}C. ET-1 (20 nM) was applied at a time point of 60s. Apocynin treatment reduced the ET-1 stimulated calcium influx in rat PASMC compared to the DMSO control under chronic hypoxia.

5.3.2 NOX4 siRNA reduced the the endothelin-1 (ET-1) stimulated calcium influx under normoxia and abolished it completely under chronic hypoxia

The role of NADPH oxidase derived ROS production in regulation of calcium influx was further strengthened by the use of NOX4 specific siRNA. The treatment of rat PASMC with two different sequences of NOX4 specific siRNA resulted in reduced ET-1 stimulated calcium influx under normoxic conditions compared to scrambled control and complete disappearance of calcium influx under hypoxia (Fig. 26 a and b). Although ET-1 primed calcium influx was much lower in scrambled hypoxic cells compared to scrambled normoxic cells, the basal calcium levels (before ET-1 stimulation) were higher (Fig. 26 a and b). Both sequences of NOX4 siRNA abolished the transient calcium peak induced by ET-1 and delayed the overall calcium influx under normoxia (Fig. 26 a). Sequence-2 of NOX4 siRNA was more effective than sequence-1 in delaying the sustained calcium increase and reducing the overall calcium influx under normoxia (Fig. 26 a), whereas under hypoxia both sequences abolished the calcium influx while sequence-2 being marginally more effective than sequence-1 (Fig. 26 b).

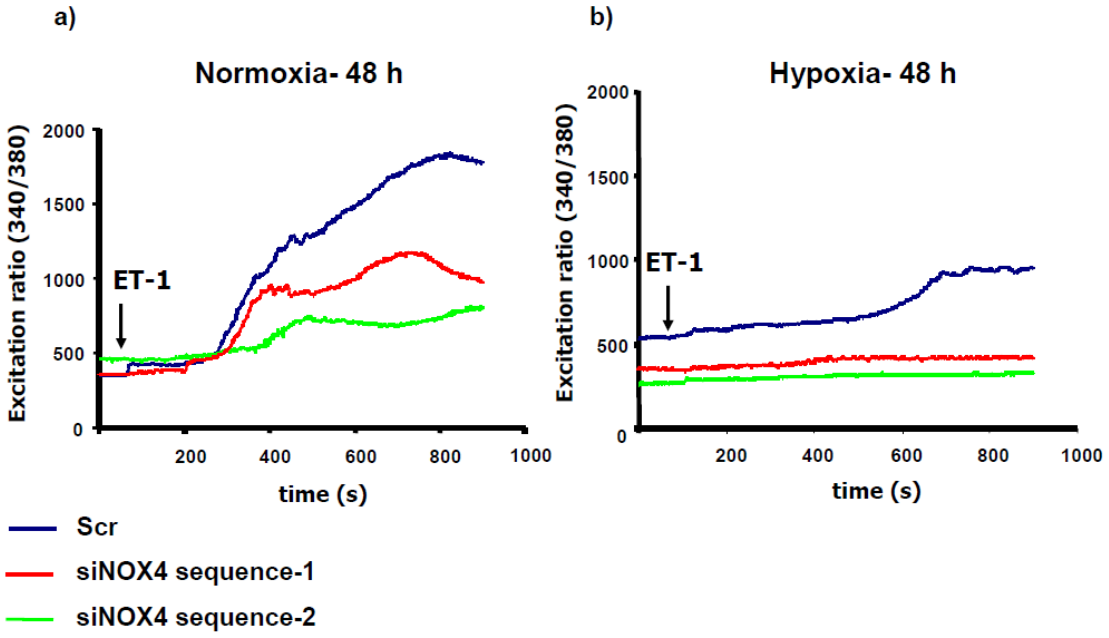

Figure 26. Measurement of intracellular calcium in rat PASMC treated with NOX4 siRNA under normoxic and hypoxic conditions. a) NOX4 siRNA reduced the endothelin-1 (ET-1) primed calcium influx in rat PASMC under normoxic conditions. ET-1 (20 nM) was applied at a time point of 60 s. The PASMC were loaded with Fura-2 for 1 h at 37 °C. Two different sequences of NOX4 siRNA were used to reproduce the effect. Sequence 2 of NOX4 siRNA was used previously in electrophysiology. b) NOX4 siRNA completely abolished the ET-1 stimulated calcium influx under hypoxia compared to scrambled siRNA control. The basal calcium level was higher in scrambled siRNA treated hypoxic cells compared to scrambled normoxic control. The data is averaged from three independent experiments on the cells isolated from two rats.

5.3.3 Increased ROS production and its attenuation with NOX4 siRNA in rat PASMC under chronic hypoxia

To reproduce the previously reported effect of NOX4 on ROS production in human PASMC (Fig. 16), the ROS was measured in rat PASMC using another oxidation sensitive dye i.e. dichloro flourescein diacetate (DCF-DA). An increased ROS production was observed in PASMC exposed to 48 h and 72 h of hypoxia and treatment with NOX4 siRNA attenuated this increase (Fig. 27 a, b). In addition, ET-1 stimulated ROS production was significantly reduced in PASMC treated with NOX4 siRNA (Fig. 27 c). This finding can be correlated with the reduced calcium influx on ET-1 stimulation in siNOX4 treated PASMC (Fig. 27 c and Fig. 26).

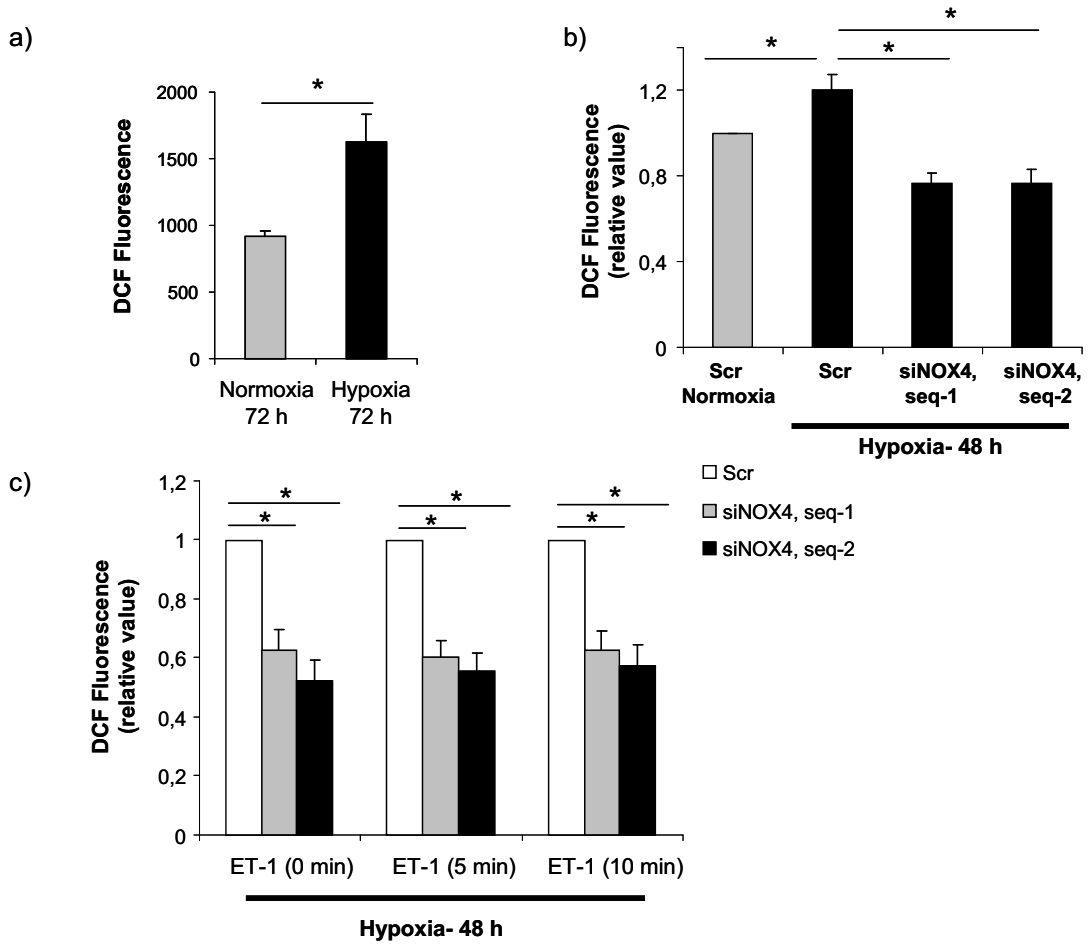

Figure 27. ROS measurement in rat PASMC treated with NOX4 siRNA under chronic hypoxia.
a) ROS was measured using oxidation sensitive dye DCF-DA in rat PASMC exposed to chronic hypoxia. A significantly increased ROS production was observed in PASMC under chronic hypoxia (72 h) compared to normoxic control. b) The bar graph shows the basal ROS level in rat PASMC without ET-1 stimulation. scrambled siRNA treated hypoxic (48 h) cells were found to produce significantly more ROS compared to normoxic scrambled siRNA control and treatment with NOX4 siRNA attenuated the ROS increase in hypoxic PASMC. c) The bar graph depicts the ET-1 stimulated increase in ROS in rat PASMC treated with NOX4 siRNA exposed to chronic hypoxia. ET-1 stimulated ROS production was significantly reduced in rat PASMC treated with NOX4 siRNA. The data is averaged from three independent experiments from the cells isolated from three rats. * $p<0.05$.

6 DISCUSSION

Acute alveolar hypoxia induces constriction of pulmonary artery vessels, which is an essential mechanism to adapt perfusion to ventilation, and thus to optimise pulmonary gas exchange [5;49]. Previous reports from our laboratory have suggested that $p47^{phox}$ knockout mice exhibited reduced acute HPV, while vasoconstriction elicited by the thromboxane mimetic U46619 was not affected [49]. In contrast to the beneficial effects of HPV for regional alveolar hypoxia, chronic alveolar hypoxia induces remodeling of the pulmonary vasculature, characterised by hypertrophy of the vessel media, and thus a narrowing of the vascular lumen. This leads to an increased pulmonary vascular resistance, pulmonary hypertension and may result in right heart failure [122].

The role of oxidative stress in hypertrophy of vascular media has been widely recognised for some time and NADPH oxidase-generated ROS has been demonstrated in a mouse model to contribute to vascular hypertrophy [5;94;117-119]. However, little is known regarding the downstream target of NADPH oxidase derived ROS which induces vascular hypertrophy. The current thesis demonstrated the regulation of NADPH oxidases and their ability to regulate K_{DR} channels and calcium influx under chronic hypoxia via ROS production.

6.1 *Screening of NADPH oxidases for their potential role in the development of hypoxia induced pulmonary hypertension*

With respect to the lung, relatively few reports of the expression and regulation of the recently identified new vascular NADPH oxidase subunits exist. Hoidal and coworkers [119] have demonstrated that NOX4 is the predominant homolog in human airway and pulmonary artery smooth muscle cells [123]. In addition Hohler et al. identified a low output NADPH oxidase in pulmonary artery endothelial cells [124].

Thus, in screening for the hypoxic regulation of NADPH oxidases in the lung homogenate of the mice exposed to three days and three weeks of hypoxia, a significant up-regulation of NOX4 was observed by real time PCR. In contrast, NOX1 and NOX2 did not exhibit any significant regulation and the other subunits were downregulated. Investigations of the recently identified new isoforms of phagocytic NADPH oxidase subunits in the lung is of interest, since NADPH oxidases have been proposed as possible pulmonary oxygen sensors [5;119]. With respect to an additional role for non-phagocytic NADPH oxidase subunits in the pathophysiology of hypoxia-induced pulmonary hypertension, the present study focused on

NOX4, because: 1) NOX4 is the only non-phagocytic NADPH oxidase subunit prominently expressed in the media of mouse pulmonary arteries which has been suggested as the main site of oxygen sensing, 2) NOX4 was significantly up-regulated in chronic hypoxia in homogenised mouse lung tissue, 3) NOX4 acts as an oxygen sensor to regulate TASK-1 activity in HEK 293 cells [125] and 4) it was recently suggested that this subunit may contribute to pathophysiological changes in the systemic vasculature and in the pulmonary arteries [31;123]. In two recent investigations, a prominent expression of NOX1 and NOX4 was demonstrated in colon and kidney, respectively, by northern blotting [34;126]. In a previous study, an NADPH oxidase homolog NOX1 was identified in homogenised rabbit lungs, and in PASMC [127]. Recently, NOX4 was suggested to be the predominant NOX2-homolog in human airway and pulmonary arterial smooth muscle cells [119;123] and Liu and colleagues provided evidence that the phagocytic NADPH oxidase subunit NOX2 plays an important role in the development of hypoxia-induced pulmonary hypertension [99]. With respect to the current findings Suliman and coworkers have also supported a possible role for NOX4 in the context of oxygen sensing in the mouse kidney, demonstrating induced expression of the renal-specific NADPH oxidase (NOX4) under hypoxic conditions [128]. The selective up-regulation of NOX4 in chronic hypoxic mouse lung may indicate its importance in vascular remodeling process.

6.2 *Comparison of hypoxic regulation of NOX2 and NOX4 in the pulmonary vasculature*

Remodeling of small pulmonary arteries is considered to be the major cause of the increase in vascular resistance occurring during chronic hypoxia, therefore hypoxia-dependent regulation of NOX4 and NOX2 mRNA was investigated in the vessels of the murine pulmonary vasculature, since NOX2 has been suggested to play a pivotal role in the development of chronic hypoxia-induced pulmonary hypertension by Liu *et al.* [99]. Real time PCR analysis revealed that NOX4, in contrast to NOX2, is elevated in the pulmonary vasculature by chronic hypoxia: up-regulation of NOX4 but not of NOX2 occurred in the pulmonary arteries within 21 days of exposure to hypoxia, as demonstrated by quantitative PCR of microdissected vessels. Moreover, *in situ* hybridization revealed that NOX4 transcripts were localized to the pulmonary artery smooth muscle layer. The hypoxia-dependent increase in NOX4 expression levels in the pulmonary vasculature correlated well with the development of pulmonary hypertension [129] and was corroborated further at the protein level: 1) NOX4-immunoreactivity was detected in the pulmonary vasculature by immunostaining, and 2) the percentage of NOX4 immunoreactive vessels was strongly increased by chronic alveolar hypoxia with an increase in the number of NOX4-positive small vessels. The up-regulation at

the protein level preceded the regulation on the mRNA level. This suggests that NOX4 can be regulated on both the mRNA and the protein level. The differential regulation of NOX4 and NOX2 can also be due to their different activation mechanisms. While the activation of NOX1, NOX2 and NOX3 is dependent on the presence of additional cytosolic subunits such as $p47^{phox}$ and $p67^{phox}$ (for NOX2 activation) or NOXO1 and NOXA1 (for NOX1 activation), the activation of NOX4 is independent of such cytosolic subunits [130]. The co-expression studies done by Kawahara *et al.* have demonstrated that NOX4 can generate ROS independent of the cytosolic subunits [130]. The Real time PCR analysis of lung homogenates from mice exposed to hypoxia revealed a selective up-regulation of NOX4 and down-regulation of the other cytosolic subunits essential for NOX1 and NOX2 activation. In this regard, the up-regulation of NOX4 can be viewed as significantly more important in the state of chronic hypoxia compared to NOX2, which is more dependent on the presence of cytosolic subunits for its activation. At the subcellular level, the perinuclear localisation of NOX4 in the PASMC supports the notion of the presence of the protein in the endoplasmic reticulum (ER), as recently demonstrated in microvascular endothelial cells by Görlach and coworkers [131]. The presence of NOX4 in the ER further suggests an important role of NOX4 in maintaining the redox potential and Ca^{2+}-homeostasis in PASMC [132].

The findings of Liu *et al.* that NOX2 is essential for development of hypoxia-induced pulmonary hypertension, together with the fact that we as well as Liu *et al.* were unable to detect regulation of NOX2 in pulmonary arteries by hypoxia, are suggestive that NOX2 and NOX4 may play a differential role in the development of hypoxia-induced pulmonary hypertension. Hypothetically, endothelial ROS generation by NOX2 may stimulate NOX4 up-regulation in the vessel media, which would be important for hypoxia-dependent PASMC proliferation. In line with this argumentation is the detection primarily of NOX2 in pulmonary vascular endothelial cells in the current study, as well as two recent reports demonstrating a ROS-dependent up-regulation of NOX4 in cardiac cells [133;134].

6.3 *Role of NOX4 in idiopathic pulmonary arterial hypertension (IPAH) and regulation of human PASMC proliferation by ROS generation*

A possible role of NOX4 in the pathogenesis of pulmonary hypertension in general was supported by the fact that NOX4 is up-regulated in the vessel media of lung sections from patients with IPAH that underwent lung transplantation, compared to healthy donor lungs. The fact that NOX4 is up-regulated in the vessel media in both hypoxia-induced pulmonary

hypertension and in human IPAH may be explained by distinct or common regulators of NOX4. With regard to the latter it has been shown that TGF-β can upregulate NOX4 in human PASMC [123], that hypoxia can increase TGF-β in PASMC [135], and that interference with TGF-β blocks hypoxia-induced vascular remodeling [136]. Interestingly, it has been shown that TGF-β can *vice versa* be regulated by ROS [137]. In addition, it appears that NOX4 dependent regulation of human PASMC proliferation is via ROS generation as silencing of NOX4 reduced human PASMC proliferation and ROS production. These findings are in agreement with the recent work of Sturrock *et al.* who also observed up-regulation of NOX4 by TGF-β and reduced proliferation of human PASMC on silencing of NOX4 [123]. Thus, hypoxia-induced and human IPAH may share some common pathophysiological mechanisms with regard to NOX4.

6.4 *NOX4 mediated regulation of K_{DR} channels Kv1.5 and Kv2.1 at the functional level (electrophysiology)*

The K_{DR} channels belong to a subfamily of voltage-gated K^+ channels and are responsible for maintaining the membrane potential of resistance PASMC due to their high abundance in the lower segments of pulmonary vasculature [63;138] . Many reports have documented that vascular remodeling in chronic hypoxia induced pulmonary hypertension is due to reduced K_{DR} channel function and increased calcium influx in PASMC [59]. The selective inhibition of K_{DR} channels in the pulmonary vasculature has attracted much attention with the aim to identify the underlying mechanism behind this process. The role of oxidative stress has recently been shown by several reports in the regulation of Kv channels by oxidative modification at key cysteine residues [139] [112]. There are several sources of oxidative stress in the cell including mitochondria, xanthine oxidases, cyclooxygenase, uncoupled nitric oxide synthase and NADPH oxidases. Of these various sources, NADPH oxidases have recently gained the focus of main ROS producing enzymes in the vessels [140]. Previous reports have indicated that $gp91^{phox}$ (NOX2) at least is not responsible for hypoxia mediated inhibition of Kv current in the mouse lung [141]. However, there is no evidence yet which suggests the involvement of NOX4-derived ROS in the regulation of K_{DR} channels in the lung vasculature. Thus, to delineate the downstream signaling pathway of NOX4, two hypoxia-sensitive members of the K_{DR} subfamily, Kv1.5 and Kv2.1, were investigated since: 1) Kv2.1 channel has been shown to be an important determinant in maintaining the resting *Em* in resistance PASMC and application of an antibody against Kv2.1 in electrophysiological preparation abolished further hypoxic inhibition of I_{Kv} in PASMC [115;116], 2) both of these channels are abundantly expressed

in resistance PASMC at protein and mRNA level [88], 3) the expression of both channels is down-regulated in PASMC under chronic hypoxia at the mRNA and protein levels [86;87], 4) Kv1.5 knockout mice exhibit impaired hypoxic pulmonary vasoconstriction [67] and 5) down-regulation of Kv channels in hypoxia has been linked to decreased apoptosis and increased proliferation due to intracellular inhibition of caspases [90;142].

Therefore, in an attempt to investigate a functional relationship between NOX4 and K_{DR} channels, a strong co-localisation of NOX4 with Kv1.5 and Kv2.1 channels on both rat lung sections and isolated PASMC was observed. The NOX4 mediated regulation of K_{DR} currents in rat PASMC was corroborated at the functional level by electrophysiology (whole cell configuration). The treatment of rat PASMC with 0.5 mM apocynin under hypoxia resulted in a significant increase in the whole cell K_{DR} current. When antibodies specific for Kv1.5 and Kv2.1 channels were added in the intracellular pipette solution, a significant 55% inhibition of the whole cell K_{DR} current was observed, indicating that both channels conduct a large portion of the K_{DR} current. Similar observations have been noted in previous reports [115, 116]. No time dependent attenuation of K_{DR} current (wash out or run down) was observed until 22 min after establishment of the whole cell configuration. The portion of the whole cell K_{DR} current blocked by Kv1.5 and Kv2.1 antibodies was equivalent to the current blocked by hypoxia, since no further inhibition of K_{DR} currents by Kv1.5 and Kv2.1 antibodies was observed in hypoxic cells. From this observation, it is clear that both channels conduct the main hypoxia sensitive component of the whole cell K_{DR} current in rat PASMC, which has also been indicated in previous reports [115;116]. However, apocynin treatment of cells under hypoxia resulted in the reappearance of Kv1.5 and Kv2.1 specific current formerly blocked by hypoxia. Since apocynin has been suggested to be a ROS scavenger in PASMC [143], it can be suggested that the reduced function of K_{DR} channels under chronic hypoxic conditions is most likely due to increased ROS production. The role of ROS in regulation of pulmonary vascular tone is still controversial. Whereas some reports suggested an increase of ROS [29;30] others reports suggestsed a decrease under hypoxia [3;25]. In this regard, in the current study an increased ROS production was observed under chronic hypoxia, whereas the treatment with NOX4 siRNA caused a pronounced decrease in ROS production. Along this line, Cogolludo *et al.* have demonstrated that U46619 inhibited Kv currents in rat PASMC by an increase in ROS and that treatment of rat PASMC with apocyin reverted this effect [144]. The data were further supported by the use of NOX4 specific siRNA in rat PASMC which also significantly increased the whole cell K_{DR} current under chronic hypoxic conditions. Intriguingly, the

stimulatory effect of apocynin and NOX4 siRNA on the whole cell K_{DR} current was observed only under chronic hypoxia, whereas under normoxia, apocynin and NOX4 siRNA had no significant effect on the K_{DR} current (data not shown). These findings suggest that NOX4 mediated inhibition of K_{DR} channels is operational only under chronic hypoxia. This fact is further strengthened by the up-regulation of NOX4 under chronic hypoxia which can generate a large amount of oxidative species such as O_2^- and H_2O_2 which may exert an inhibitory effect on K_{DR} channel function. In this regard, it has previously been shown that oxidant production decreases the activity of cloned shaker K^+ channels (Kv1.3, Kv1.4 and Kv1.5), shaw (Kv3.4) and an inward rectifier K^+ channel (IRK3) in *Xenopus* oocytes, whereas Kv1.2, Kv2.1 and Kv2.2 were resistant to oxidants [145]. Similar findings have been reported in frog cardiac myocytes and in rat PASMC [144;146]. The action of oxidants on the K^+ channel activity is conferred by the oxidative modification at key cystine and methionine residues at the N-terminal inactivation ball domain and pore domain. Oxidants can affect two different inactivation mechanisms of Kv channels: involving N-type inactivation, which is mediated by N-terminal ball and chain mechanism; and P/C type inactivation which involves constriction of the ion conductance pathway. Oxidants can disrupt the N-type inactivation of shaker type K^+ channels by methionine oxidation [113] and may accelerate P/C type inactivation of shaker type K^+ channels in the absence of N-type inactivation [147]. The kinetics of a calcium activated K^+ channel (BK_{ca}) are also affected by H_2O_2, where calcium dependent activation of the BK_{Ca} channel is disrupted by modification of a cysteine residue near the C-terminal calcium bowl domain [112].

Against this background, a significantly increased activation of K_{DR} current and a shift towards more hyperpolarised potentials by siNOX4 treatment under chronic hypoxia was observed. The conductance voltage relationship can be described by the Boltzman equation, $G/Gmax=1/(1+e^{-(V-V_{1/2})}/K)^n$, where K is the slope factor, V is the test potential and $V_{1/2}$ is the voltage required for half maximal conductance. Using this equation Kv1.5 channels have been reported to have $V_{1/2}$ and K values around -10 mV and 7 mV respectively, whereas for Kv2.1 and Kv2.2 channels these values are 10 mV and 5 to 19 mV respectively [148]. In this regard, we have observed that the activation kinetics of K_{DR} current under chronic hypoxia is very similar to that observed for Kv2.1 and Kv2.2 channels. However, the activation kinetics after NOX4 siRNA treatment under chronic hypoxia resembles the pattern observed for the Kv1.5 channel. This finding may indicate that the effect of NOX4-derived ROS production may specifically inhibit oxidation-sensitive K_{DR} channels such as Kv1.5, which is in agreement

with the previous finding that the Kv1.5 channel is sensitive to oxidant production, whereas the Kv2.1 and Kv2.2 channels are resistant to any inhibition by oxidants [145]. However, further investigations are required to understand the ROS mediated inhibition of the K_{DR} channels under chronic hypoxia.

6.5 *Role of NOX4 in regulation of calcium influx under chronic hypoxia*

Calcium is an important intracellular signaling molecule responsible for various physiological and pathological processes such as contraction, cell growth and proliferation, gene expression and vascular remodeling [55]. Calcium homeostasis in the cell is achieved by the presence of at least three different categories of Ca^{2+} channel which are: 1) voltage dependent Ca^{2+} channels (VDCC) such as L-type Ca^{2+} channels which are regulated by changes in membrane potential, 2) receptor operated Ca^{2+} channels (ROC) which are activated by the interaction of agonists with the respective receptors such as ryanodine receptor Ca^{2+} release channels in the endoplasmic reticulum (ER), and 3) store operated Ca^{2+} channels (SOC) which are opened by depletion of Ca^{2+} from ER and lead to influx of Ca^{2+} ions from extracellular source, a mechanism known as capacitative Ca^{2+} entry (CCE) [149]. Recent investigations have suggested that calcium regulation in PASMC in response to hypoxia is an intricate signaling process involving a cross talk between extracellular calcium influx and intracellular calcium release. This complex signaling network of calcium regulation is due to the presence of multiple Ca^{2+} channel present in the plasma membrane which differ in their regulatory mechanism by different stimuli. Moreover, presence of intracellular calcium stores such as ryanodine sensitive calcium stores in the ER, IP_3 sensitive calcium stores and mitochondria further increases this complexity. It is suggested that chronic hypoxia induced vascular remodeling is mediated by increased levels of calcium in PASMC [55]. Many reports have been published on the regulation of calcium influx under chronic hypoxia in the last decade which has greatly enhanced our understanding of calcium regulation during chronic hypoxia. But still there are many unresolved questions: 1) it is not clear yet what is the primary stimulus mediating calcium influx during acute HPV, 2) which calcium channels are responsible for maintaining increased calcium levels during chronic hypoxia and how they are regulated. Focussing on the regulation of calcium influx during chronic hypoxia, the role of NADPH oxidase generated oxidative stress was investigated in these processes in rat PASMC on ET-1 stimulation. Previous reports have suggested that ET-1 is up-regulated during chronic hypoxia induced pulmonary hypertension, and stimulates a biphasic calcium response in PASMC, consisting of a rapid transient peak followed by a sustained increase in intracellular calcium levels [13;150].

This biphasic response has been suggested due to a complex signaling process involving 1) calcium influx via L-type calcium channels due to ET-1 mediated inhibition of Kv channels and 2) calcium release from intracellular ryanodine and IP_3 sensitive calcium stores by a calcium induced calcium release (CICR) mechanism [151]. In this regard, a very similar biphasic response to ET-1 stimulation was observed in rat PASMC in the current investigation. Moreover apocynin treatment of rat PASMC abolished the ET-1 stimulated transient calcium increase and delayed the sustained increase in calcium. In addition, the overall ET-1 stimulated calcium influx under chronic hypoxia was lower in apocynin treated PASMC compared to the DMSO treated controls. These findings were further supported by the use of NOX4 specific siRNA which decreased the ET-1 stimulated calcium influx under normoxic conditions and abolished it completely under chronic hypoxia. These data thus provide the evidence that ET-1 mediated calcium influx under chronic hypoxia is mainly mediated by NOX4 derived ROS production. However, under normoxic conditions, there could be additional regulatory mechanisms which could regulate ET-1 mediated calcium influx independent of NOX4. The specific role of NOX4 derived oxidative stress in regulation of calcium influx under chronic hypoxia is also in agreement with the real time PCR data which revealed a selective up-regulation of NOX4 in chronic hypoxic mouse lung homogenate. Analogous to these findings, Rathore *et al.* have recently reported that the acute hypoxia mediated increase in calcium levels was attenuated after apocynin treatment and in isolated PASMC from $p47^{phox}$ knockout mice [50].

According to the classical theory of redox oxygen sensing, the L-type calcium channels are responsible for the calcium influx during acute HPV and may also be responsible for sustaining increased calcium levels in PASMC during chronic hypoxia [24]. Supporting this hypothesis some reports have suggested that blockers of L-type calcium channels such as nifedipine and verapamil attenuate hypoxia induced pulmonary hypertension [152]. In contrast, another group reported that nifedipine did not affect hypoxia induced pulmonary hypertension in chronically hypoxic rats [153]. However, it has been recently recognised that under chronic hypoxic conditions besides L-type calcium channels, other calcium channels such as store operated and receptor operated calcium channels are important regulators of the calcium influx [150, 93]. The classical transient receptor potential channels (TRPC) constitute the alternative pathways of calcium entry in PASMC. Seven members are included in TRPC gene family (TRPC1-TRPC7). Of these, TRPC1 exhibits store operated calcium entry whereas TRPC3 and TRPC6 are involved in receptor operated calcium entry. Lin. et al have

demonstrated that TRPC1, TRPC3 and TRPC6 are expressed in rat PASMC whereas TRPC1 and TRPC6 are up-regulated under chronic hypoxia [93]. Furthermore, recently published data from our laboratory showed in TRPC6 knockout a complete disappearance of the acute phase of hypoxia induced pulmonary vasoconstriction [54].

To date, there is no report in the literature which suggests the role NOX4 in regulation of calcium influx under chronic hypoxia. In this regard the current study demonstrated for the first time an essential role of NOX4 in ET-1 mediated calcium influx under chronic hypoxia. However, the mechanism of NOX4 mediated regulation of calcium influx has to be further investigated. It is also not clear if NOX4 regulates the calcium influx from the extracellular milieu or the release of calcium from the intracellular stores under chronic hypoxia. Possible mechanisms may include ET-1 mediated activation of NOX4 in the ER or plasma membrane resulting in superoxide production which can increase the calcium influx via TRPC channels, L-type calcium channels or from intracellular compartments such as ryanodine sensitive and IP_3 sensitive calcium stores (Fig. 28). Regarding this possibility an increased ROS production was observed in PASMC on ET-1 stimulation under chronic hypoxia. Moreover, ET-1 stimulated ROS production was significantly decreased in PASMC treated with NOX4 siRNA. Along this line it has been demonstrated previously that ET-1 can increase ROS production by NADPH oxidase activation and can also increase the open probability of L-type calcium channels [97;154;155]. Moreover, oxidants such as hydrogen peroxide have recently been shown to accelerate calcium release from intracellular stores in rat PASMC and NOX4 has been shown to produce a large amount of hydrogen peroxide [156;157]. In contrast to this, a reduced ET-1 stimulated calcium influx was observed under chronic hypoxia in spite of a NOX4 up-regulation. The potential reason behind this discrepancy could be high levels of calcium which can activate some adaptive mechanisms inside the hypoxic PASMC to prevent further calcium increase by oxidative stress coming from NOX4 (Fig. 28). For example, Shimoda *et al.* have shown that high levels of calcium may desensitise ryanodine sensitive calcium channels in ER. Thus, calcium induced calcium release (CICR) from intracellular stores is inhibited [150]. Nevertheless, NOX4 seems to be essential for ET-1 stimulated calcium release under chronic hypoxia. However, a complete understanding of this mechanism requires further investigation.

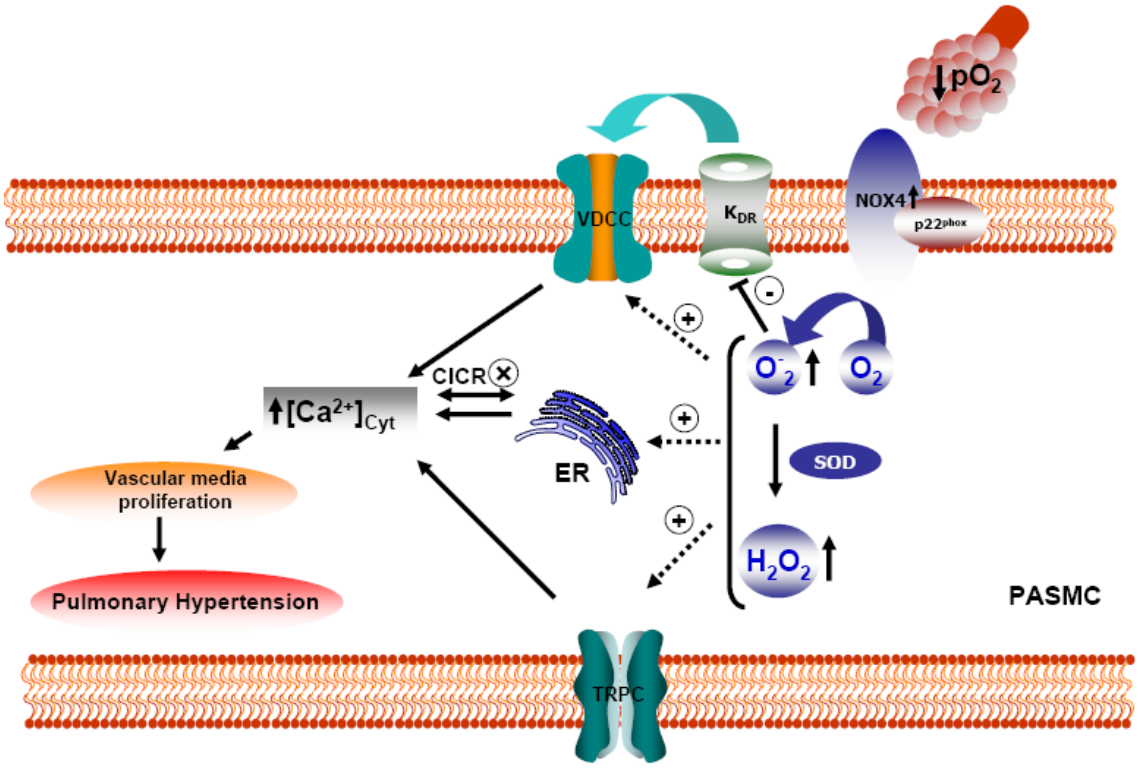

Fig.28 Schematic presentation of NOX4 mediated regulation of K_{DR} channels and calcium influx under chronic hypoxia in PASMC. Under chronic hypoxia an up-regulation of NOX4 can inhibit K_{DR} channel function possibly by oxidative modification of cysteine residues due to increased ROS production and regulating N-type inactivation or P/C type inactivation. In addition, NOX4 derived ROS production may regulate calcium influx via affecting voltage dependent calcium channels (VDCC) such as L-type calcium channels, canonical transient receptor potential channels (TRPC) or through the ryanodine sensitive calcium release channels in endoplasmic reticulum (ER). High intracellular calcium concentration can lead to vascular media proliferation and pulmonary hypertension. SOD- superoxide dismutase; CICR- calcium induced calcium release.

In conclusion, presented data in the current study suggest that 1) NOX4 is significantly up-regulated in pulmonary arterial vessels during chronic hypoxia, both at the transcriptional and protein levels, 2) NOX4 plays an important role in regulating PASMC proliferation, 3) NOX4 may be involved in the pathogenesis of IPAH, 4) NOX4 derived ROS inhibit K_{DR} channel function under chronic hypoxia and 5) NOX4 is important for the ET-1 mediated calcium influx under chronic hypoxia.

Together these findings suggest a role for NOX4 and its downstream signaling pathway in chronic hypoxia-induced vascular remodeling process. With regard to the up-regulation of NOX4 in hypoxia-induced pulmonary hypertension and IPAH patients, a functional interference with NOX4 or its down-stream pathway may offer a new therapeutic approach for the treatment of this disease. However, further investigations, for example on NOX4 are needed to fully prove the relevance of NOX4 in pathogenesis of hypoxia-induced pulmonary hypertension.

7 SUMMARY

The pulmonary vasculature has the unique ability to undergo vasoconstriction in response to acute hypoxia, a physiological mechanism known as hypoxic pulmonary vasoconstriction (HPV). Sustained or chronic hypoxia, however, leads to proliferation of vascular smooth muscle cells of pulmonary arterioles, which causes a permanent increase in pulmonary vascular resistance, and may lead to right heart dysfunction. The underlying mechanisms of vascular proliferation under chronic hypoxia have not been fully defined. The NADPH oxidases are one family of recently discovered molecules which generate reactive oxygen species (ROS) and have been suggested to be important for cellular signaling under physiological conditions. However, NADPH oxidase generated oxidative stress can also lead to inflammation, vascular smooth muscle cell proliferation and endothelial damage under pathological conditions. Many homologs of NADPH oxidases exist, the classical homolog is gp91phox or NOX2, and the recently discovered homologs include NOX1, NOX3, NOX4, NOX5, DUOX1 and DUOX2. Superoxide production by classical gp91phox is induced by assembly of the cytosolic subunits such as p40phox, p47phox and p67phox with membrane-bound gp91phox complex. A previous report from our laboratory has shown that the knockout mice of $p47^{phox}$ subunit exhibit reduced acute HPV as compared to wild type mice suggesting an essential role of NADPH oxidases in regulation of vascular tone in acute hypoxia. Against this background, the current thesis aimed to elucidate the role of NADPH oxidases in vascular remodeling in chronic hypoxia, and its possible downstream mediators. Screening of NADPH oxidase expression revealed that all subunits were expressed in the lung homogenate and that NOX4 was prominently up-regulated under chronic hypoxia. The NOX4 mRNA was also up-regulated in the microdissected vessels of mice exposed up to three weeks of chronic hypoxia. In addition, a functional interference with NOX4 using NOX4 siRNA resulted in reduced ROS production and reduced proliferation of pulmonary arterial smooth muscle cells (PASMC) revealing an important contribution of NOX4 in PASMC proliferation and particularly in hypoxia induced pulmonary hypertension. Intriguingly, a similar reflection was found in lungs of patients with idiopathic pulmonary hypertension that underwent lung transplantation. Further experiments demonstrated that NOX4 inhibited voltage-gated delayed rectifier K^+ channels (K_{DR}) under hypoxia. Pharmacological inhibition with apocynin and genetic ablation with NOX4siRNA resulted in increased K_{DR} current under hypoxia. In addition, the current study demonstrated that NOX4 is essential for ET-1 mediated calcium influx in PASMC as NOX4 knockdown using NOX4 siRNA abolished the ET-1 mediated

calcium influx under chronic hypoxia. Thus, the NOX4-ROS-K_{DR}-[Ca^{2+}] pathway may contribute to the development of pulmonary hypertension.

8 ZUSAMMENFASUNG

Das pulmonale Gefäßsystem besitzt die besondere Eigenschaft, auf akute Hypoxie mit einer Vasokonstriktion zu reagieren. Dies ist ein physiologischer Mechanismus, der als hypoxische pulmonale Vasokonstriktion (HPV) bezeichnet wird. Anhaltende oder chronische Hypoxie führt darüberhinaus zu einer Proliferation der Media der Lungenarteriolen, das einen permanenten Anstieg des pulmonalen Gefäßwiderstandes auslöst, der im weiteren zu einem *Cor pulmonale* führen kann. Die der HPV zu Grunde liegenden Mechanismen sind bisher noch nicht umfassend geklärt worden. NADPH-Oxidasen sind eine vor kurzem entdeckte Proteinfamilie, die reaktive Sauerstoffspezies (ROS) generieren können und unter physiologischen Bedingungen für die zelluläre Signaltransduktion wichtig sind. Andererseits können die von NADPH-Oxidasen stammenden ROS unter pathologischen Bedingungen zu Entzündung und Proliferation von vaskulären glatten Muskelzellen und zur Schädigung des Endothels führen. In der Literatur sind mehrere Homologe von NADPH-Oxidasen beschrieben, wobei das klassische Homolog als gp91phox oder NOX2 bekannt ist. Weitere, erst kürzlich entdeckte Homologe umfassen NOX1, NOX3, NOX4, NOX5, DUOX1 und DUOX2. Die Superoxidproduktion der klassischen gp91phox wird durch die Anlagerung der zytosolischen Untereinheiten p40phox, p47phox und p67phox an gp91phox induziert. Unsere bisherigen Daten zeigen, dass Mäuse mit einer p47phox-Defizienz im Vergleich zu Wildtyp-Mäusen eine geringere akute HPV aufweisen, das auf eine essentielle Rolle der NADPH-Oxidasen für die Regulation des vaskulären Tonus unter akuter Hypoxie hinweist.

Ziel der vorliegenden Arbeit war, die Rolle der NADPH-Oxidasen für den vaskulären Umbauprozess unter chronischer Hypoxie und deren Signaltransduktionsmechanismen aufzuklären. Untersuchungen der NADPH-Oxidasen Expression zeigten, dass alle Untereinheiten im Lungenhomogenat exprimiert waren und die Expression von NOX4 unter chronischer Hypoxie stark hochreguliert war. Darüberhinaus war die NOX4-mRNA auch in den durch Mikrodissektion gewonnenen Gefäßen der Mäuse, die 3 Wochen unter chronischer Hypoxie gehalten wurden, hochreguliert. Zusätzlich bewirkte eine funktionelle Interferenz von NOX4 mit NOX4-siRNA eine reduzierte ROS-Produktion und eine verringerte Proliferation der pulmonalarteriellen glatten Muskelzellen (PASMC). Dies weist auf eine bedeutungsvolle Rolle von NOX4 für die Proliferation von PASMC, insbesondere bei Hypoxia-induzierter pulmonaler Hypertonie, hin. Interessanterweise wurden ähnliche Ergebnisse in Lungen von Patienten mit idiopatischer pulmonaler Hypertonie nach Transplantation der Lunge gewonnen. Weitere Experimente zeigten, dass NOX4 unter

chronischer Hypoxie die *voltage gated delayed rectifier* K^+-Kanäle (K_{DR}) hemmt. Eine pharmakologische Inhibition von NOX4 mittels Apocynin oder eine genetische Ablation durch siRNA erhöhten den K_{DR}-Strom unter chronischer Hypoxie. Zusätzlich ist in der vorliegenden Arbeit gezeigt, dass NOX4 essentiell für den ET-1 vermittelten Kalziumeinstrom ist, da durch Reduzierung von NOX4 mittels NOX4 siRNA der ET-1 vermittelte Kalziumeinstrom unter chronischer Hypoxie nicht mehr vorhanden war.

Zusammengefasst gesagt, könnte der NOX4-ROS-K_{DR}-[Ca^{2+}]-Signalweg somit zur Entstehung der pulmonalen Hypertonie beitragen.

9 ABBREVIATIONS

Apo	apocynin
AOS	activated oxygen species
ADP	adeonsine di-phosphate
ATP	adenosine triphosphate
BSA	bovine serum albumin
CCE	capacitative calcium entry
cGMP	cyclic guanosine monophosphate
cADPR	cyclic adeonsine di-phosphate riobse
CO	carbon mono oxide
CYP	cytochrome p-450
$[Ca^{2+}]i$	intracellular calcium concentration
DMSO	dimethylsulfoxide
DUOX	dual oxidase
EDTA	ethylenediaminetetraacetic acid
EETs	epoxyeicosatetraenoic acid
EGTA	ethylene glycol-bis (2-aminoethylether)-N,N,N',N'-tetraacetic acid
EMSA	electromobility shift assay
ER	endoplasmic reticulum
ET-1	endothelin-1
ETC	electron transport chain
FCS	foetal Calf Serum
FITC	fluorescein Isothiocyanate
g	gramm
G	gauge
H_2O_2	hydrogen per oxide
HETEs	hydroepoxyeicosatetraenoic acid
HIF	hypoxia Inducible Factor
HO	heme oxygenase
HOX	hypoxia
HPV	hypoxic Pulmonary Vasoconstriction
HRE	hypoxia responsive element
IPAH	idioptathic pulmonary arterial hypertension
$BKCa^{2+}$	calcium activate potassium channel
K^+	potassium ion
K_A	A-type potassium channel
K_{DR}	delayed rectifier potassium channel
Kir	inward rectifier potassium channel
K^+ATP	ATP sensitive potassium channel
kg	kilogramm
Kv-channel	voltage-dependend potassium channel
l	liter
M	molar
mRNA	messenger ribo nucleic acid
ml	milliliter
mM	millimolar
µM	micromolar
n	number of experiments
NADP	nicotinamide adenine di-nucleotide phosphate (oxidised)

NADPH	nicotinamide adenine di-nucleotide phosphate (reduced)
nM	nanomolar
NO	nitric oxide
NOS	nitric oxide synthase
NOX	normoxic
NOX1	NADPH oxidase homolog 1
NOX2	NADPH oxidase homolog 2 (gp 91phox)
NOX4	NADPH oxidase homolog 4 (Renox)
O_2^-	superoxidradikal
O_2	oxygen
OH^-	hydroxyl radical
PASMC	pulmonary Arterial Smooth Muscle cells
pA/pF	current density
PBS	phosphatpufferlösung
Po	open probability of channel
pCO_2	partial pressure of carbon di-oxide
pO_2	partial pressure of oxygen
ps	pico siemens
PAP	pulmonary arterial pressure
PIP_2	phosphatidylinositolbisphosphate
PKC	proteinkinase C
PKG	proteinkinase G
RT-PCR	reverse transcriptase polymerase chain reaction
PLC	phospholipase C
pVHL	von Hippel-Lindau
ROC	receptor-operated Ca^{2+}channel
ROS	reactive oxygen species
RyRs	ryanodine receptors
rpm	revolution per minute
sGC	soluble guanylyl cyclase
siRNA	small interfering RNA
SEM	standard error of mean
SOD	super oxide dismutase
SR	sarcoplasmic reticulum
TWIK	weakly inward rectifying potassium channel
SMC	smooth muscle cell
SM-α Actin	alpha-smooth muscle actin
SOC	store-operated Ca^{2+}channel
U	units
VDCC	voltage-dependent Ca^{2+} channel
Vm	membrane potential
WT	wildtype

10 REFERENCE LIST

1. Hillier, S. C., J. A. Graham, C. C. Hanger, P. S. Godbey, R. W. Glenny, and W. W. Wagner, Jr. 1997. Hypoxic vasoconstriction in pulmonary arterioles and venules. *J.Appl.Physiol* 82:1084-1090.

2. Staub, N. C. 1985. Site of hypoxic pulmonary vasoconstriction. *Chest* 88:240S-245S.

3. Moudgil, R., E. D. Michelakis, and S. L. Archer. 2005. Hypoxic pulmonary vasoconstriction. *J.Appl.Physiol* 98:390-403.

4. Yamaguchi, K., K. Suzuki, K. Naoki, K. Nishio, N. Sato, K. Takeshita, H. Kudo, T. Aoki, Y. Suzuki, A. Miyata, et al. 1998. Response of intra-acinar pulmonary microvessels to hypoxia, hypercapnic acidosis, and isocapnic acidosis. *Circ.Res.* 82:722-728.

5. Weissmann, N., N. Sommer, R. T. Schermuly, H. A. Ghofrani, W. Seeger, and F. Grimminger. 2006. Oxygen sensors in hypoxic pulmonary vasoconstriction. *Cardiovasc.Res.* 71:620-629.

6. Marshall, B. E. and C. Marshall. 1980. Continuity of response to hypoxic pulmonary vasoconstriction. *J.Appl.Physiol* 49:189-196.

7. Maggiorini, M. and F. Leon-Velarde. 2003. High-altitude pulmonary hypertension: a pathophysiological entity to different diseases. *Eur.Respir.J.* 22:1019-1025.

8. Stenmark, K. R., K. A. Fagan, and M. G. Frid. 2006. Hypoxia-induced pulmonary vascular remodeling: cellular and molecular mechanisms. *Circ.Res.* 99:675-691.

9. Means, A. R. 1994. Calcium, calmodulin and cell cycle regulation. *FEBS Lett.* 347:1-4.

10. Murray, T. R., L. Chen, B. E. Marshall, and E. J. Macarak. 1990. Hypoxic contraction of cultured pulmonary vascular smooth muscle cells. *Am.J.Respir.Cell Mol.Biol.* 3:457-465.

11. Bennie, R. E., C. S. Packer, D. R. Powell, N. Jin, and R. A. Rhoades. 1991. Biphasic contractile response of pulmonary artery to hypoxia. *Am.J.Physiol* 261:L156-L163.

12. Ward, J. P. and T. P. Robertson. 1995. The role of the endothelium in hypoxic pulmonary vasoconstriction. *Exp.Physiol* 80:793-801.

13. Aaronson, P. I., T. P. Robertson, and J. P. Ward. 2002. Endothelium-derived mediators and hypoxic pulmonary vasoconstriction. *Respir.Physiol Neurobiol.* 132:107-120.

14. Toda, N. and T. Okamura. 2003. The pharmacology of nitric oxide in the peripheral nervous system of blood vessels. *Pharmacol.Rev.* 55:271-324.

15. Lincoln, T. M. 1989. Cyclic GMP and mechanisms of vasodilation. *Pharmacol.Ther.* 41:479-502.

16. Lincoln, T. M. and T. L. Cornwell. 1993. Intracellular cyclic GMP receptor proteins. *FASEB J.* 7:328-338.

17. Burke, T. M. and M. S. Wolin. 1987. Hydrogen peroxide elicits pulmonary arterial relaxation and guanylate cyclase activation. *Am.J.Physiol* 252:H721-H732.

18. Cai, H., Z. Li, S. Dikalov, S. M. Holland, J. Hwang, H. Jo, S. C. Dudley, Jr., and D. G. Harrison. 2002. NAD(P)H oxidase-derived hydrogen peroxide mediates endothelial nitric oxide production in response to angiotensin II. *J.Biol.Chem.* 277:48311-48317.

19. Le Cras, T. D. and I. F. McMurtry. 2001. Nitric oxide production in the hypoxic lung. *Am.J.Physiol Lung Cell Mol.Physiol* 280:L575-L582.

20. Fleming, I. and R. Busse. 1999. Signal transduction of eNOS activation. *Cardiovasc.Res.* 43:532-541.

21. Thannickal, V. J. and B. L. Fanburg. 2000. Reactive oxygen species in cell signaling. *Am.J.Physiol Lung Cell Mol.Physiol* 279:L1005-L1028.

22. Leach, R. M., H. S. Hill, V. A. Snetkov, and J. P. Ward. 2002. Hypoxia, energy state and pulmonary vasomotor tone. *Respir.Physiol Neurobiol.* 132:55-67.

23. Kobertz, W. R., C. Williams, and C. Miller. 2000. Hanging gondola structure of the T1 domain in a voltage-gated K(+) channel. *Biochemistry* 39:10347-10352.

24. Archer, S. L., J. A. Will, and E. K. Weir. 1986. Redox status in the control of pulmonary vascular tone. *Herz* 11:127-141.

25. Archer, S. L., J. Huang, T. Henry, D. Peterson, and E. K. Weir. 1993. A redox-based O2 sensor in rat pulmonary vasculature. *Circ.Res.* 73:1100-1112.

26. Leach, R. M., H. M. Hill, V. A. Snetkov, T. P. Robertson, and J. P. Ward. 2001. Divergent roles of glycolysis and the mitochondrial electron transport chain in hypoxic pulmonary vasoconstriction of the rat: identity of the hypoxic sensor. *J.Physiol* 536:211-224.

27. Waypa, G. B., N. S. Chandel, and P. T. Schumacker. 2001. Model for hypoxic pulmonary vasoconstriction involving mitochondrial oxygen sensing. *Circ.Res.* 88:1259-1266.

28. Rounds, S. and I. F. McMurtry. 1981. Inhibitors of oxidative ATP production cause transient vasoconstriction and block subsequent pressor responses in rat lungs. *Circ.Res.* 48:393-400.

29. Guzy, R. D. and P. T. Schumacker. 2006. Oxygen sensing by mitochondria at complex III: the paradox of increased reactive oxygen species during hypoxia. *Exp.Physiol* 91:807-819.

30. Waypa, G. B., J. D. Marks, M. M. Mack, C. Boriboun, P. T. Mungai, and P. T. Schumacker. 2002. Mitochondrial reactive oxygen species trigger calcium increases during hypoxia in pulmonary arterial myocytes. *Circ.Res.* 91:719-726.

31. Cai, H., K. K. Griendling, and D. G. Harrison. 2003. The vascular NAD(P)H oxidases as therapeutic targets in cardiovascular diseases. *Trends Pharmacol.Sci.* 24:471-478.

32. Babior, B. M., J. D. Lambeth, and W. Nauseef. 2002. The neutrophil NADPH oxidase. *Arch.Biochem.Biophys.* 397:342-344.

33. Bokoch, G. M. and U. G. Knaus. 2003. NADPH oxidases: not just for leukocytes anymore! *Trends Biochem.Sci.* 28:502-508.

34. Suh, Y. A., R. S. Arnold, B. Lassegue, J. Shi, X. Xu, D. Sorescu, A. B. Chung, K. K. Griendling, and J. D. Lambeth. 1999. Cell transformation by the superoxide-generating oxidase Mox1. *Nature* 401:79-82.

35. Cheng, G., Z. Cao, X. Xu, E. G. van Meir, and J. D. Lambeth. 2001. Homologs of gp91phox: cloning and tissue expression of Nox3, Nox4, and Nox5. *Gene* 269:131-140.

36. Lambeth, J. D., G. Cheng, R. S. Arnold, and W. A. Edens. 2000. Novel homologs of gp91phox. *Trends Biochem.Sci.* 25:459-461.

37. Geiszt, M., J. B. Kopp, P. Varnai, and T. L. Leto. 2000. Identification of renox, an NAD(P)H oxidase in kidney. *Proc.Natl.Acad.Sci.U.S.A* 97:8010-8014.

38. Geiszt, M. 2006. NADPH oxidases: new kids on the block. *Cardiovasc.Res.* 71:289-299.

39. Griendling, K. K., D. Sorescu, and M. Ushio-Fukai. 2000. NAD(P)H oxidase: role in cardiovascular biology and disease. *Circ.Res.* 86:494-501.

40. Lassegue, B. and R. E. Clempus. 2003. Vascular NAD(P)H oxidases: specific features, expression, and regulation. *Am.J.Physiol Regul.Integr.Comp Physiol* 285:R277-R297.

41. Bedard, K. and K. H. Krause. 2007. The NOX family of ROS-generating NADPH oxidases: physiology and pathophysiology. *Physiol Rev.* 87:245-313.

42. Banfi, B., R. A. Clark, K. Steger, and K. H. Krause. 2003. Two novel proteins activate superoxide generation by the NADPH oxidase NOX1. *J.Biol.Chem.* 278:3510-3513.

43. Geiszt, M., K. Lekstrom, J. Witta, and T. L. Leto. 2003. Proteins homologous to p47phox and p67phox support superoxide production by NAD(P)H oxidase 1 in colon epithelial cells. *J.Biol.Chem.* 278:20006-20012.

44. Uchizono, Y., R. Takeya, M. Iwase, N. Sasaki, M. Oku, H. Imoto, M. Iida, and H. Sumimoto. 2006. Expression of isoforms of NADPH oxidase components in rat pancreatic islets. *Life Sci.* 80:133-139.

45. Miller, A. A., G. R. Drummond, H. H. Schmidt, and C. G. Sobey. 2005. NADPH oxidase activity and function are profoundly greater in cerebral versus systemic arteries. *Circ.Res.* 97:1055-1062.

46. Miller, A. A., G. R. Drummond, A. E. Mast, H. H. H. W. Schmidt, and C. G. Sobey. 2007. Effect of Gender on NADPH-Oxidase Activity, Expression and Function in the Cerebral Circulation: Role of Estrogen. *Stroke*.

47. Wolin, M. S., T. M. Burke-Wolin, and H. Mohazzab. 1999. Roles for NAD(P)H oxidases and reactive oxygen species in vascular oxygen sensing mechanisms. *Respir.Physiol* 115:229-238.

48. Marshall, C., A. J. Mamary, A. J. Verhoeven, and B. E. Marshall. 1996. Pulmonary artery NADPH-oxidase is activated in hypoxic pulmonary vasoconstriction. *Am.J.Respir.Cell Mol.Biol.* 15:633-644.

49. Weissmann, N., S. Zeller, R. U. Schafer, C. Turowski, M. Ay, K. Quanz, H. A. Ghofrani, R. T. Schermuly, L. Fink, W. Seeger, et al. 2006. Impact of mitochondria and NADPH oxidases on acute and sustained hypoxic pulmonary vasoconstriction. *Am.J.Respir.Cell Mol.Biol.* 34:505-513.

50. Rathore, R., Y. M. Zheng, C. F. Niu, Q. H. Liu, A. Korde, Y. S. Ho, and Y. X. Wang. 2008. Hypoxia activates NADPH oxidase to increase [ROS]i and [Ca2+]i through the mitochondrial ROS-PKCepsilon signaling axis in pulmonary artery smooth muscle cells. *Free Radic.Biol.Med.* 45:1223-1231.

51. Dietrich, A., H. Kalwa, B. Fuchs, F. Grimminger, N. Weissmann, and T. Gudermann. 2007. In vivo TRPC functions in the cardiopulmonary vasculature. *Cell Calcium* 42:233-244.

52. Ward, J. P., T. P. Robertson, and P. I. Aaronson. 2005. Capacitative calcium entry: a central role in hypoxic pulmonary vasoconstriction? *Am.J.Physiol Lung Cell Mol.Physiol* 289:L2-L4.

53. McDaniel, S. S., O. Platoshyn, J. Wang, Y. Yu, M. Sweeney, S. Krick, L. J. Rubin, and J. X. Yuan. 2001. Capacitative Ca(2+) entry in agonist-induced pulmonary vasoconstriction. *Am.J.Physiol Lung Cell Mol.Physiol* 280:L870-L880.

54. Weissmann, N., A. Dietrich, B. Fuchs, H. Kalwa, M. Ay, R. Dumitrascu, A. Olschewski, U. Storch, M. Schnitzler, H. A. Ghofrani, et al. 2006. Classical transient receptor potential channel 6 (TRPC6) is essential for hypoxic pulmonary vasoconstriction and alveolar gas exchange. *Proc.Natl.Acad.Sci.U.S.A* 103:19093-19098.

55. Landsberg, J. W. and J. X. Yuan. 2004. Calcium and TRP channels in pulmonary vascular smooth muscle cell proliferation. *News Physiol Sci.* 19:44-50.

56. Dipp, M., P. C. Nye, and A. M. Evans. 2001. Hypoxic release of calcium from the sarcoplasmic reticulum of pulmonary artery smooth muscle. *Am.J.Physiol Lung Cell Mol.Physiol* 281:L318-L325.

57. Wilson, H. L., M. Dipp, J. M. Thomas, C. Lad, A. Galione, and A. M. Evans. 2001. Adp-ribosyl cyclase and cyclic ADP-ribose hydrolase act as a redox sensor. a primary role for cyclic ADP-ribose in hypoxic pulmonary vasoconstriction. *J.Biol.Chem.* 276:11180-11188.

58. Okabe, E., Y. Tsujimoto, and Y. Kobayashi. 2000. Calmodulin and cyclic ADP-ribose interaction in Ca2+ signaling related to cardiac sarcoplasmic reticulum: superoxide anion radical-triggered Ca2+ release. *Antioxid.Redox.Signal.* 2:47-54.

59. Remillard, C. V. and J. X. Yuan. 2005. High altitude pulmonary hypertension: role of K+ and Ca2+ channels. *High Alt.Med.Biol.* 6:133-146.

60. Yuan, J. X. 2001. Oxygen-sensitive K(+) channel(s): where and what? *Am.J.Physiol Lung Cell Mol.Physiol* 281:L1345-L1349.

61. Coppock, E. A., J. R. Martens, and M. M. Tamkun. 2001. Molecular basis of hypoxia-induced pulmonary vasoconstriction: role of voltage-gated K+ channels. *Am.J.Physiol Lung Cell Mol.Physiol* 281:L1-12.

62. Patel, A. J. and E. Honore. 2001. Molecular physiology of oxygen-sensitive potassium channels. *Eur.Respir.J.* 18:221-227.

63. Michelakis, E. D., H. L. Reeve, J. M. Huang, S. Tolarova, D. P. Nelson, E. K. Weir, and S. L. Archer. 1997. Potassium channel diversity in vascular smooth muscle cells. *Can.J.Physiol Pharmacol.* 75:889-897.

64. Post, J. M., C. H. Gelband, and J. R. Hume. 1995. [Ca2+]i inhibition of K+ channels in canine pulmonary artery. Novel mechanism for hypoxia-induced membrane depolarization. *Circ.Res.* 77:131-139.

65. Yuan, X. J. 1995. Voltage-gated K+ currents regulate resting membrane potential and [Ca2+]i in pulmonary arterial myocytes. *Circ.Res.* 77:370-378.

66. Platoshyn, O., Y. Yu, E. A. Ko, C. V. Remillard, and J. X. Yuan. 2007. Heterogeneity of hypoxia-mediated decrease in I(K(V)) and increase in [Ca2+](cyt) in pulmonary artery smooth muscle cells. *Am.J.Physiol Lung Cell Mol.Physiol* 293:L402-L416.

67. Archer, S. L., B. London, V. Hampl, X. Wu, A. Nsair, L. Puttagunta, K. Hashimoto, R. E. Waite, and E. D. Michelakis. 2001. Impairment of hypoxic pulmonary vasoconstriction in mice lacking the voltage-gated potassium channel Kv1.5. *FASEB J.* 15:1801-1803.

68. Pozeg, Z. I., E. D. Michelakis, M. S. McMurtry, B. Thebaud, X. C. Wu, J. R. Dyck, K. Hashimoto, S. Wang, R. Moudgil, G. Harry, et al. 2003. In vivo gene transfer of the O2-sensitive potassium channel Kv1.5 reduces pulmonary hypertension and restores hypoxic pulmonary vasoconstriction in chronically hypoxic rats. *Circulation* 107:2037-2044.

69. Durmowicz, A. G., S. Hofmeister, T. K. Kadyraliev, A. A. Aldashev, and K. R. Stenmark. 1993. Functional and structural adaptation of the yak pulmonary circulation to residence at high altitude. *J.Appl.Physiol* 74:2276-2285.

70. Rhodes, J. 2005. Comparative physiology of hypoxic pulmonary hypertension: historical clues from brisket disease. *J.Appl.Physiol* 98:1092-1100.

71. Hislop, A. and L. Reid. 1977. Changes in the pulmonary arteries of the rat during recovery from hypoxia-induced pulmonary hypertension. *Br.J.Exp.Pathol.* 58:653-662.

72. Dempsey, E. C., M. G. Frid, A. A. Aldashev, M. Das, and K. R. Stenmark. 1997. Heterogeneity in the proliferative response of bovine pulmonary artery smooth muscle cells to mitogens and hypoxia: importance of protein kinase C. *Can.J.Physiol Pharmacol.* 75:936-944.

73. Frid, M. G., E. P. Moiseeva, and K. R. Stenmark. 1994. Multiple phenotypically distinct smooth muscle cell populations exist in the adult and developing bovine pulmonary arterial media in vivo. *Circ.Res.* 75:669-681.

74. Steudel, W., F. Ichinose, P. L. Huang, W. E. Hurford, R. C. Jones, J. A. Bevan, M. C. Fishman, and W. M. Zapol. 1997. Pulmonary vasoconstriction and hypertension in mice with targeted disruption of the endothelial nitric oxide synthase (NOS 3) gene. *Circ.Res.* 81:34-41.

75. Steudel, W., M. Scherrer-Crosbie, K. D. Bloch, J. Weimann, P. L. Huang, R. C. Jones, M. H. Picard, and W. M. Zapol. 1998. Sustained pulmonary hypertension and right ventricular hypertrophy after chronic hypoxia in mice with congenital deficiency of nitric oxide synthase 3. *J.Clin.Invest* 101:2468-2477.

76. Schermuly, R. T., E. Dony, H. A. Ghofrani, S. Pullamsetti, R. Savai, M. Roth, A. Sydykov, Y. J. Lai, N. Weissmann, W. Seeger, et al. 2005. Reversal of experimental pulmonary hypertension by PDGF inhibition. *J.Clin.Invest* 115:2811-2821.

77. Ambalavanan, N., A. Bulger, and J. B. Philips III. 1999. Hypoxia-induced release of peptide growth factors from neonatal porcine pulmonary artery smooth muscle cells. *Biol.Neonate* 76:311-319.

78. Eddahibi, S., M. Humbert, E. Fadel, B. Raffestin, M. Darmon, F. Capron, G. Simonneau, P. Dartevelle, M. Hamon, and S. Adnot. 2001. Serotonin transporter overexpression is responsible for pulmonary artery smooth muscle hyperplasia in primary pulmonary hypertension. *J.Clin.Invest* 108:1141-1150.

79. Eddahibi, S., B. Raffestin, M. Hamon, and S. Adnot. 2002. Is the serotonin transporter involved in the pathogenesis of pulmonary hypertension? *J.Lab Clin.Med.* 139:194-201.

80. Growcott, E. J., K. H. Banner, and J. Wharton. 2005. Hypoxia amplifies the proliferative capacity of distal human pulmonary artery smooth-muscle cells. *Chest* 128:600S-601S.

81. Marcos, E., S. Adnot, M. H. Pham, A. Nosjean, B. Raffestin, M. Hamon, and S. Eddahibi. 2003. Serotonin transporter inhibitors protect against hypoxic pulmonary hypertension. *Am.J.Respir.Crit Care Med.* 168:487-493.

82. Xin, X., A. D. Johnson, T. Scott-Burden, D. Engler, and W. Casscells. 1994. The predominant form of fibroblast growth factor receptor expressed by proliferating human arterial smooth muscle cells in culture is type I. *Biochem.Biophys.Res.Commun.* 204:557-564.

83. Sommer, N., A. Dietrich, R. T. Schermuly, H. A. Ghofrani, T. Gudermann, R. Schulz, W. Seeger, F. Grimminger, and N. Weissmann. 2008. Regulation of hypoxic pulmonary vasoconstriction: basic mechanisms. *Eur.Respir.J.* 32:1639-1651.

84. Weir, E. K. and A. Olschewski. 2006. Role of ion channels in acute and chronic responses of the pulmonary vasculature to hypoxia. *Cardiovasc.Res.* 71:630-641.

85. Smirnov, S. V., T. P. Robertson, J. P. Ward, and P. I. Aaronson. 1994. Chronic hypoxia is associated with reduced delayed rectifier K+ current in rat pulmonary artery muscle cells. *Am.J.Physiol* 266:H365-H370.

86. Wang, J., L. Weigand, W. Wang, J. T. Sylvester, and L. A. Shimoda. 2005. Chronic hypoxia inhibits Kv channel gene expression in rat distal pulmonary artery. *Am.J.Physiol Lung Cell Mol.Physiol* 288:L1049-L1058.

87. Platoshyn, O., Y. Yu, V. A. Golovina, S. S. McDaniel, S. Krick, L. Li, J. Y. Wang, L. J. Rubin, and J. X. Yuan. 2001. Chronic hypoxia decreases K(V) channel expression and function in pulmonary artery myocytes. *Am.J.Physiol Lung Cell Mol.Physiol* 280:L801-L812.

88. Moudgil, R., E. D. Michelakis, and S. L. Archer. 2006. The role of k+ channels in determining pulmonary vascular tone, oxygen sensing, cell proliferation, and apoptosis: implications in hypoxic pulmonary vasoconstriction and pulmonary arterial hypertension. *Microcirculation.* 13:615-632.

89. Yu, Y., O. Platoshyn, J. Zhang, S. Krick, Y. Zhao, L. J. Rubin, A. Rothman, and J. X. Yuan. 2001. c-Jun decreases voltage-gated K(+) channel activity in pulmonary artery smooth muscle cells. *Circulation* 104:1557-1563.

90. Remillard, C. V. and J. X. Yuan. 2004. Activation of K+ channels: an essential pathway in programmed cell death. *Am.J.Physiol Lung Cell Mol.Physiol* 286:L49-L67.

91. Moudgil, R., E. D. Michelakis, and S. L. Archer. 2005. Hypoxic pulmonary vasoconstriction. *J.Appl.Physiol* 98:390-403.

92. Shimoda, L. A., J. S. Sham, T. H. Shimoda, and J. T. Sylvester. 2000. L-type Ca(2+) channels, resting [Ca(2+)](i), and ET-1-induced responses in chronically hypoxic pulmonary myocytes. *Am.J.Physiol Lung Cell Mol.Physiol* 279:L884-L894.

93. Lin, M. J., G. P. Leung, W. M. Zhang, X. R. Yang, K. P. Yip, C. M. Tse, and J. S. Sham. 2004. Chronic hypoxia-induced upregulation of store-operated and receptor-operated Ca2+ channels in pulmonary arterial smooth muscle cells: a novel mechanism of hypoxic pulmonary hypertension. *Circ.Res.* 95:496-505.

94. Fortuno, A., J. G. San, M. U. Moreno, J. Diez, and G. Zalba. 2005. Oxidative stress and vascular remodelling. *Exp.Physiol* 90:457-462.

95. Wu, W., O. Platoshyn, A. L. Firth, and J. X. Yuan. 2007. Hypoxia divergently regulates production of reactive oxygen species in human pulmonary and coronary artery smooth muscle cells. *Am.J.Physiol Lung Cell Mol.Physiol* 293:L952-L959.

96. Li, H., S. J. Chen, Y. F. Chen, Q. C. Meng, J. Durand, S. Oparil, and T. S. Elton. 1994. Enhanced endothelin-1 and endothelin receptor gene expression in chronic hypoxia. *J.Appl.Physiol* 77:1451-1459.

97. Wedgwood, S., R. W. Dettman, and S. M. Black. 2001. ET-1 stimulates pulmonary arterial smooth muscle cell proliferation via induction of reactive oxygen species. *Am.J.Physiol Lung Cell Mol.Physiol* 281:L1058-L1067.

98. Lambeth, J. D., K. H. Krause, and R. A. Clark. 2008. NOX enzymes as novel targets for drug development. *Semin.Immunopathol.* 30:339-363.

99. Liu, J. Q., I. N. Zelko, E. M. Erbynn, J. S. Sham, and R. J. Folz. 2006. Hypoxic pulmonary hypertension: role of superoxide and NADPH oxidase (gp91phox). *Am.J.Physiol Lung Cell Mol.Physiol* 290:L2-10.

100. Lassegue, B. and R. E. Clempus. 2003. Vascular NAD(P)H oxidases: specific features, expression, and regulation. *Am.J.Physiol Regul.Integr.Comp Physiol* 285:R277-R297.

101. Lachmanova, V., O. Hnilickova, V. Povysilova, V. Hampl, and J. Herget. 2005. N-acetylcysteine inhibits hypoxic pulmonary hypertension most effectively in the initial phase of chronic hypoxia. *Life Sci.* 77:175-182.

102. Zungu, M., M. E. Young, W. C. Stanley, and M. F. Essop. 2008. Expression of mitochondrial regulatory genes parallels respiratory capacity and contractile function in a rat model of hypoxia-induced right ventricular hypertrophy. *Mol.Cell Biochem.* 318:175-181.

103. Fink, L., W. Seeger, L. Ermert, J. Hanze, U. Stahl, F. Grimminger, W. Kummer, and R. M. Bohle. 1998. Real-time quantitative RT-PCR after laser-assisted cell picking. *Nat.Med.* 4:1329-1333.

104. Fink, L. and R. M. Bohle. 2002. Internal standards for laser microdissection. *Methods Enzymol.* 356:99-113.

105. Fink, L., S. Kohlhoff, M. M. Stein, J. Hanze, N. Weissmann, F. Rose, E. Akkayagil, D. Manz, F. Grimminger, W. Seeger, et al. 2002. cDNA array hybridization after laser-assisted microdissection from nonneoplastic tissue. *Am.J.Pathol.* 160:81-90.

106. Kwapiszewska, G., M. Meyer, R. Bogumil, R. M. Bohle, W. Seeger, N. Weissmann, and L. Fink. 2004. Identification of proteins in laser-microdissected small cell numbers by SELDI-TOF and Tandem MS. *BMC.Biotechnol.* 4:30.

107. Ord, J. J., E. H. Streeter, I. S. Roberts, D. Cranston, and A. L. Harris. 2005. Comparison of hypoxia transcriptome in vitro with in vivo gene expression in human bladder cancer. *Br.J.Cancer* 93:346-354.

108. Wingler, K., S. Wunsch, R. Kreutz, L. Rothermund, M. Paul, and H. H. Schmidt. 2001. Upregulation of the vascular NAD(P)H-oxidase isoforms Nox1 and Nox4 by the renin-angiotensin system in vitro and in vivo. *Free Radic.Biol.Med.* 31:1456-1464.

109. Goyal, P., N. Weissmann, F. Rose, F. Grimminger, H. J. Schafers, W. Seeger, and J. Hanze. 2005. Identification of novel Nox4 splice variants with impact on ROS levels in A549 cells. *Biochem.Biophys.Res.Commun.* 329:32-39.

110. Rose, F., F. Grimminger, J. Appel, M. Heller, V. Pies, N. Weissmann, L. Fink, S. Schmidt, S. Krick, G. Camenisch, et al. 2002. Hypoxic pulmonary artery fibroblasts trigger proliferation of vascular smooth muscle cells: role of hypoxia-inducible transcription factors. *FASEB J.* 16:1660-1661.

111. Weissmann, N., A. Dietrich, B. Fuchs, H. Kalwa, M. Ay, R. Dumitrascu, A. Olschewski, U. Storch, Y. S. Mederos, H. A. Ghofrani, et al. 2006. Classical transient receptor potential channel 6 (TRPC6) is essential for hypoxic pulmonary vasoconstriction and alveolar gas exchange. *Proc.Natl.Acad.Sci.U.S.A* 103:19093-19098.

112. McCartney, C. E., H. McClafferty, J. M. Huibant, E. G. Rowan, M. J. Shipston, and I. C. Rowe. 2005. A cysteine-rich motif confers hypoxia sensitivity to mammalian large conductance voltage- and Ca-activated K (BK) channel alpha-subunits. *Proc.Natl.Acad.Sci.U.S.A* 102:17870-17876.

113. Ciorba, M. A., S. H. Heinemann, H. Weissbach, N. Brot, and T. Hoshi. 1997. Modulation of potassium channel function by methionine oxidation and reduction. *Proc.Natl.Acad.Sci.U.S.A* 94:9932-9937.

114. Ruppersberg, J. P., M. Stocker, O. Pongs, S. H. Heinemann, R. Frank, and M. Koenen. 1991. Regulation of fast inactivation of cloned mammalian IK(A) channels by cysteine oxidation. *Nature* 352:711-714.

115. Archer, S. L., E. Souil, A. T. nh-Xuan, B. Schremmer, J. C. Mercier, Y. A. El, L. Nguyen-Huu, H. L. Reeve, and V. Hampl. 1998. Molecular identification of the role of voltage-gated K+ channels, Kv1.5 and Kv2.1, in hypoxic pulmonary vasoconstriction and control of resting membrane potential in rat pulmonary artery myocytes. *J.Clin.Invest* 101:2319-2330.

116. Hogg, D. S., A. R. Davies, G. McMurray, and R. Z. Kozlowski. 2002. K(V)2.1 channels mediate hypoxic inhibition of I(KV) in native pulmonary arterial smooth muscle cells of the rat. *Cardiovasc.Res.* 55:349-360.

117. Wang, H. D., S. Xu, D. G. Johns, Y. Du, M. T. Quinn, A. J. Cayatte, and R. A. Cohen. 2001. Role of NADPH oxidase in the vascular hypertrophic and oxidative stress response to angiotensin II in mice. *Circ.Res.* 88:947-953.

118. Weber, D. S., P. Rocic, A. M. Mellis, K. Laude, A. N. Lyle, D. G. Harrison, and K. K. Griendling. 2005. Angiotensin II-induced hypertrophy is potentiated in mice overexpressing p22phox in vascular smooth muscle. *Am.J.Physiol Heart Circ.Physiol* 288:H37-H42.

119. Hoidal, J. R., S. S. Brar, A. B. Sturrock, K. A. Sanders, B. Dinger, S. Fidone, and T. P. Kennedy. 2003. The role of endogenous NADPH oxidases in airway and pulmonary vascular smooth muscle function. *Antioxid.Redox.Signal.* 5:751-758.

120. Stenmark, K. R., K. A. Fagan, and M. G. Frid. 2006. Hypoxia-induced pulmonary vascular remodeling: cellular and molecular mechanisms. *Circ.Res.* 99:675-691.

121. Sylvester, J. T. 2001. Hypoxic pulmonary vasoconstriction: a radical view. *Circ.Res.* 88:1228-1230.

122. Jeffery, T. K. and J. C. Wanstall. 2001. Pulmonary vascular remodeling: a target for therapeutic intervention in pulmonary hypertension. *Pharmacol.Ther.* 92:1-20.

123. Sturrock, A., B. Cahill, K. Norman, T. P. Huecksteadt, K. Hill, K. Sanders, S. V. Karwande, J. C. Stringham, D. A. Bull, M. Gleich, et al. 2006. Transforming growth factor-beta1 induces

Nox4 NAD(P)H oxidase and reactive oxygen species-dependent proliferation in human pulmonary artery smooth muscle cells. *Am.J.Physiol Lung Cell Mol.Physiol* 290:L661-L673.

124. Hohler, B., B. Holzapfel, and W. Kummer. 2000. NADPH oxidase subunits and superoxide production in porcine pulmonary artery endothelial cells. *Histochem.Cell Biol.* 114:29-37.

125. Lee, Y. M., B. J. Kim, Y. S. Chun, I. So, H. Choi, M. S. Kim, and J. W. Park. 2006. NOX4 as an oxygen sensor to regulate TASK-1 activity. *Cell Signal.* 18:499-507.

126. Shiose, A., J. Kuroda, K. Tsuruya, M. Hirai, H. Hirakata, S. Naito, M. Hattori, Y. Sakaki, and H. Sumimoto. 2001. A novel superoxide-producing NAD(P)H oxidase in kidney. *J.Biol.Chem.* 276:1417-1423.

127. Weissmann, N., A. Tadic, J. Hanze, F. Rose, S. Winterhalder, M. Nollen, R. T. Schermuly, H. A. Ghofrani, W. Seeger, and F. Grimminger. 2000. Hypoxic vasoconstriction in intact lungs: a role for NADPH oxidase-derived H(2)O(2)? *Am.J.Physiol Lung Cell Mol.Physiol* 279:L683-L690.

128. Suliman, H. B., M. Ali, and C. A. Piantadosi. 2004. Superoxide dismutase-3 promotes full expression of the EPO response to hypoxia. *Blood* 104:43-50.

129. Weissmann, N., D. Manz, D. Buchspies, S. Keller, T. Mehling, R. Voswinckel, K. Quanz, H. A. Ghofrani, R. T. Schermuly, L. Fink, et al. 2005. Congenital erythropoietin over-expression causes "anti-pulmonary hypertensive" structural and functional changes in mice, both in normoxia and hypoxia. *Thromb.Haemost.* 94:630-638.

130. Kawahara, T., D. Ritsick, G. Cheng, and J. D. Lambeth. 2005. Point mutations in the proline-rich region of p22phox are dominant inhibitors of Nox1- and Nox2-dependent reactive oxygen generation. *J.Biol.Chem.* 280:31859-31869.

131. Petry, A., T. Djordjevic, M. Weitnauer, T. Kietzmann, J. Hess, and A. Gorlach. 2006. NOX2 and NOX4 mediate proliferative response in endothelial cells. *Antioxid.Redox.Signal.* 8:1473-1484.

132. Gorlach, A., P. Klappa, and T. Kietzmann. 2006. The endoplasmic reticulum: folding, calcium homeostasis, signaling, and redox control. *Antioxid.Redox.Signal.* 8:1391-1418.

133. Djordjevic, T., A. Pogrebniak, R. S. BelAiba, S. Bonello, C. Wotzlaw, H. Acker, J. Hess, and A. Gorlach. 2005. The expression of the NADPH oxidase subunit p22phox is regulated by a redox-sensitive pathway in endothelial cells. *Free Radic.Biol.Med.* 38:616-630.

134. Buggisch, M., B. Ateghang, C. Ruhe, C. Strobel, S. Lange, M. Wartenberg, and H. Sauer. 2007. Stimulation of ES-cell-derived cardiomyogenesis and neonatal cardiac cell proliferation by reactive oxygen species and NADPH oxidase. *J.Cell Sci.* 120:885-894.

135. Jiang, Y., A. Dai, Q. Li, and R. Hu. 2007. Hypoxia induces transforming growth factor-beta1 gene expression in the pulmonary artery of rats via hypoxia-inducible factor-1alpha. *Acta Biochim.Biophys.Sin.(Shanghai)* 39:73-80.

136. Chen, Y. F., J. A. Feng, P. Li, D. Xing, Y. Zhang, R. Serra, N. Ambalavanan, E. Majid-Hassan, and S. Oparil. 2006. Dominant negative mutation of the TGF-beta receptor blocks hypoxia-induced pulmonary vascular remodeling. *J.Appl.Physiol* 100:564-571.

137. Jackson, I. L., L. Chen, I. Batinic-Haberle, and Z. Vujaskovic. 2007. Superoxide dismutase mimetic reduces hypoxia-induced O2*-, TGF-beta, and VEGF production by macrophages. *Free Radic.Res.* 41:8-14.

138. Turner, J. L. and R. Z. Kozlowski. 1997. Relationship between membrane potential, delayed rectifier K+ currents and hypoxia in rat pulmonary arterial myocytes. *Exp.Physiol* 82:629-645.

139. Tang, X. D., M. L. Garcia, S. H. Heinemann, and T. Hoshi. 2004. Reactive oxygen species impair Slo1 BK channel function by altering cysteine-mediated calcium sensing. *Nat.Struct.Mol.Biol.* 11:171-178.

140. Paravicini, T. M. and R. M. Touyz. 2008. NADPH oxidases, reactive oxygen species, and hypertension: clinical implications and therapeutic possibilities. *Diabetes Care* 31 Suppl 2:S170-S180.

141. Archer, S. L., H. L. Reeve, E. Michelakis, L. Puttagunta, R. Waite, D. P. Nelson, M. C. Dinauer, and E. K. Weir. 1999. O2 sensing is preserved in mice lacking the gp91 phox subunit of NADPH oxidase. *Proc.Natl.Acad.Sci.U.S.A* 96:7944-7949.

142. Remillard, C. V., D. D. Tigno, O. Platoshyn, E. D. Burg, E. E. Brevnova, D. Conger, A. Nicholson, B. K. Rana, R. N. Channick, L. J. Rubin, et al. 2007. Function of Kv1.5 channels and genetic variations of KCNA5 in patients with idiopathic pulmonary arterial hypertension. *Am.J.Physiol Cell Physiol* 292:C1837-C1853.

143. Heumuller, S., S. Wind, E. Barbosa-Sicard, H. H. Schmidt, R. Busse, K. Schroder, and R. P. Brandes. 2008. Apocynin is not an inhibitor of vascular NADPH oxidases but an antioxidant. *Hypertension* 51:211-217.

144. Cogolludo, A., G. Frazziano, L. Cobeno, L. Moreno, F. Lodi, E. Villamor, J. Tamargo, and F. Perez-Vizcaino. 2006. Role of reactive oxygen species in Kv channel inhibition and vasoconstriction induced by TP receptor activation in rat pulmonary arteries. *Ann.N.Y.Acad.Sci.* 1091:41-51.

145. Duprat, F., E. Guillemare, G. Romey, M. Fink, F. Lesage, M. Lazdunski, and E. Honore. 1995. Susceptibility of cloned K+ channels to reactive oxygen species. *Proc.Natl.Acad.Sci.U.S.A* 92:11796-11800.

146. Valenzeno, D. P. and M. Tarr. 1991. Membrane photomodification of cardiac myocytes: potassium and leakage currents. *Photochem.Photobiol.* 53:195-201.

147. Chen, J., V. Avdonin, M. A. Ciorba, S. H. Heinemann, and T. Hoshi. 2000. Acceleration of P/C-type inactivation in voltage-gated K(+) channels by methionine oxidation. *Biophys.J.* 78:174-187.

148. Coetzee, W. A., Y. Amarillo, J. Chiu, A. Chow, D. Lau, T. McCormack, H. Moreno, M. S. Nadal, A. Ozaita, D. Pountney, et al. 1999. Molecular diversity of K+ channels. *Ann.N.Y.Acad.Sci.* 868:233-285.

149. Mauban, J. R., C. V. Remillard, and J. X. Yuan. 2005. Hypoxic pulmonary vasoconstriction: role of ion channels. *J.Appl.Physiol* 98:415-420.

150. Shimoda, L. A., J. S. Sham, T. H. Shimoda, and J. T. Sylvester. 2000. L-type Ca(2+) channels, resting [Ca(2+)](i), and ET-1-induced responses in chronically hypoxic pulmonary myocytes. *Am.J.Physiol Lung Cell Mol.Physiol* 279:L884-L894.

151. Shimoda, L. A., J. T. Sylvester, and J. S. Sham. 2000. Mobilization of intracellular Ca(2+) by endothelin-1 in rat intrapulmonary arterial smooth muscle cells. *Am.J.Physiol Lung Cell Mol.Physiol* 278:L157-L164.

152. Fike, C. D. and M. R. Kaplowitz. 1999. Nifedipine inhibits pulmonary hypertension but does not prevent decreased lung eNOS in hypoxic newborn pigs. *Am.J.Physiol* 277:L449-L456.

153. Oka, M., K. G. Morris, and I. F. McMurtry. 1993. NIP-121 is more effective than nifedipine in acutely reversing chronic pulmonary hypertension. *J.Appl.Physiol* 75:1075-1080.

154. Lund, A. K., S. L. Peterson, G. S. Timmins, and M. K. Walker. 2005. Endothelin-1-mediated increase in reactive oxygen species and NADPH Oxidase activity in hearts of aryl hydrocarbon receptor (AhR) null mice. *Toxicol.Sci.* 88:265-273.

155. Zeng, Q., Q. Zhou, F. Yao, S. T. O'Rourke, and C. Sun. 2008. Endothelin-1 regulates cardiac L-type calcium channels via NAD(P)H oxidase-derived superoxide. *J.Pharmacol.Exp.Ther.* 326:732-738.

156. Lin, M. J., X. R. Yang, Y. N. Cao, and J. S. Sham. 2007. Hydrogen peroxide-induced Ca2+ mobilization in pulmonary arterial smooth muscle cells. *Am.J.Physiol Lung Cell Mol.Physiol* 292:L1598-L1608.

157. Martyn, K. D., L. M. Frederick, L. K. von, M. C. Dinauer, and U. G. Knaus. 2006. Functional analysis of Nox4 reveals unique characteristics compared to other NADPH oxidases. *Cell Signal.* 18:69-82.

11 ACKNOWLEDGEMENT

I would like to reveal my sincere acknowledgement to Prof. Dr. Werner Seeger for this wonderful opportunity of learning science in an international environment of graduate college. Prof. Seeger, you have ever been the first and final source of inspiration for me.

I would like to disclose my sincere gratitude to Prof. Norbert Weißmann, my supervisor, for his efforts and contribution to my learning. I am greatly impressed by his friendly personality, patience and team approach of successfully exploring science.

My sincere thanks go to Prof. Gabriel Haddad at University of California San Diego (USA) for giving me an opportunity to learn electrophysiology at his lab. I thank a lot to Dr. Xiang Q Gu for teaching me complicated technique of patch clamp. I was highly impressed by his humbleness, patience and hard working nature. You were an inspiration for me to overcome my frustration when I could not get even a single patch for three months. Thank a lot Xiang for bearing with me at that difficult time.

I would like to express my sincere thanks to Dr. Oliver Eickelberg, Director of the International Graduate Program MBML, and his MBML team for their constant efforts to make the program intensive, effective and a success. You, as a program director, were absolutely right to assume that students needed adequate pressure, and you deserve heartfelt appreciation. My special thanks go to my colleagues in MBML for their contribution to make the study an interactive, interesting and enjoying of its kind.

I would like to acknowledge Dr. Markus Roth for the guidance throughout all the experiments and for his support and motivation whenever I needed. I thank Dr. Bakytbek Egemnazaraov, Dr. Eva Dony and Dr. Beate Füchs for “Zussamenfassug”. Thanks also go to Dr. Rory Morty and Dr. Nirmal Parajuli for linguistic editing. I thank all the technical staffs in the lab, and especially Carmen Homberger, Ingrid Breitenborn Müller and Karin Quanz for their assistance in experiments. I thank Dr. Oleg Pak for helping me in calcium measurement

It goes without saying that my beloved parents ever deserve my deepest gratitude. Finally, I express thanks to my wife Neha Bansal, for bearing with me at difficult time.

Giessen, Germany

April 2009

ACADEMIC HONORS/SCHOLARSHIPS

- International Trainee Travel Award (ITTA) from American Thoracic Society (ATS) San Diego, 2009
- Travel bursary from European Respiratory Society (ERS) for attending 5th ERS lung science conference in Taormina, Italy 2007
- Faculty of Medicine and Veterinary Medicine research scholarship from The University of Edinburgh (Scotland, U.K) 2003-2004

PUBLICATIONS

- O'Reilly M, Marshall E, Macgillivray T, **Mittal M**, Xue W, Kenyon CJ, Brown RW. Dietary electrolyte-driven responses in the renal WNK kinase pathway in vivo. *J Am Soc Nephrol.* 2006 Sep;17(9):2402-13

- **Mittal M**, Roth M, König P, Hofmann S, Dony E, Goyal P, Selbitz AC, Schermuly RT, Ghofrani HA, Kwapiszewska G, Kummer W, Klepetko W, Hoda MA, Fink L, Hänze J, Seeger W, Grimminger F, Schmidt HH, Weissmann N. Hypoxia-Dependent Regulation of Nonphagocytic NADPH Oxidase Subunit NOX4 in the Pulmonary Vasculature. *Circ Res* 2007 Aug 3;101(3):258-67

- Roth M, Rupp M, Hofmann S, **Mittal M**, Sommer N, Quanz K, Schubert D, Dony E, Schermuly RT, Ghofrani H A, Rutschmann K, Wilhelm S, Seeger W, Ruth P, Grimminger F, Sausbier M, and Weissmann N. Vascular effects of heme oxygenase-2 and the BK-channel in acute, sustained, and chronic alveolar hypoxia. *Am J Respir Crit Care Med.* 2009 Aug 15;180(4):353-64.

- Weissmann N, Hackemack S, Dahal BK, Pullamsetti SS, Savai R, **Mittal M**, Fuchs B, Medebach T, Dumitrascu R, Eickels MV, Ghofrani HA, Seeger W, Grimminger F, Schermuly RT. The soluble guanylate cyclase activator HMR1766 reverses hypoxia-induced experimental pulmonary hypertension in mice. *Am J Physiol Lung Cell Mol Physiol.* 2009 Oct;297(4):L658-65.

- **Mittal M**, Roth M, Gu XQ, Pak O, Schermuly RT, Ghofrani HA, Seeger W, Grimminger F, Haddad GG and Weissmann N. NOX4 regulates K_{DR} channels and calcium influx under chronic hypoxia (Under preparation)

POSTER PRESENTATIONS

- **Mittal M**, Roth M, Gu XQ, Pak O, Schermuly RT, Ghofrani HA, Seeger W, Grimminger F, Haddad GG and Weissmann N. Role of NADPH oxidase derived ROS in regulation of K_{DR} channels and calcium influx under chronic hypoxia.*Hypoxia and Consequences: From Molecule to Malady, New York Academy of Sciences, New York, U.S.A, 12-14 March. 2009*

- **Mittal M**, Roth M, König P, Hofmann S, Dony E, Goyal P, Selbitz AC, Schermuly RT, Ghofrani HA, Kwapiszewska G, Kummer W, Klepetko W, Hoda MA, Fink L, Hänze J, Seeger W, Grimminger F, Schmidt HH, Weissmann N. (2007) Hypoxia dependent regulation of non phagocytic NADPH oxidase subunit NOX4 in pulmonary vasculature. *European Respiratory Society, Stockholm, Sweden,15-19 Sep.2007*

- **Mittal M**, Roth M, König P, Hofmann S, Dony E, Goyal P, Selbitz AC, Schermuly RT, Ghofrani HA, Kwapiszewska G, Kummer W, Klepetko W, Hoda MA, Fink L, Hänze J, Seeger W, Grimminger F, Schmidt HH, Weissmann N. (2007) Hypoxia driven up-regulation of non phagocytic NADPH oxidase subunit NOX4 in pulmonary vasculature. *American Thoracic Society, San Francisco, USA,18-23 May 2007*

- **Mittal M**, Roth M, König P, Hofmann S, Dony E, Goyal P, Selbitz AC, Schermuly RT, Ghofrani HA, Kwapiszewska G, Kummer W, Klepetko W, Hoda MA, Fink L, Hänze J, Seeger W, Grimminger F, Schmidt HH, Weissmann N. (2007) Hypoxia dependent up-regulation of NADPH oxidase subunit NOX4 in pulmonary vasculature. *European Respiratory Society. Taormina, Italy, March 2007*

ORAL PRESENTATIONS

- **Mittal M**, Roth M, Gu XQ, Pak O, Schermuly RT, Ghofrani HA, Seeger W, Grimminger F, Haddad GG and Weissmann N. NOX4 regulates K_{DR} channels and calcium influx under chronic hypoxia. *American Thoracic Society, San Diego, USA, 2009*

- **Mittal M**, Roth M, König P, Hofmann S, Dony E, Goyal P, Selbitz AC, Schermuly RT, Ghofrani HA, Kwapiszewska G, Kummer W, Klepetko W, Hoda MA, Fink L, Hänze J, Seeger W, Grimminger F, Schmidt HH, Weissmann N. (2007) Hypoxia dependent up-regulation of NADPH oxidase subunit NOX4 in pulmonary vasculature. *Sonder Forschungs Bereich symposium, Giessen,Germany,May 2007*

- **Mittal M**, Roth M, König P, Hofmann S, Dony E, Goyal P, Selbitz AC, Schermuly RT, Ghofrani HA, Kwapiszewska G, Kummer W, Klepetko W, Hoda MA, Fink L, Hänze J, Seeger W, Grimminger F, Schmidt HH, Weissmann N. (2006) Localisation of NADPH oxidases and their role in hypoxia induced pulmonary hypertension. *European respiratory society. Munich,Germany,2-6 Sep.2006*

- **Mittal M**, Roth M, Hänze J, Schermuly RT, Ghofrani HA, Seeger W, Grimminger F, Schmidt HH, Weissmann N. (2005) Role of NADPH oxidases and Kv channels in hypoxia induced pulmonary hypertension. *Annual retreat of Molecular Biology and Medicine of Lung, Giessen, July 2006*

- **Mittal M**, Roth M, Hänze J, Schermuly RT, Ghofrani HA, Seeger W, Grimminger F, Schmidt HH, Weissmann N. (2005) Role of NADPH oxidases and Kv channels in hypoxia induced pulmonary hypertension. *Annual retreat of Molecular Biology and Medicine of Lung, Giessen, July 2005*

13 DECLARATION

I declare that I have completed this dissertation single-handedly without the unauthorized help of a second party and only with the assistance acknowledged therein. I have appropriately acknowledged and referenced all text passages that are derived literally from or are based on the content of published or unpublished work of others, and all information that relates to verbal communications. I have abided by the principles of good scientific conduct laid down in the charter of the Justus Liebig University of Giessen in carrying out the investigations described in the dissertation.

"Ich erkläre: Ich habe die vorgelegte Dissertation selbständig, ohne unerlaubte fremde Hilfe und nur mit den Hilfen angefertigt, die ich in der Dissertation angegeben habe. Alle Textstellen, die wörtlich oder sinngemäß aus veröffentlichten oder nicht veröffentlichten Schriften entnommen sind, und alle Angaben, die auf mündlichen Auskünften beruhen, sind als solche kenntlich gemacht. Bei den von mir durchgeführten und in der Dissertation erwähnten Untersuchungen habe ich die Grundsätze guter wissenschaftlicher Praxis, wie sie in der „Satzung der Justus-Liebig-Universität Gießen zur Sicherung guter wissenschaftlicher Praxis" niedergelegt sind, eingehalten."

Manish Mittal

Giessen
April 2009